

Appendix A

Los Peñasquitos Lagoon Sediment TMDL Modeling - Final

Submitted to:



City of San Diego
Storm Water Department
9370 Chesapeake Drive, Suite 100
San Diego, CA 92123

Submitted by:



Tetra Tech, Inc.
1230 Columbia St., Suite 1000
San Diego, CA 92101

October 12, 2010



Contents

Introduction	1
Watershed Description	2
Lagoon Description	3
Data Inventory and Analysis	3
Land Use	3
Topography	5
Soil Characteristics	6
Meteorological Data	8
Streamflow Data	10
Suspended Sediment Data	15
Overview of Modeling Approach	24
Watershed Model Description	24
Watershed Model Setup	25
Catchment Delineation	25
Configuration of Key Model Components	28
Lagoon Model Description	29
Lagoon Model Setup	29
Grid Generation	30
Boundary Conditions	32
Initial Conditions	35
Model Calibration and Validation	36
Watershed Model Calibration and Validation	36
Lagoon Model Calibration	51
Summary and Conclusions	72
References	73
Appendix A: Model Hydrology Parameters	A-1
Appendix B: Model Sediment Parameters	B-1

Tables

Table 1.	Area and percent land use distribution	5
Table 2.	Sand, silt, and clay distribution by hydrologic soil group	8
Table 3.	Hourly rainfall gages	9
Table 4.	Potential evapotranspiration (PET) stations	10
Table 5.	TSS measurements at USGS stations on Los Peñasquitos Creek	16
Table 6.	Rainfall and TSS measurements at the MLS and TWAS stations on Los Peñasquitos Creek	17
Table 7.	Pollutograph measurements of TSS (mg/L) at Carmel Creek	19
Table 8.	Pollutograph measurements of TSS (mg/L) at Carroll Canyon Creek	20
Table 9.	Pollutograph measurements of TSS (mg/L) at Los Peñasquitos Creek	21
Table 10.	TSS (mg/L) EMCs for the pollutograph and MLS stations on Los Peñasquitos Creek	22
Table 11.	Impervious fraction by land use type	27
Table 12.	Sediment fractions by hydrologic soil group	28
Table 13.	Sediment fractions adjusted for watershed delivery	28
Table 14.	LSPC hydrologic model performance - entire simulation period	41
Table 15.	Comparison of modeled and measured sediment fractions for each storm event	49
Table 16.	Lagoon calibration data summary	51
Table A-1.	110 pwat-parm2	A-1
Table A-2.	120 pwat-parm3	A-2
Table A-3.	130 pwat-parm4	A-4
Table B-1.	Impervious surface coefficients (KEIM and JEIM) by landuse	B-2
Table B-2.	Sediment fractions by hydrologic soil group	B-2
Table B-3.	Sediment fractions adjusted for watershed delivery	B-2
Table B-4.	Model reach parameters	B-2
Table B-5.	Model reach sand and silt stress and erodibility coefficients	B-3

Figures

Figure 1.	Location of the Los Peñasquitos watershed and lagoon	2
Figure 2.	Land use distribution in the Los Peñasquitos watershed	4
Figure 3.	Topography in the Los Peñasquitos watershed	6
Figure 4.	Hydrologic soil groups in the Los Peñasquitos watershed	7
Figure 5.	Meteorological stations within and near the Los Peñasquitos watershed	9
Figure 6.	USGS monitoring locations in the Los Peñasquitos watershed	11
Figure 7.	Stormwater monitoring locations in the Los Peñasquitos watershed	12
Figure 8.	Measured flows at TMDL monitoring locations	12
Figure 9.	Cumulative volumes at TMDL monitoring locations	13
Figure 10.	Photos near the Carroll Canyon Creek monitoring station	13
Figure 11.	Photo at the Los Peñasquitos Creek monitoring station	14
Figure 12.	Comparison of flows at the MLS and USGS gaging station (11023340)	14
Figure 13.	Comparison of cumulative volumes at the MLS and USGS gaging stations	15
Figure 14.	Relationship between rainfall and TSS measured at the MLS	18
Figure 15.	EMC/Median TSS and 95th percentile confidence intervals for all sampling events	22
Figure 16.	Particle size distribution for the 11/30/2007 storm event	23
Figure 17.	Particle size distribution for the 12/7/2007 storm event	23
Figure 18.	Schematic of LSPC Hydrology Components	24
Figure 19.	Catchment delineation in the Los Peñasquitos watershed	26
Figure 23.	Mean monthly flow for calibration period (USGS 11023340)	37
Figure 24.	Mean monthly flow for validation period (USGS 11023340)	37
Figure 25.	Monthly median and percentile flow comparison – calibration period	38
Figure 26.	Monthly median and percentile flow comparison – validation period	38



Figure 27.	Flow exceedence output comparison – calibration period	39
Figure 28.	Flow exceedence output comparison – validation period	39
Figure 29.	Cumulative volume comparison – calibration period	40
Figure 30.	Cumulative volume comparison – validation period.....	40
Figure 31.	Time-series streamflow measured on Los Peñasquitos Creek	42
Figure 32.	Baseflow and storm volumes measured on Los Peñasquitos Creek.....	42
Figure 33.	Comparison of modeled and observed flows at the USGS and MLS stations – 11/30/2007 storm	43
Figure 34.	Comparison of modeled and observed flows at the USGS and MLS stations – 12/7/2007 storm	44
Figure 35.	Comparison of modeled and observed flows at the USGS and MLS stations – 2/3/2008 storm	45
Figure 36.	Comparison of EMC and 95 th Percentile TSS data collected during each storm event	46
Figure 37.	Pollutograph TSS calibration at Carmel Creek	47
Figure 38.	Pollutograph TSS calibration at Los Peñasquitos Creek	47
Figure 39.	Pollutograph TSS calibration at Carroll Canyon Creek	48
Figure 40.	Comparison of modeled and measured TSS with 95 th percentile confidence intervals	50
Figure 41.	Measured TSS before/after construction of the El Cuervo Norte wetlands	51
Figure 42.	Calibration stations within Los Peñasquitos Lagoon	52
Figure 43.	Water surface elevation calibration results.....	54
Figure 44.	Temperature calibration results	55
Figure 45.	Salinity Calibration results for all stations (including Station W2).....	57
Figure 46.	TSS calibration at Ocean Inlet – entire calibration period	59
Figure 47.	TSS calibration at Ocean Inlet – 11/30/2007 storm	59
Figure 48.	TSS calibration at Ocean Inlet – 12/7/2007 storm	60
Figure 49.	TSS calibration at Ocean Inlet – 2/3/2008 storm	60
Figure 50.	Modeled vs. observed sand fraction at Ocean Inlet – 11/30/2007 storm.....	61
Figure 51.	Modeled vs. observed sand fraction at Ocean Inlet – 12/7/2007 storm.....	61
Figure 52.	Modeled vs. observed sand fraction at Ocean Inlet – 2/3/2008 storm	62
Figure 53.	Modeled vs. observed silt fraction at Ocean Inlet – 11/30/2007 storm.....	62
Figure 54.	Modeled vs. observed silt fraction at Ocean Inlet – 12/7/2007 storm.....	63
Figure 55.	Modeled vs. observed silt fraction at Ocean Inlet – 2/3/2008 storm.....	63
Figure 56.	Modeled vs. observed clay fraction at Ocean Inlet – 11/30/2007 storm	64
Figure 57.	Modeled vs. observed clay fraction at Ocean Inlet – 12/7/2007 storm	64
Figure 58.	Modeled vs. observed clay fraction at Ocean Inlet – 2/3/2008 storm	65
Figure 59.	TSS calibration at Lagoon Segment – entire calibration period.....	65
Figure 60.	TSS calibration at Lagoon Segment – 11/30/2007 storm.....	66
Figure 61.	TSS calibration at Lagoon Segment – 12/7/2007 storm.....	66
Figure 62.	TSS calibration at Lagoon Segment – 2/3/2008 storm.....	67
Figure 63.	Modeled vs. observed sand fraction at Lagoon Segment – 11/30/2007 storm.....	67
Figure 64.	Modeled vs. observed sand fraction at Lagoon Segment – 12/7/2007 storm.....	68
Figure 65.	Modeled vs. observed sand fraction at Lagoon Segment – 2/3/2008 storm.....	68
Figure 66.	Modeled vs. observed silt fraction at Lagoon Segment – 11/30/2007 storm	69
Figure 67.	Modeled vs. observed silt fraction at Lagoon Segment – 12/7/2007 storm	69
Figure 68.	Modeled vs. observed silt fraction at Lagoon Segment – 2/3/2008 storm	70
Figure 69.	Modeled vs. observed clay fraction at Lagoon Segment – 11/30/2007 storm	70
Figure 70.	Modeled vs. observed clay fraction at Lagoon Segment – 12/7/2007 storm	71
Figure 71.	Modeled vs. observed clay fraction at Lagoon Segment – 2/3/2008 storm	71

Introduction

The Los Peñasquitos watershed and lagoon are located in central San Diego County (Figure 1). Both the watershed and lagoon are included in the Los Peñasquitos Hydrologic Unit (906), which also includes Mission Bay and several coastal tributaries¹. The lagoon was included in the Clean Water Act's (CWA) Section 303(d) list for sediment/siltation and is the primary focus of this study. Increasing urban development has altered hydrology within the watershed and modified the geomorphic conditions of the three main tributaries that feed into the lagoon. These conditions have resulted in sedimentation in the lagoon-watershed interface and within lagoon channels (City of San Diego, 2009).

Tetra Tech (Tt) is supporting the City of San Diego and stakeholders by developing and calibrating models to support ongoing sediment TMDL development efforts for Los Peñasquitos Lagoon. Water quality simulation models are needed to link potential sources of sediment loading to lagoon impacts for TMDL development and analysis of management scenarios. The linked watershed and lagoon models were developed based on models that were previously configured for the U.S. Environmental Protection Agency (EPA) and the Regional Water Quality Control Board. These models were refined with additional calibration and validation based on monitoring data that were recently collected by the watershed stakeholders.

This report describes the approach that was used to develop and refine the Los Peñasquitos watershed and lagoon models. Model calibration/validation results are also presented and discussed. The watershed model used information on watershed soils, land use, topography, and stream networks to simulate the hydrology and sediment input to the lagoon. The lagoon model incorporates watershed inputs and oceanic forcings (tidal flooding) to mimic the circulation and sediment transport within the lagoon. This modeling framework will eventually be used to simulate existing (baseline) conditions within the watershed and lagoon, calculate the numeric TMDL target, identify required sediment load reductions, and evaluate possible management actions.

¹ http://www.projectcleanwater.org/html/ws_penasquitos.html

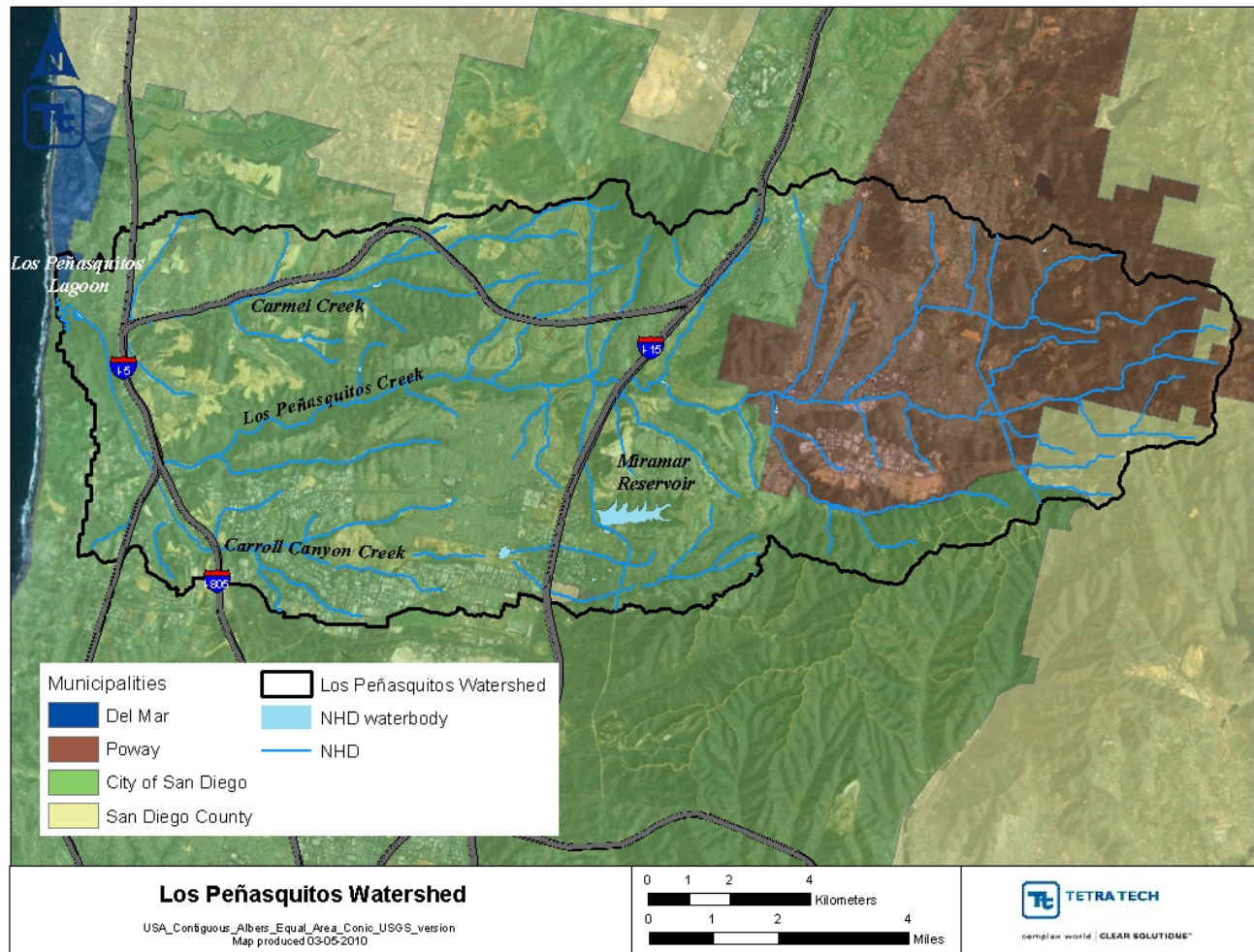


Figure 1. Location of the Los Peñasquitos watershed and lagoon

Watershed Description

The Los Peñasquitos Lagoon watershed is a 93 mi² coastal watershed located in central San Diego County. The watershed includes portions of the cities of San Diego, Poway, and Del Mar. In addition, a small portion of San Diego County is located in the eastern headwaters area. Three major streams drain the watershed and flow into the tidal lagoon. Los Peñasquitos Creek is the largest catchment in the watershed draining 59 mi² through its central portion. Carroll Canyon Creek is the second largest catchment (18 mi²) and drains the southern portion of the watershed. Carmel Creek is located along the northern, coastal area and drains the remaining 16 mi². Los Peñasquitos Creek and Carroll Canyon Creek confluence together prior to entering the lagoon. There is one major dam in the Carroll Canyon Creek watershed, which drains approximately 1 mi² and forms Miramar Reservoir. Key watershed characteristics, including land use, soils, and other features that are important for model representation are described in later sections.

Lagoon Description

The Los Peñasquitos Lagoon is a relatively small salt marsh lagoon (0.6 mi²) that is part of the Torrey Pines State Reserve. Given the status of “Natural Preserve” by the California State Parks, the lagoon is one of the few remaining native salt marsh lagoons in California and provides a home to several endangered species. The lagoon is ecologically diverse, supporting a variety of plant species, and providing habitat for numerous bird, fish, and small mammal populations. The lagoon also serves as a stopover for migratory birds and provides habitat for coastal marine and salt marsh species.

The lagoon is listed as impaired on the CWA’s Section 303(d) list due to sediment/siltation impacts that originate from watershed sediment contributions. Tidal flows enter the lagoon during periods when the lagoon mouth is open to the ocean. Currently, the lagoon mouth is open throughout most of the year. Mouth closures are typically caused by coastal processes (deposition of sand and cobble from nearshore sources) and structures, such as the Highway 101 abutments. Mechanical dredging is used when needed to eliminate blockages and allow for tidal flow into the lagoon in order to improve water quality conditions and support salt marsh species. Most of the freshwater input flows through Los Peñasquitos Canyon into the lagoon. Carroll Canyon Creek to the south and Carmel Creek to the north also contribute freshwater to the lagoon. Historically, Los Peñasquitos Creek was the only tributary that flowed year-round, while Carroll Canyon and Carmel Creeks only flowed during significant rainfall events. Beginning in the 1980’s, these drainages also began flowing year-round due to increasing urban development within the watershed. Carroll Canyon Creek confluences with Los Peñasquitos Creek upstream and the combined stream channel extends into the lagoon along the western side of the railroad track berm. This berm acts as a barrier between the eastern and western portions of the lagoon for much of its length. The railroad trestle along the northern side provides the only connection between eastern and western portions of the lagoon. The lagoon channel that receives flow from Carmel Creek crosses through this area.

The regional climate is characterized by higher precipitation during winter months and lower precipitation (and corresponding high lagoon salinity) during the dry summer months (Williams, 1997). Storm events transport sediment into the lagoon which deposits on the salt flats and within lagoon channels. These sediment deposits have gradually built-up over the years due to increased sediment loading and inadequate flushing, which directly and indirectly affects lagoon functions and salt marsh characteristics.

Data Inventory and Analysis

Multiple data sources were used to characterize the watershed and lagoon, in particular flow and water quality conditions. Much of this information was recently collected by the watershed stakeholders to assist with model development. Data describing the watershed’s topography, land use, and soil characteristics were compiled and used to develop the watershed model. Stream flows and total suspended sediment concentrations were used to calibrate both the lagoon and watershed model components. The lagoon was also characterized using available bathymetric survey information, data sondes analyzing pressure and salinity, and sediment grab samples.

Land Use

Land use information was used in the model to characterize watershed imperviousness and the amount of sediment that washes off land surfaces, depending on land use type. Data detailing land use in the Los Peñasquitos watershed was based on the San Diego Association of Governments 2000 land use coverage² (Figure 2). The largest single land use type in the Los Peñasquitos watershed is open space. Approximately 54 percent of

² http://www.sandag.org/resources/maps_and_gis/gis_downloads/downloads/zip/Land/CurrentLand/lu.zip

the watershed has been developed, with 46 percent of that area classified as impervious. The area and percent distribution of land uses within the watershed is presented in Table 1.

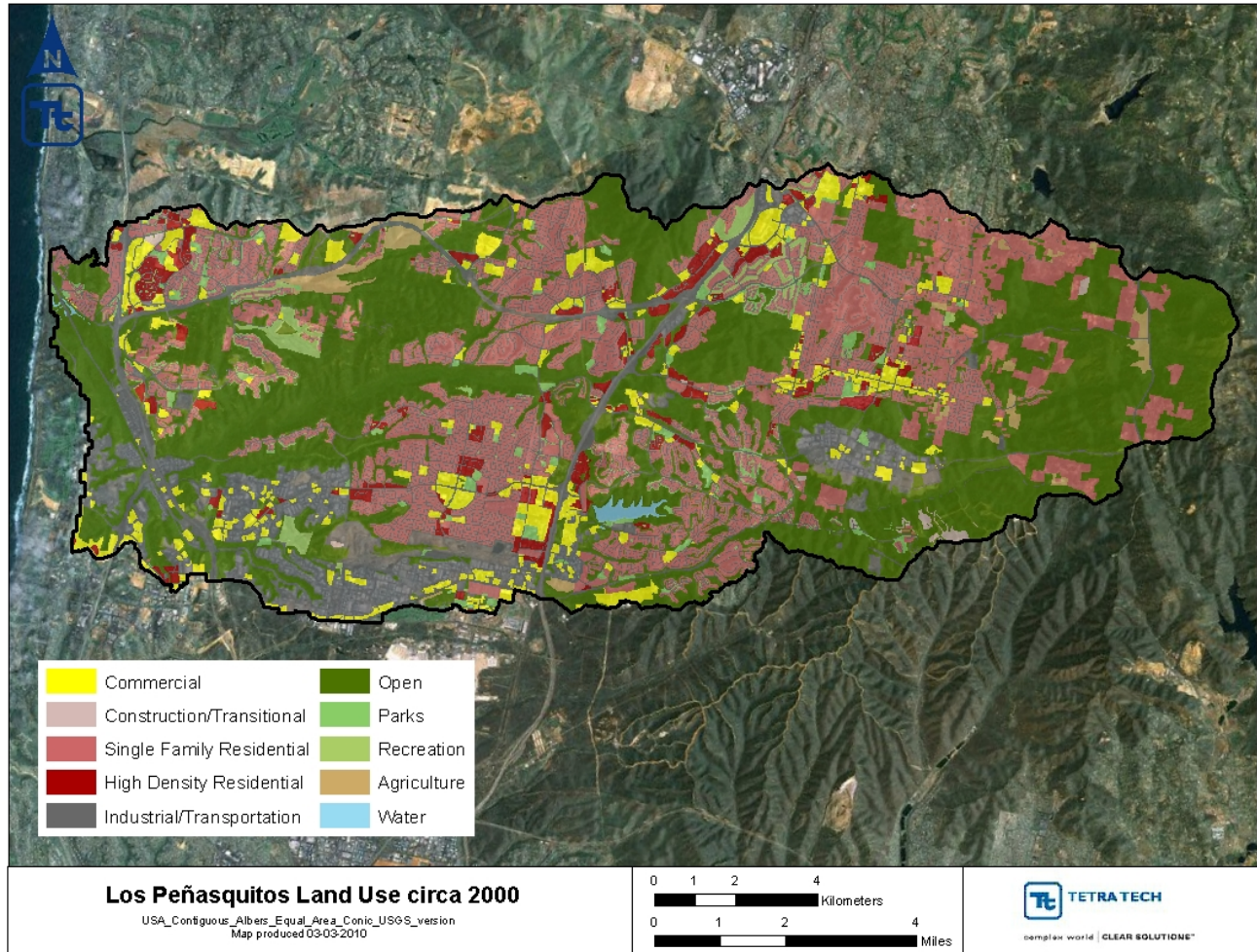


Figure 2. Land use distribution in the Los Peñasquitos watershed



Table 1. Area and percent land use distribution

Land Use Group	Land Use area (acres)	Percent Total
Agriculture	741	1.2%
Commercial Institutional	3,596	6.0%
High Density Residential	1,855	3.1%
Industrial/Transportation	11,658	19.5%
Low Density Residential	14,254	23.8%
Open	25,497	42.6%
Open Recreational	713	1.2%
Parks Recreational	1,335	2.2%
Transitional	171	0.3%

Topography

Topographical information was primarily used to describe the slope of the main tributaries within the watershed. Ten meter elevation data were obtained from the San Diego Association of Governments³. Elevation within the watershed rises from sea level to 2,600 ft in the headwaters (Figure 3).

³ http://www.sandag.org/resources/maps_and_gis/gis_downloads/downloads/zip/elev10grd.zip

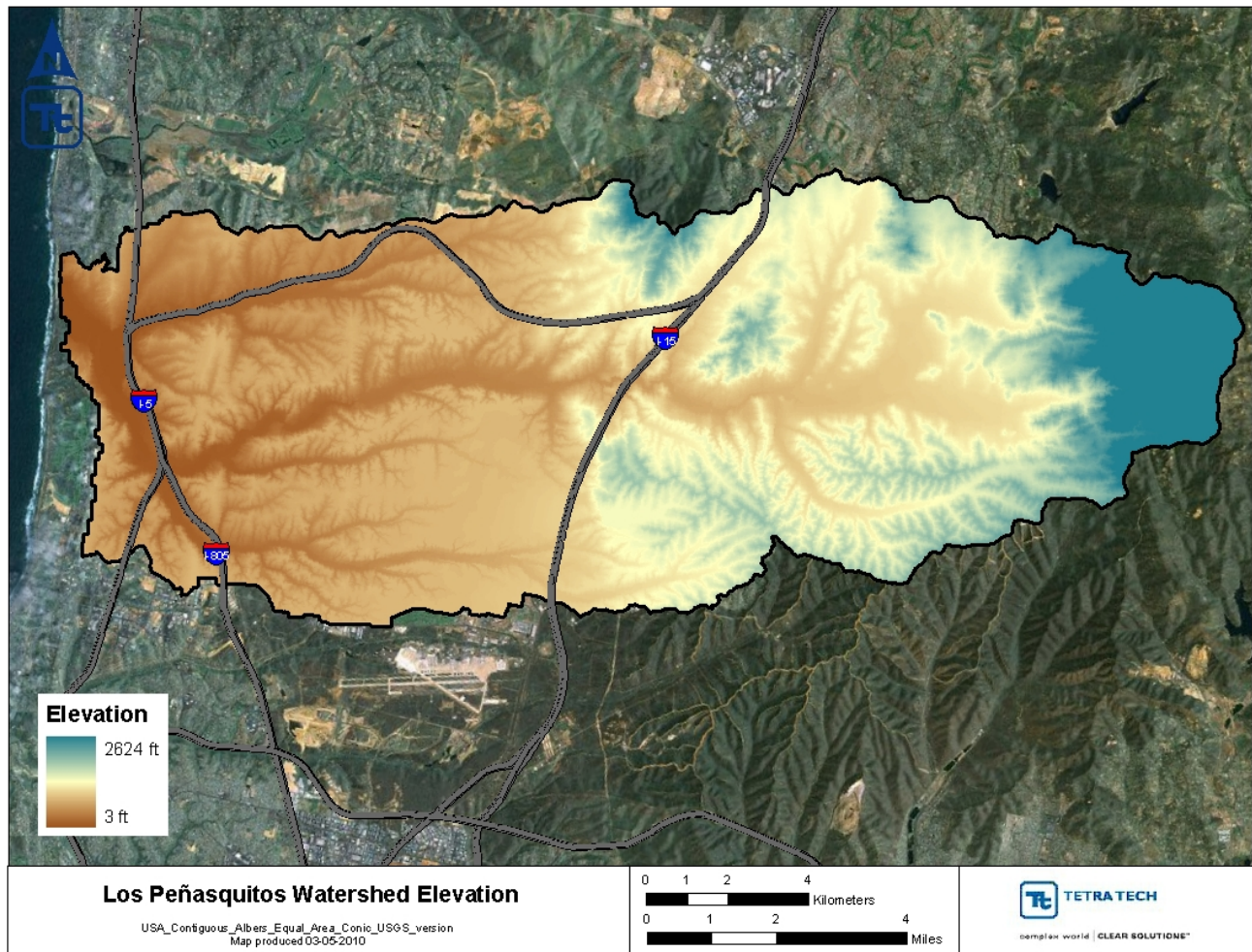


Figure 3. Topography in the Los Peñasquitos watershed

Soil Characteristics

Soils data for the Los Peñasquitos watershed were used to group watershed catchments based on differing infiltration rates. The Soil Survey Geographic (SSURGO) Database⁴ was used to characterize the soils. The majority of the watershed is located within hydrologic soil group D, which is indicative of a low infiltration rate and a high potential for surface runoff (Figure 4). As a result, Group D soils are more susceptible to erosion and can contribute significant sediment loads.

Soil erodibility values (K factor) were obtained from the SSURGO database and used in conjunction with slope information to calculate the coefficient in the soil detachment equation (KRER) for each land use/hydrologic soil group combination. The proportion of sand, silt and clay within each hydrologic soil group (particle size distribution) was also extracted from the SSURGO database. Soils that are more easily transported typically have higher proportions of smaller particles sizes (silt and clay fractions), as compared to local parent soils, because of differences in settling rates and other sediment transport characteristics. To account for these differences, soils

⁴<http://soils.usda.gov/survey/geography/ssurgo/>. National Resources Conservation Service. Accessed September 2008

transported by surface runoff were assumed to be composed of 5 percent sand, twice as much clay as the percentage of clay within each hydrologic soil group, and the remainder assigned to the silt fraction (Table 2).

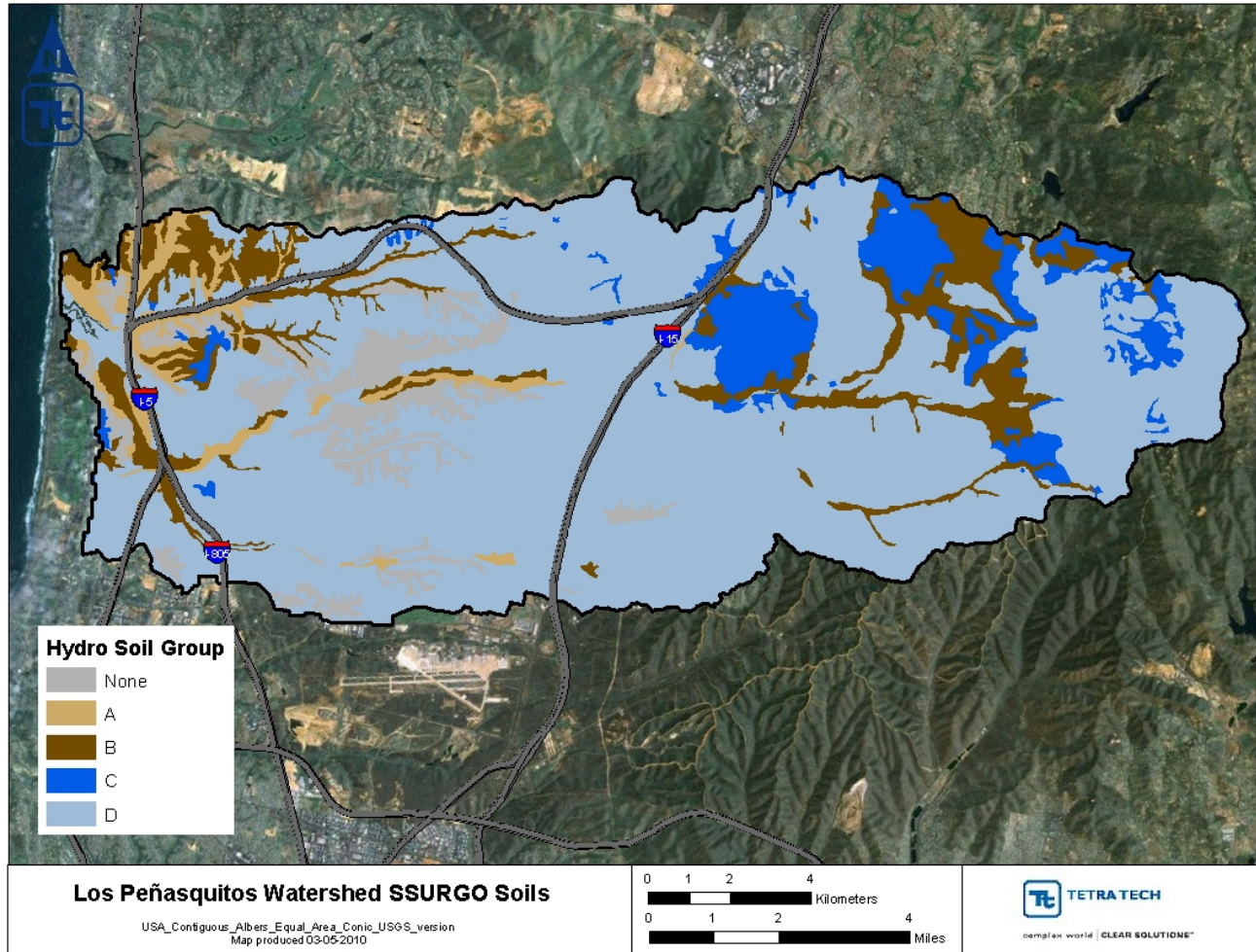


Figure 4. Hydrologic soil groups in the Los Peñasquitos watershed

Table 2. Sand, silt, and clay distribution by hydrologic soil group

	Hydrologic Soils Group		
	B	C	D
SSURGO Soil Fractionation			
SAND	60 %	26 %	14 %
SILT	67 %	19 %	14 %
CLAY	47 %	32 %	21 %
Surface Soil Runoff Fractionation			
SAND	5 %	5 %	5 %
SILT	67 %	67 %	54 %
CLAY	28 %	28 %	41 %

Meteorological Data

Surface runoff and associated pollutant transport is dependent on the water balance, including precipitation inputs and evapotranspiration outputs. Meteorological data describing rainfall and potential evapotranspiration (PET) were compiled to describe the hydrologic cycle of the watershed. Precipitation data were obtained from two local Alert weather stations: 24 and 22 (available from the San Diego County Flood Control District) (Figure 5). Rainfall from Alert station 24 was used to represent the upper portion of the watershed and Alert station 22 the lower portion. Data collected at these stations were available from 1/1/1990 through 6/30/2008 (Table 3). Additional rainfall data were collected by the City of San Diego (2009) at three flow monitoring stations between 9/13/2007 and 6/16/2008.

The PET time series was developed from nearby California Irrigation Management Information System (CIMIS) stations⁵ (Figure 5). CIMIS station 74 was primarily used to assign hourly PET values to each weather station. For days when the station did not record PET, a secondary station (CIMIS 62) was used to patch the missing dates (Table 4). CIMIS station 62 is located 30 miles to the northwest of the watershed in Temecula. A ratio of the average annual PET over the simulation period was used to scale the secondary PET values, as needed.

⁵ <http://www.cimis.water.ca.gov/cimis/welcome.jsp>

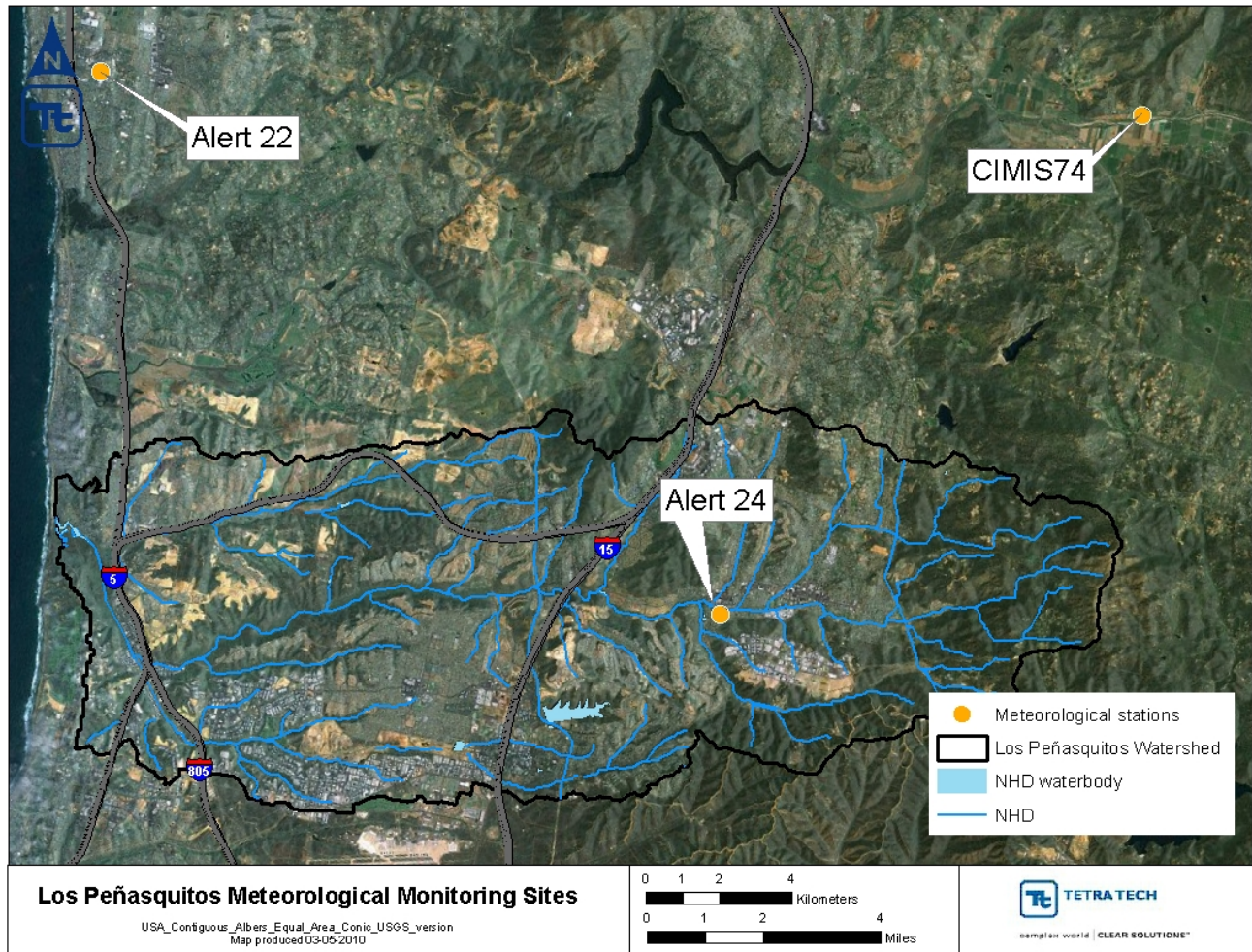


Figure 5. Meteorological stations within and near the Los Peñasquitos watershed

Table 3. Hourly rainfall gages

Station Name	Elevation (ft)	Data Collection Period		Precipitation (in/yr)
		Start	End	
Alert 24	446	1/1/1990	6/30/2008	8.14
Alert 22	250	1/1/1990	6/30/2008	6.96



Table 4. Potential evapotranspiration (PET) stations

Station Name	Elevation (ft)	Data Collection Period		Percent Missing
		Start	End	
CIMIS 74	450	1/1/1990	12/20/1998	48%
CIMIS 62	1420	1/1/1990	6/30/2008	3%

Streamflow Data

Available streamflow data collected within the watershed were compiled for model calibration and validation. The United States Geological Survey (USGS) maintains a long term flow gage (11023340) in the upper Los Peñasquitos watershed (Figure 6). Daily data from 1990 through 2008 were downloaded for calibration of model hydrologic parameters⁶. Total suspended solids (TSS) data were also collected at this location and a downstream USGS sediment monitoring station (325423117124501). Sediment monitoring data are described in the following section.

⁶ http://waterdata.usgs.gov/nwis/dv/?site_no=11023340&referred_module=sw

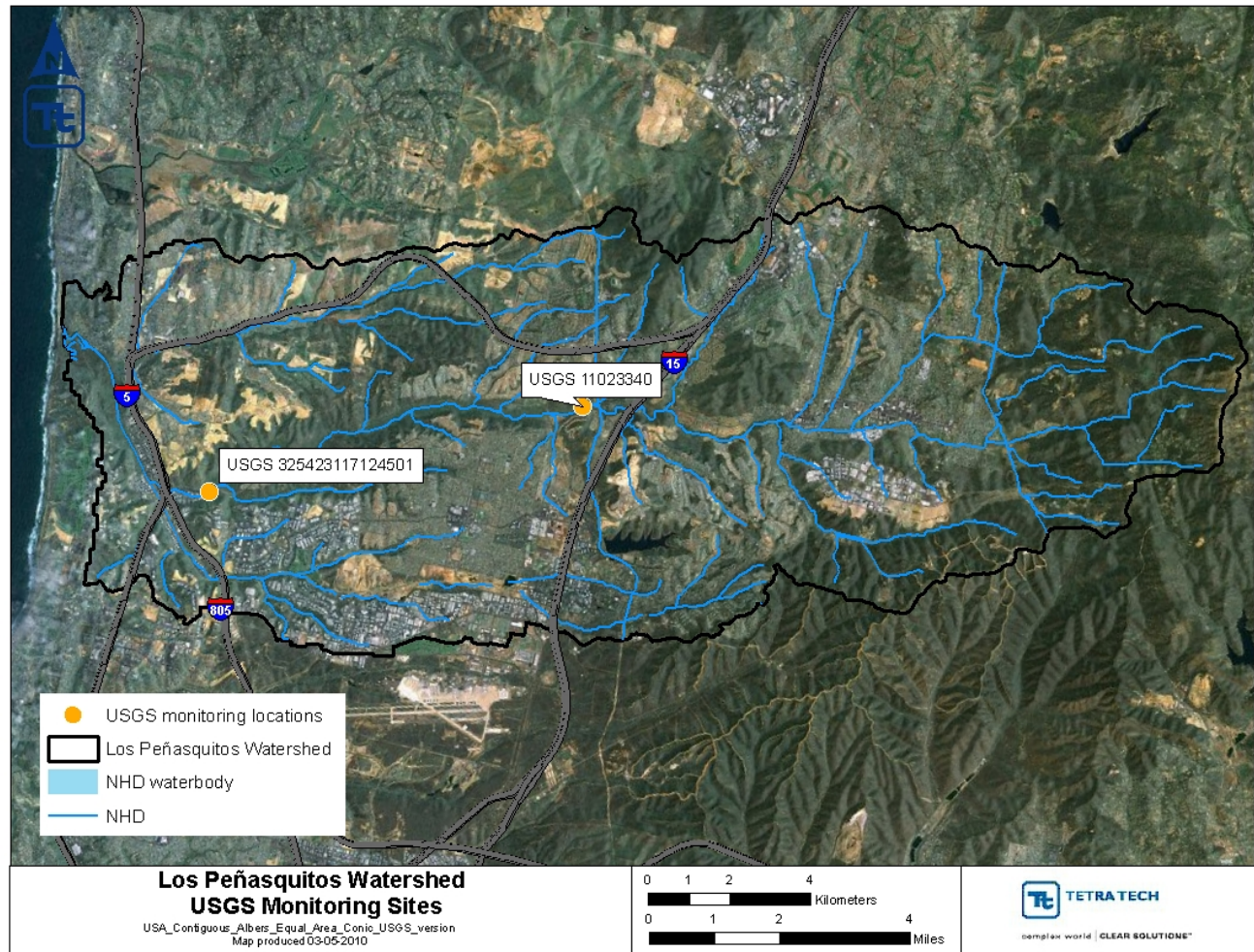


Figure 6. USGS monitoring locations in the Los Peñasquitos watershed

Additional streamflow data were collected at the base of Los Peñasquitos, Carroll Canyon, and Carmel Creeks as part of the Los Peñasquitos TMDL monitoring study (City of San Diego, 2009) (Figure 7). The Los Peñasquitos TMDL monitoring station was co-located with the long term Los Peñasquitos Creek Mass Loading Station (MLS) that undergoes routine water quality monitoring. Note that two additional monitoring stations within the watershed (LPC-TWAS-1 and LPC-TWAS-2) are shown in Figure 7 and are described in the following section. Flows were determined by applying the Manning’s Equation to data collected with Sigma 950 or 920 flow meters with area velocity meters and pressure transducers. Sampling frequency ranged from 5 to 15 minute intervals. Instruments were deployed on 9/13/2007 and retrieved on 6/16/2008.

Los Peñasquitos Creek drains the largest area within the watershed and, accordingly, recorded the highest measured flows and runoff volume (Figure 8). Median flows in Los Peñasquitos Creek were roughly twice those in Carmel Creek and two orders of magnitude greater than in Carroll Canyon Creek. A continual increase in cumulative volume for Los Peñasquitos Creek and Carmel Creek indicated consistent baseflows. By contrast, streamflow data collected on Carroll Canyon Creek included periods with little change in cumulative volume, which indicates low baseflow. Low flows at this station were within the tenth percentile (Figure 8).

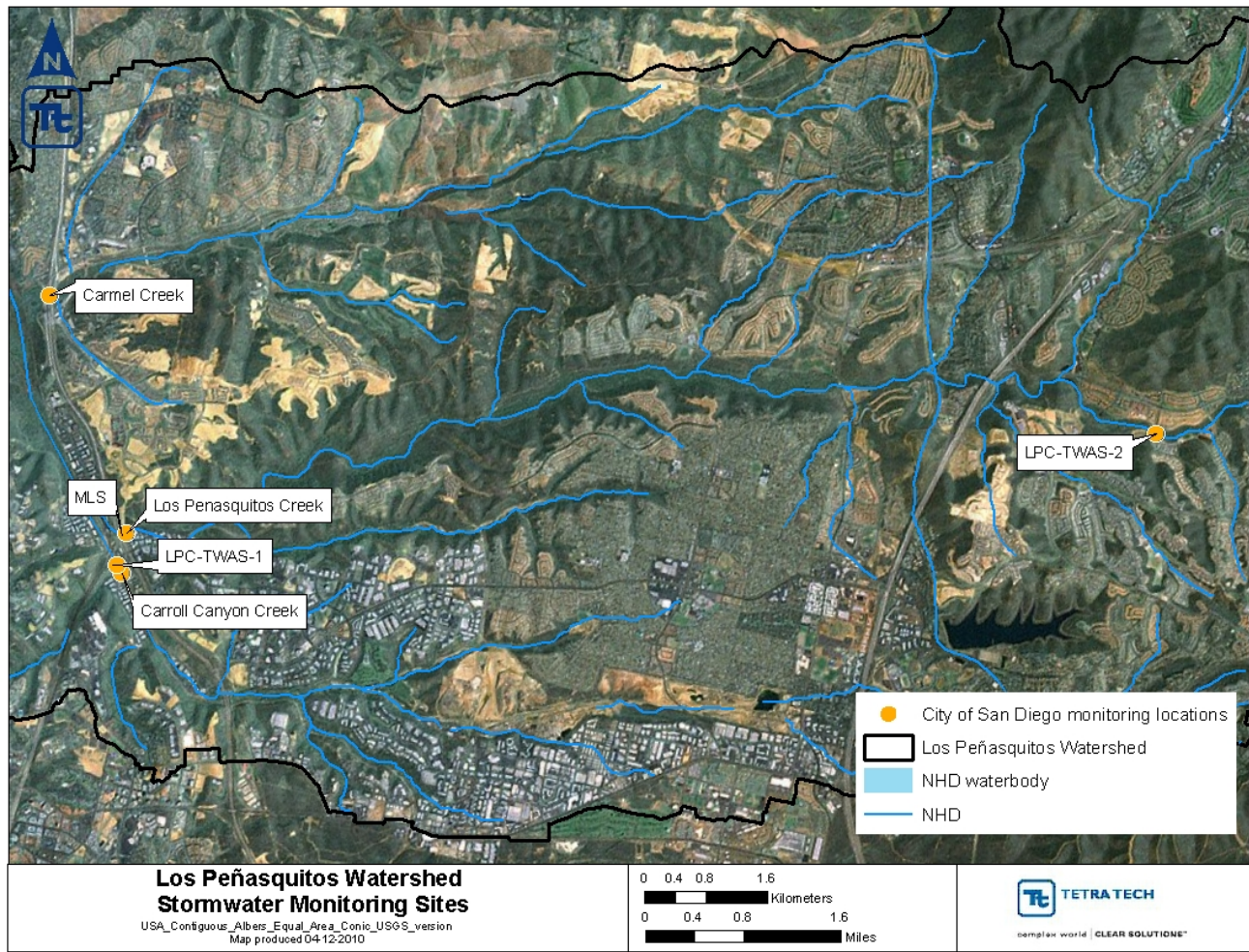


Figure 7. Stormwater monitoring locations in the Los Peñasquitos watershed

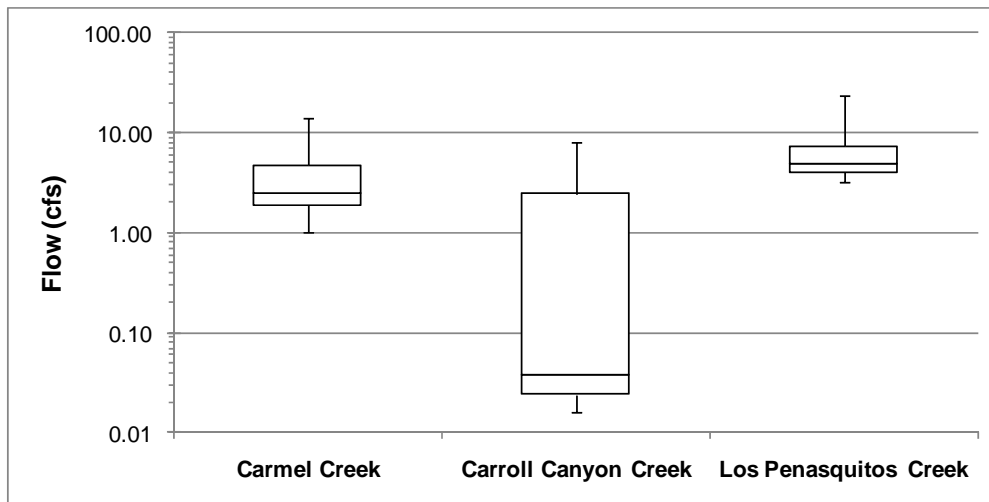


Figure 8. Measured flows at TMDL monitoring locations

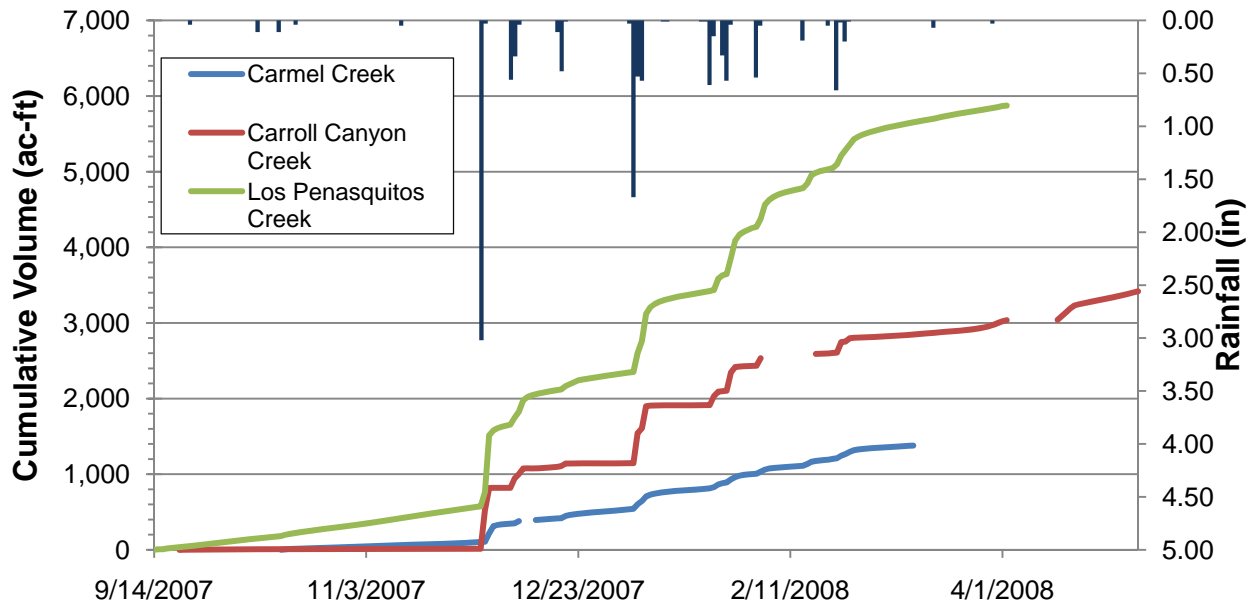


Figure 9. Cumulative volumes at TMDL monitoring locations

Measuring streamflow in the Los Peñasquitos watershed presents difficulties that are common to urban, arid watersheds. The Los Peñasquitos and Carmel Creek monitoring locations were both natural channels with heavy vegetation. During monitoring, cross section measurements were taken at each station at regular intervals with flows estimated using Manning’s equation. The Carmel Creek location had ponded conditions due to a flow control structure located downstream of the box culvert. The Carroll Canyon Creek monitoring location is a concrete lined trapezoidal channel. Median depths in Los Peñasquitos, Carmel, and Carroll Canyon Creeks were 7.0, 4.8, and 0.95 inches, respectively. Because of shallow water depths, variability in natural channel cross sections, and water not distributed uniformly across the concrete channel in Carroll Canyon Creek, flows are difficult to accurately monitor over a long period (Figures 10 and 11). Also, small differences in depths or depth homogeneity across the channel can result in large differences in flows at the lower end of the station rating tables.



Figure 10. Photos near the Carroll Canyon Creek monitoring station



Figure 11. Photo at the Los Peñasquitos Creek monitoring station

Comparison of the flow record at the Los Peñasquitos Creek MLS and the USGS gaging station upstream (11023340) shows a distinct difference in recorded flows. There was small difference in average daily flow throughout the common period of record (9/13/2007 – 3/31/2008) (Figure 12). However, when cumulative volumes are compared (Figure 13), the total volume measured at the USGS station (8,000 ac-ft) is greater than the volume measured downstream at the MLS (5,870 ac-ft). An estimate of the water volume that would need to be infiltrated by the creek over the 200 days of record, assuming an average creek width of 8 ft, results in an infiltration rate of 0.6 in/hr. This estimated infiltration rate is higher than expected and may indicate an error in the rating table at the MLS station, especially at higher flows. It is difficult to develop a rating table at the MLS, or any of the monitoring locations, during storm flows because of the high velocities in the creek and safety concerns for monitoring staff. Possible data limitations were considered during model development and calibration.

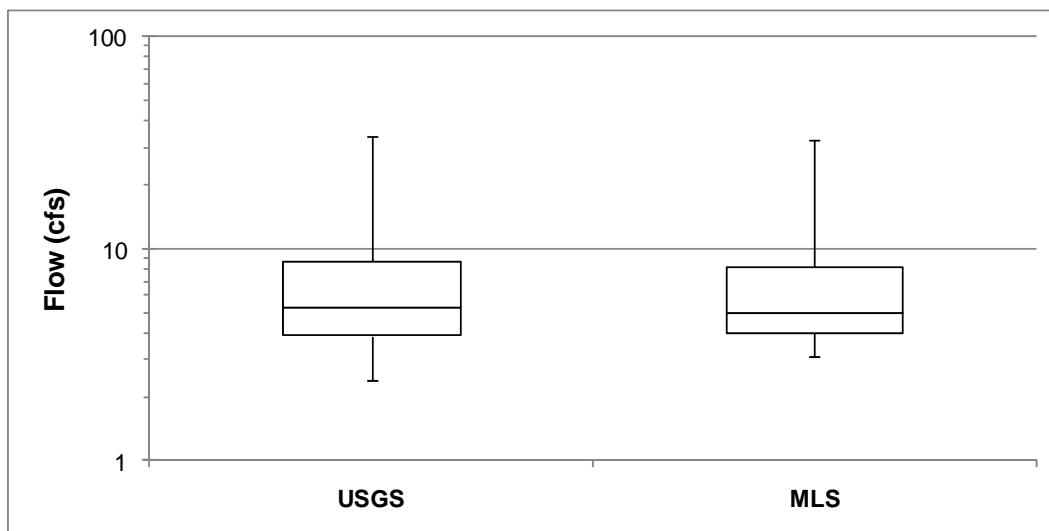


Figure 12. Comparison of flows at the MLS and USGS gaging station (11023340)

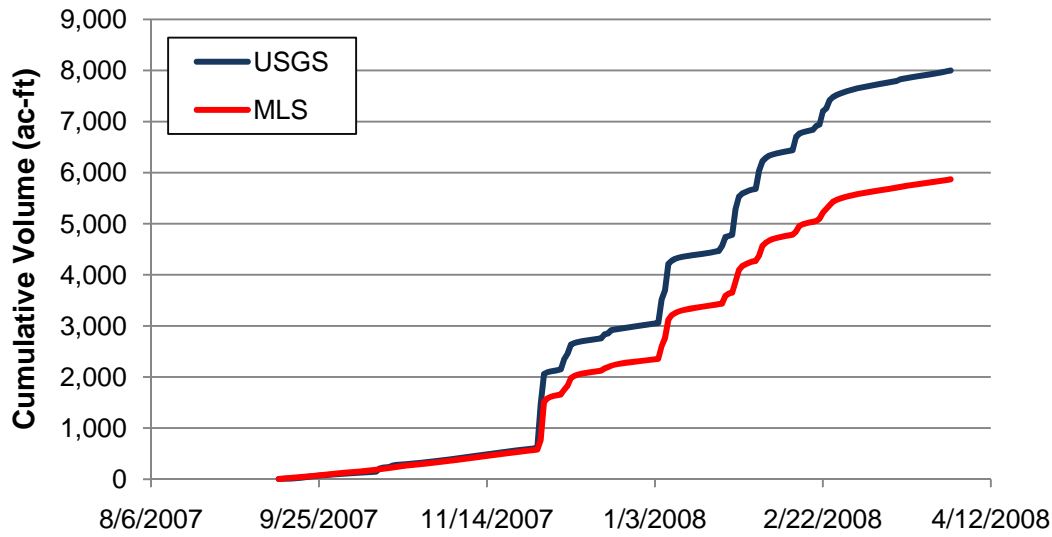


Figure 13. Comparison of cumulative volumes at the MLS and USGS gaging stations

Suspended Sediment Data

Suspended sediment and particle size data were collected at several locations within the Los Peñasquitos watershed and used to develop and calibrate the watershed model. Total suspended sediment (TSS) data were collected in the watershed by three different agencies. The USGS collected 19 samples at gage 11023340 between 11/12/1985 and 10/25/1986 and five samples at gage 325423117124501 from 1/20/1982 to 3/18/1982 (USGS, 2009) (Table 5). Event mean concentrations (EMCs) from stormwater and dry weather runoff were collected at the MLS on Los Peñasquitos Creek near the confluence with Carroll Canyon Creek. Stormwater and dry weather runoff events were also monitored at this station since 2001, in accordance with NPDES permit requirements. In addition, two Temporary Watershed Assessment Stations (TWAS) are located within the watershed on Los Peñasquitos Creek upstream (TWAS-2) and on Carroll Canyon Creek (TWAS-1). These stations were monitored on 11/30/2007 and 2/3/2008 (Figure 7 above; Table 6). The relationship between rainfall and flow at the MLS is shown in Figure 14. Collectively, these data were used to better understand the relationship between flow and sediment loading for model development purposes.



Table 5. TSS measurements at USGS stations on Los Peñasquitos Creek

USGS 11023340			USGS 325423117124501		
Date Time	Flow (cfs)	TSS Concentration (mg/L)	Date Time	Flow (cfs)	TSS Concentration (mg/L)
11/12/1985 10:00	70	362	1/20/1982 15:15	4.87	222
11/12/1985 10:30	70	365	1/21/1982 10:20	7.9	1060
11/12/1985 15:15	93	321	3/15/1982 8:40	4.33	1070
11/12/1985 16:00	100	321	3/17/1982 11:05	6.71	366
11/25/1985 13:00	460	1640	3/18/1982 16:50	10.9	245
11/25/1985 13:45	432	1400			
11/26/1985 13:00	32	252			
11/30/1985 10:30	162	605			
12/3/1985 12:30	180	570			
1/30/1986 14:40	39	120			
2/8/1986 10:15	136	436			
2/8/1986 14:00	209	334			
2/15/1986 14:30	639	1390			
2/16/1986 9:15	146	201			
3/10/1986 12:15	130	437			
3/10/1986 13:15	93	432			
3/16/1986 8:15	375	800			
9/25/1986 12:45	75	172			
10/25/1986 12:45	75	172			



Table 6. Rainfall and TSS measurements at the MLS and TWAS stations on Los Peñasquitos Creek

Date	Station	Rain (in)	TSS (mg/L)
11/29/01	MLS	0.10	<20
2/17/02	MLS	0.14	<20
3/17/02	MLS	0.35	<20
11/8/02	MLS	0.11	35
12/16/02	MLS	0.33	58
2/11/03	MLS	0.43	38
11/12/03	MLS	0.28	27
2/3/04	MLS	0.20	<20
2/18/04	MLS	0.12	<20
10/17/04	MLS	0.16	<20
2/11/05	MLS	0.52	<20
2/18/05	MLS	0.28	108
10/17/05	MLS	0.16	20
2/20/06	MLS	0.16	30
2/28/06	MLS	0.28	182
12/10/06	MLS	0.08	22
1/30/07	MLS	0.20	<20
2/19/07	MLS	1.10	81
11/30/07	MLS	3.03	130
11/30/07	TWAS-1	3.03	260
11/30/07	TWAS-2	3.03	113
2/3/08	MLS	0.59	26
2/3/08	TWAS-1	0.59	40
2/3/08	TWAS-2	0.59	200

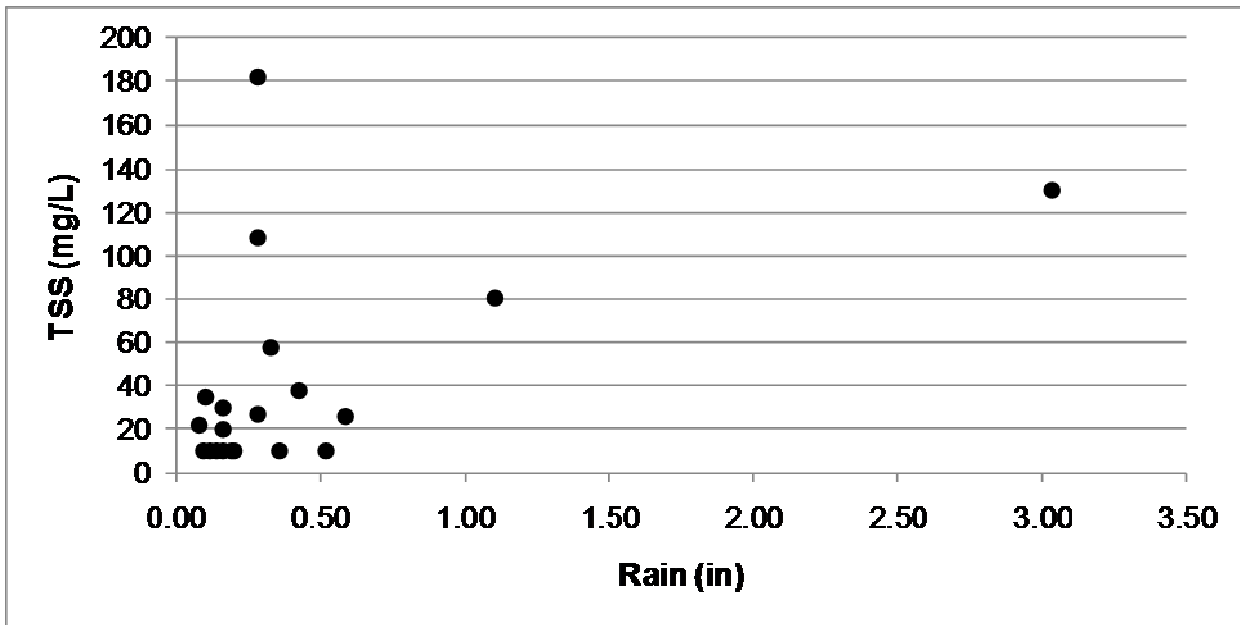


Figure 14. Relationship between rainfall and TSS measured at the MLS

Pollutograph samples characterizing suspended sediment concentration changes throughout a storm were collected during three storms in the 2007-2008 storm season as part of the TMDL monitoring study. Samples were collected from the three major streams flowing into the lagoon: Los Peñasquitos, Carroll Canyon, and Carmel Creeks (see Figure 7). The Los Peñasquitos Creek location was co-located with the MLS, which had EMC monitoring data. Pollutograph samples consist of multiple individual samples collected throughout a storm which are individually analyzed. Typically, EMCs are calculated for each monitored storm using the following equation:

$$EMC = \frac{\sum V_i * C_i}{\sum V}$$

where V is volume and C is concentration. Pollutograph samples are superior to volume- or time-weighted sampling because multiple samples provide insight into how concentrations change throughout a monitored event. The 95th percent confidence interval ($1.96 * \text{standard error of the mean}$) was calculated for each pollutograph sampling event and was used to compare to the median concentrations of the other sampling efforts.

$$CI = 1.96 \sqrt{\frac{\sum [(c_i - \bar{c})v_i]^2}{(\sum v_i)^2}}$$

Pollutograph TSS concentrations recorded during each storm event at the Los Peñasquitos, Carroll Canyon, and Carmel Creek TMDL stations are shown in Table 7 through 9.



Table 7. Pollutograph measurements of TSS (mg/L) at Carmel Creek

11/30/07 Storm		12/7/07 Storm		2/3/08 Storm	
Date Time	TSS	Date Time	TSS	Date Time	TSS
11/30/07 9:40	91	12/7/07 4:40	34	2/3/08 7:01	123.9
11/30/07 10:40	180	12/7/07 5:40	11	2/3/08 7:48	0.7*
11/30/07 11:40	56	12/7/07 6:40	8.5	2/3/08 8:18	4.3*
11/30/07 11:40	56	12/7/07 8:06	15.5	2/3/08 8:48	16
11/30/07 14:40	83	12/7/07 8:36	15.5	2/3/08 9:18	30
11/30/07 15:40	38	12/7/07 9:06	12	2/3/08 10:01	44
11/30/07 20:40	15	12/7/07 9:06	11.1	2/3/08 10:18	9.5
11/30/07 23:40	32	12/7/07 10:06	11	2/3/08 11:48	7.3
12/1/07 1:40	19.5	12/7/07 10:06	12.3	2/3/08 12:01	33.3
12/1/07 3:20	14	12/7/07 11:06	12.3	2/3/08 12:40	8.7
12/1/07 4:40	16	12/7/07 11:36	16	2/3/08 12:40	10
		12/7/07 13:06	14	2/3/08 13:01	32
		12/7/07 15:40	13	2/3/08 13:01	30.7
		12/7/07 21:02	38.3	2/3/08 13:40	10.7
				2/3/08 15:01	31.3
				2/3/08 15:10	14
				2/3/08 16:40	7
				2/3/08 17:01	62
				2/3/08 18:40	3.7*
				2/3/08 18:40	3.7*
				2/3/08 19:01	28.7
				2/3/08 20:10	4.7*
				2/3/08 21:15	15.3
				2/4/08 1:15	40
				2/4/08 1:15	2.7*
				2/4/08 5:15	21.3
				2/4/08 11:15	32
				2/4/08 15:15	24.7

* Less than reporting limit (RL)



Table 8. Pollutograph measurements of TSS (mg/L) at Carroll Canyon Creek

11/30/07 Storm		12/7/07 Storm		2/3/08 Storm	
Date Time	TSS	DateTime	TSS	DateTime	TSS
11/30/07 12:35	488	12/7/07 5:30	222	2/3/08 7:10	ND
11/30/07 13:36	340	12/7/07 7:10	130	2/3/08 7:10	1*
11/30/07 14:35	716	12/7/07 8:10	237	2/3/08 8:35	30.3
11/30/07 14:35	716	12/7/07 8:40	558	2/3/08 9:05	7.7
11/30/07 15:35	596	12/7/07 9:10	476	2/3/08 10:14	30
11/30/07 16:44	396	12/7/07 9:40	404	2/3/08 11:21	148
11/30/07 17:40	144	12/7/07 10:10	380	2/3/08 12:13	221
11/30/07 18:35	116	12/7/07 10:40	312	2/3/08 13:07	241
11/30/07 20:30	60	12/7/07 11:10	206	2/3/08 14:07	178
11/30/07 21:30	568	12/7/07 11:40	224	2/3/08 15:07	117.5
11/30/07 22:40	760	12/7/07 12:40	66	2/3/08 16:07	100
		12/7/07 15:31	29	2/3/08 17:07	106
				2/3/08 17:07	96
				2/3/08 21:37	31

* Less than reporting limit (RL)



Table 9. Pollutograph measurements of TSS (mg/L) at Los Peñasquitos Creek

11/30/07 Storm		12/7/07 Storm		2/3/08 Storm	
Date Time	TSS	Date Time	TSS	Date Time	TSS
11/30/07 11:14	53	12/7/07 7:52	3.7*	2/3/08 8:13	2*
11/30/07 14:14	35	12/7/07 11:52	5.3	2/3/08 8:13	3.3*
11/30/07 18:14	140	12/7/07 13:22	13.7	2/3/08 10:13	1.5*
11/30/07 18:14	134	12/7/07 15:01	22.3	2/3/08 12:13	ND
11/30/07 19:14	170	12/7/07 16:01	26.3	2/3/08 14:13	1*
11/30/07 21:14	68	12/7/07 17:01	23.3	2/3/08 16:13	6.7
11/30/07 22:14	60	12/7/07 18:01	17	2/3/08 17:13	12.7
12/1/07 1:14	40	12/7/07 19:01	15.7	2/3/08 19:13	17.3
12/1/07 4:14	23.3	12/7/07 22:01	5.7	2/3/08 21:13	12.7
12/1/07 6:14	78	12/8/07 1:01	4.3*	2/3/08 22:27	12.65
12/1/07 10:14	30	12/8/07 3:01	3.7*	2/4/08 0:27	7.3
		12/8/07 8:01	2.7*	2/4/08 6:27	3*
				2/4/08 6:27	1*
				2/4/08 12:16	4*

* Less than reporting limit (RL)

TSS data collected through all sampling efforts within the Los Peñasquitos watershed were compared (Figure 15). TSS concentrations recorded at the MLS on Los Peñasquitos Creek since 2001 were more than five times lower than the data collected by the USGS at both stations. There were no significant difference in TSS between the two USGS stations/sampling periods. A small difference in the TSS EMC was observed between TWAS-2 and the MLS during the first sampled storm (11/30/2007), which was a storm of 3.03 in. The second monitored storm was only 0.59 in, where TWAS-2 recorded TSS concentrations nearly an order of magnitude higher than the MLS.

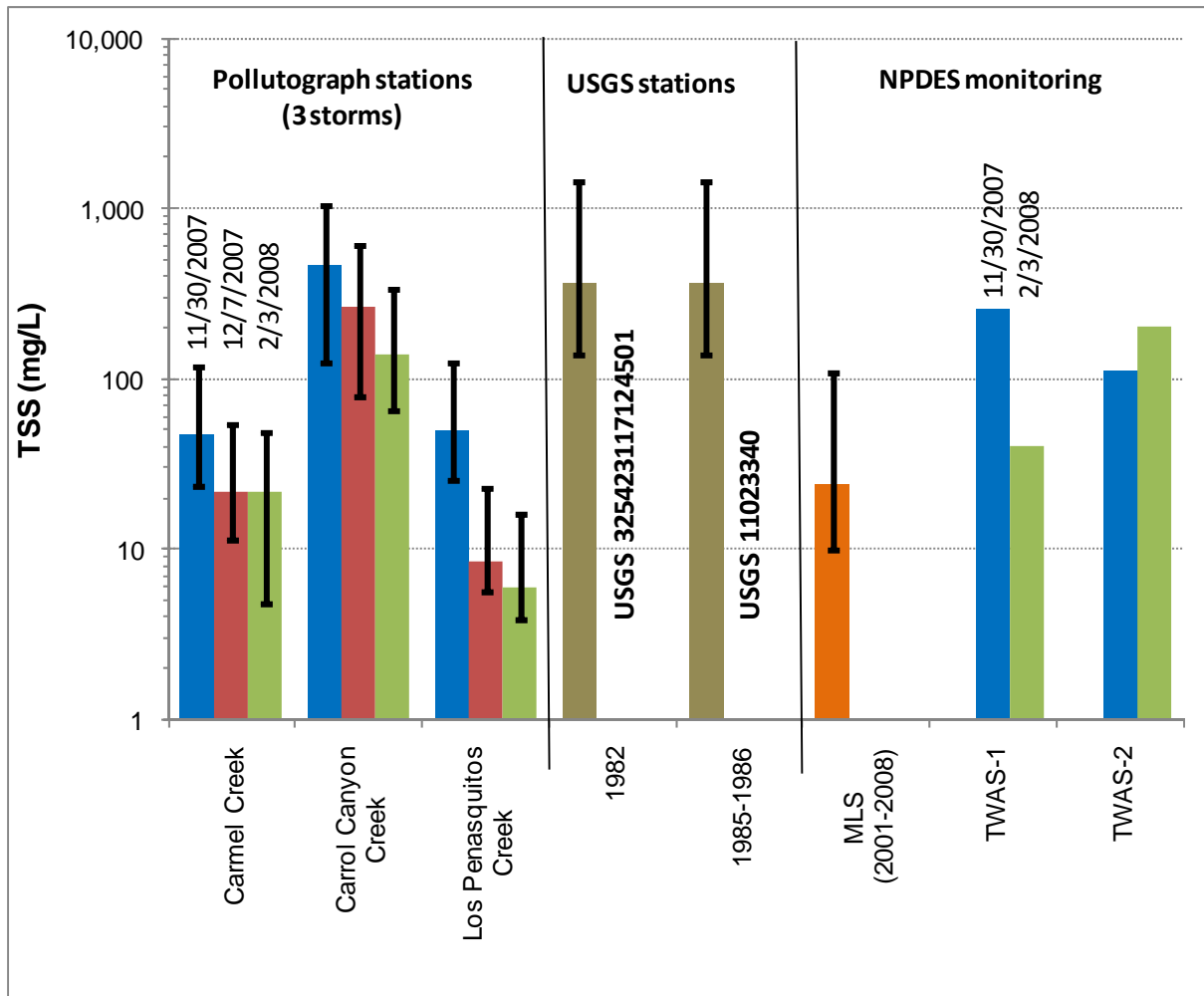


Figure 15. EMC/Median TSS and 95th percentile confidence intervals for all sampling events

Los Peñasquitos Creek was sampled using flow weighting and pollutograph sampling methods for two storms. These data showed considerable variability between the two sampling methods (Table 10). TSS EMCs were two to four times greater using the flow weighted sampling, as compared to the pollutograph sampling. The two stations were co-located and samples were collected using the same methods. Figure 11 shows this monitoring location had considerable vegetation within the creek, which may have caused significant differences in suspended particles considering depth and distance.

Table 10. TSS (mg/L) EMCs for the pollutograph and MLS stations on Los Peñasquitos Creek

	12/7/2007 Storm	2/3/2008 Storm
MLS	130	26
Pollutograph station	49.65	6.04

TSS particle size distribution was measured at the three pollutograph monitoring sites for two storms. A single composite sample was used to characterize the particle size distribution for each event. Samples were packed on ice, sent to the sample processing laboratory and analyzed with a Coulter Counter LS200. Samples from the first storm (11/30/2007) were shipped to the laboratory on 12/5/2007 and samples from the second storm (12/7/2007) were shipped on 12/11/2007. Particle size distributions for the pollutograph monitoring locations are shown in

Figure 16 and 17. Note that the particle size distributions likely do not characterize the finer particles well because they likely flocculated in the days between sampling and analysis. Li et al (2005) have shown that particles tend to flocculate together within six hours, which can affect the particle size distribution.

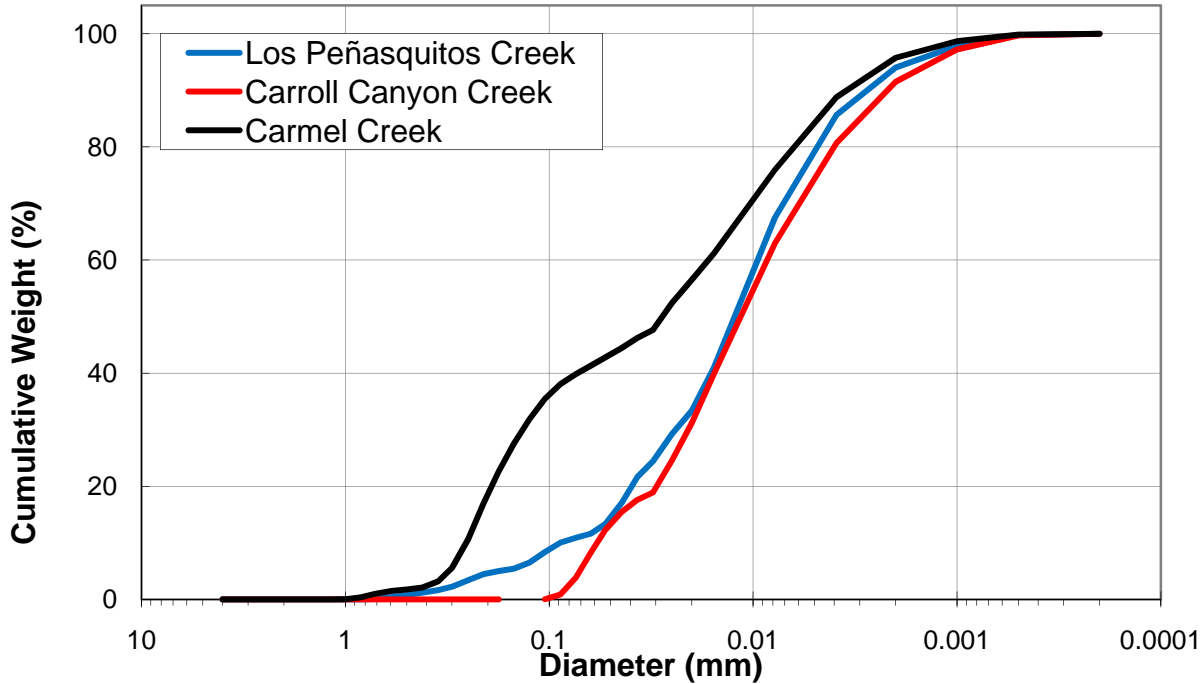


Figure 16. Particle size distribution for the 11/30/2007 storm event

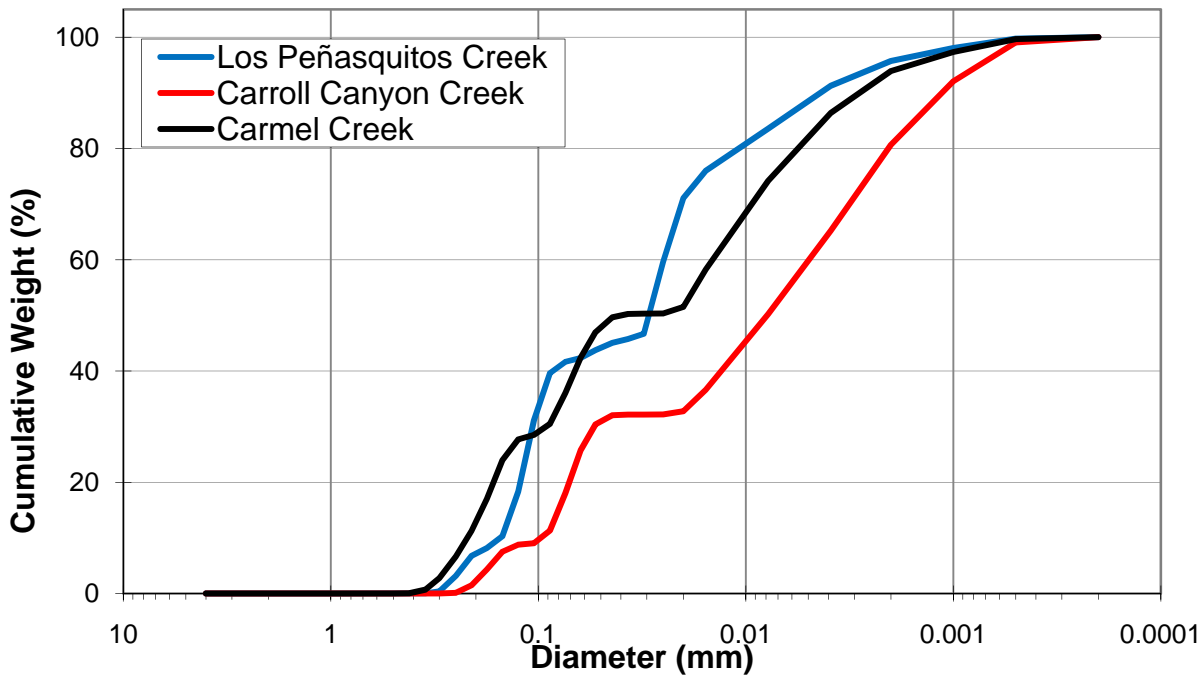


Figure 17. Particle size distribution for the 12/7/2007 storm event

Overview of Modeling Approach

The Los Peñasquitos watershed was modeled using the Loading Simulation Program in C++ (LSPC) model. The watershed model primarily uses information that details soil characteristics, land use distribution, topography, weather data, and the stream network to simulate hydrology and sediment contributions to the lagoon. Key data sources were compiled to support development of the watershed model (as described in previous sections). The Los Peñasquitos lagoon was modeled using the Environmental Fluid Dynamics Code (EFDC) model. The EFDC model incorporates meteorological data, watershed inputs, and oceanic forcings (tidal flooding). The watershed model is linked to the lagoon model through input of the LSPC results directly into the EFDC model for simulation of hydrodynamic and water quality conditions within the lagoon. Watershed model output was used to define the terrestrial inputs to the lagoon (flow and pollutant loads). Hourly watershed model flow and TSS concentrations (fractionated as sand, silt, and clay) were output for catchments 1401-1404 and 1411 and included as inputs to the EFDC lagoon model.

Watershed Model Description

LSPC (Shen et al., 2004; Tetra Tech and USEPA, 2002; USEPA, 2003) is a watershed modeling system that includes streamlined Hydrologic Simulation Program Fortran (HSPF) (Bicknell et al., 1997) algorithms for simulating hydrology, sediment, and general water quality on land, as well as a simplified stream fate and transport model. Since its original public release, the LSPC model has been expanded to include additional GQUAL components for sorption/desorption of selected water quality constituents with sediment, enhanced temperature simulation, and the HSPF RQUAL module for simulating dissolved oxygen, nutrients, and algae. LSPC has also been customized to address simulation of other pollutants such as nutrients and fecal coliform bacteria.

The hydrologic (water budget) process is complex and interconnected within LSPC (Figure 18). Rain falls and lands on various constructed landscapes, vegetation, and bare soil areas within a watershed. Varying soil types allow the water to infiltrate at different rates while evaporation and plant matter exert a demand on this rainfall. Water flows overland and through the soil matrix. There may also be point source discharge and water withdrawals/intakes. The land representation in the LSPC model environment considers three flowpaths; surface, interflow, and groundwater outflow.

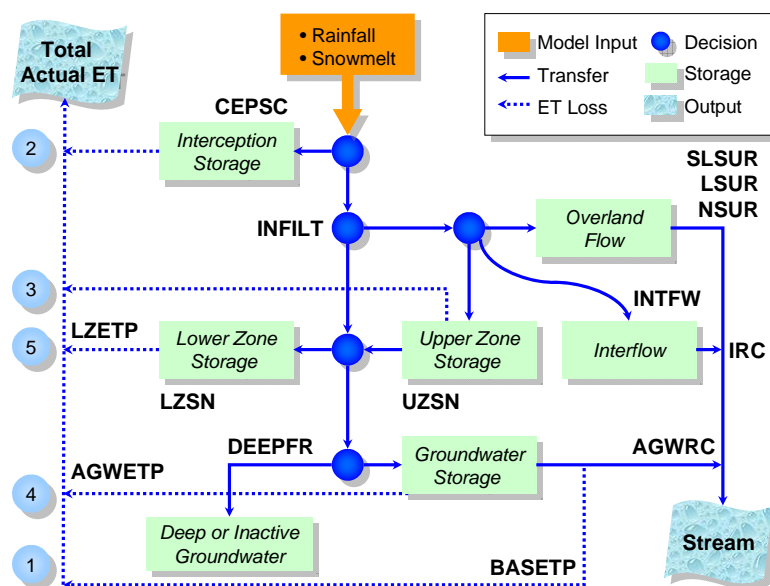


Figure 18. Schematic of LSPC Hydrology Components

The sediment routine in LSPC represents the general detachment of sediment due to rainfall, overland and in-stream transport, attachment when there is no rainfall, and scour. Land disturbance may occur from construction or agricultural practices, disturbing native vegetative cover and leaving the soil susceptible to erosion. With the native cover disturbed, a rainfall event may not only cause detachment, but can also provide sufficient rainfall in combination with the lack of vegetative cover to cause scour and further erosion as the overland flow proceeds to a defined channel. From impervious areas, a different process occurs where sediment builds up over time to a maximum value for each impervious land use type. For both pervious and impervious land uses, the amount of sediment that can be transported is a function of runoff. Sediment carried by runoff is fractionated into sand, silt, and clay portions depending on the underlying soil types. Once the sediment is in the stream channel, it is transported downstream where it can flow through the reach or settle out. If the stream velocity is sufficient, additional sediment can be mobilized via high shear stresses.

Watershed Model Setup

The Los Peñasquitos watershed model was developed to provide continuous sediment input to the EFDC lagoon model. Many data sources were used to develop the LSPC model of the Los Peñasquitos watershed. Smaller catchments within the watershed were delineated using available elevation data. Information about the soils and land use within each of those catchments was used to develop model parameters describing flow and sediment transport characteristics within the watershed.

Catchment Delineation

The Los Peñasquitos watershed was divided into smaller catchments for modeling efficiency based on 10 meter resolution digital elevation model (DEM) and hydrography. Catchment sizes ranged from 0.43 to 16.56 mi² with a median size of 7.19 mi² (Figure 19). The size of the catchments was determined to be adequate based on the accuracy needed for model predictions and linkage to the lagoon model. Delineation was based on several factors including, land use and soil information, stream channel characteristics, and the location of monitoring stations throughout the watershed for calibration purposes. Catchment 1404 receives flow from both Los Peñasquitos and Carroll Canyon Creeks. The lagoon is represented by Catchment 1402 and receives flow from Catchments 1401 (small direct drainage to the north), 1403 (Carmel Creek), and 1404 (Los Peñasquitos and Carroll Canyon Creeks).

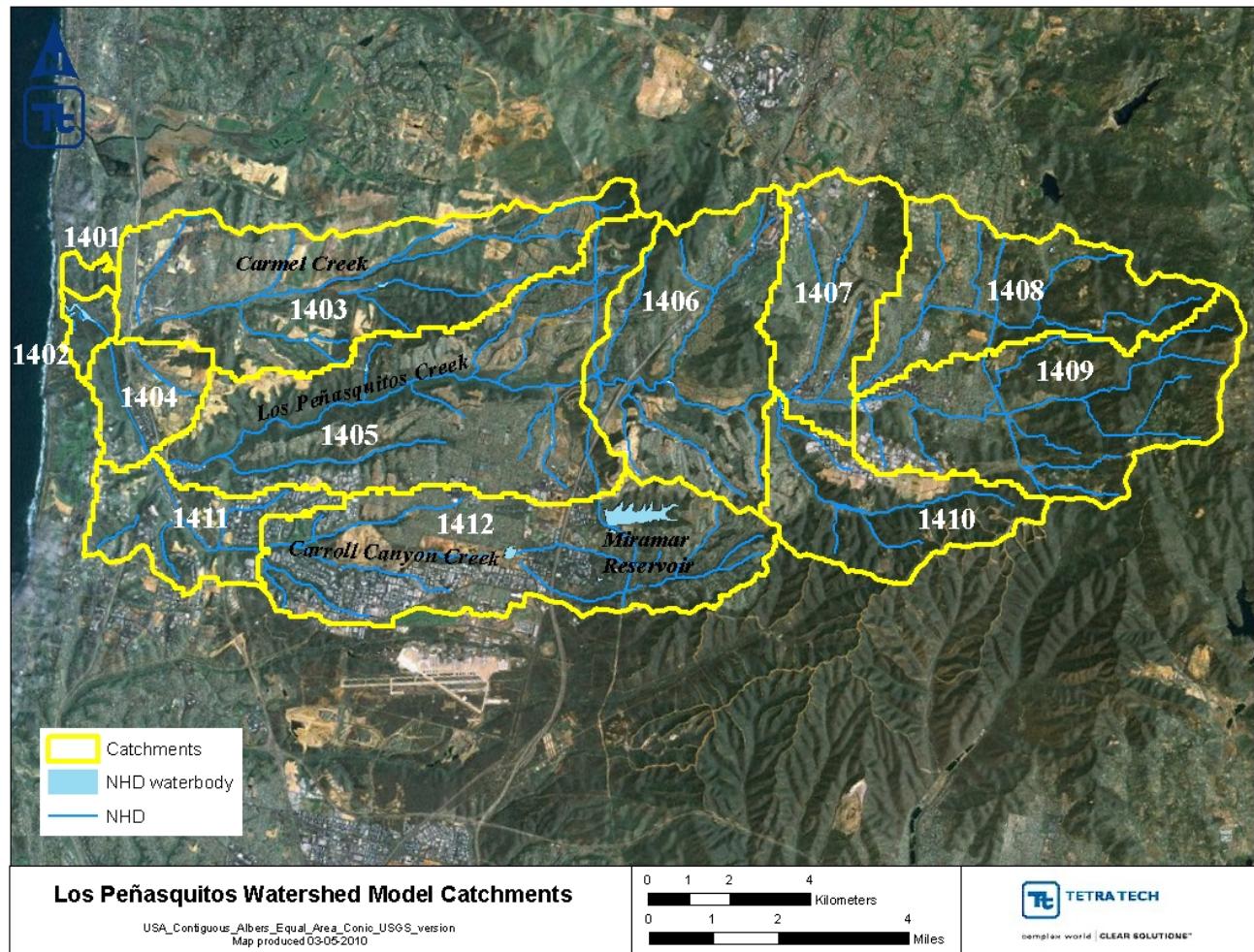


Figure 19. Catchment delineation in the Los Peñasquitos watershed

Streams

Each delineated catchment is represented with a single stream segment, as depicted in the National Hydrography Dataset (NHD), and assumed to be a completely mixed, one-dimensional segment with a trapezoidal cross-section. Once the representative reaches were identified, slopes were calculated based on elevation data (10 m DEM) and stream lengths measured from the original NHD stream coverage. In addition to stream slope and length, mean depths and channel widths are required to route flow and pollutants. Detailed cross section information did not exist for the watershed, therefore, mean stream depth and channel width were estimated using regression curves that relate upstream drainage area to stream dimensions available in the LSPC model setup spreadsheet that is described in the LSPC manual (Tetra Tech and USEPA, 2002). Manning’s n values ranging from 0.03 to 0.2 reflected very different stream types, including streams with concrete channels to heavily vegetated channels.

Land Use

LSPC algorithms require land use in each catchment to be divided into pervious and impervious categories. The overall watershed land use distribution is shown above in Table 1. The estimated impervious fraction for each land use type was calculated by multiplying the total area by an impervious factor (Table 11).

Table 11. Impervious fraction by land use type

Land Use	Percent Impervious
Agriculture	0 %
Commercial Institutional	85 %
High Density Residential	65 %
Industrial/Transportation	72 %
Low Density Residential	15 %
Open	0 %
Open Recreational	0 %
Parks Recreational	12 %
Transitional	0 %

Soils

Soil characteristics within each catchment were calculated using SSURGO data, as described previously. The average soils class within each catchment was calculated. The majority of the catchments were within hydrologic soil group D areas, which typically have high surface runoff rates and low infiltration.

Irrigation

Irrigation is an important component of the water balance in Southern California. Through changes in soil moisture storages, irrigation can affect storm runoff, as well as baseflow conditions.

The irrigation demand for the Los Peñasquitos watershed model was calculated based on information presented in “A Guide to Estimating Irrigation Water Needs of Landscape Plantings in California” (University of California Cooperative Extension, 2000). This guide recommends comparing daily precipitation to water demand to determine the amount of irrigation water.

The estimated hourly PET was based on data collected at the nearby California irrigation measurement station, CIMIS 74 (Figure 5). Hourly values were summed over each day to determine the daily PET depth in inches. To convert PET depth to the water demand for a specific crop or vegetation type, a crop-specific coefficient is multiplied by the PET. The University of California Cooperative Extension (2000) suggests a crop coefficient of 0.6 for lawns planted with warm season grasses and 0.65 for agricultural citrus production. For the purposes of this analysis, a crop coefficient of 0.8 was used to estimate the daily water demand for residential and commercial lawns and 0.85 for agricultural areas.

The difference between daily water demand and daily precipitation was calculated for each day. If precipitation exceeded water demand, then the irrigation demand was set to zero. Precipitation was used to offset water demand from the following days until all of the precipitation was lost from the system. To estimate the amount of irrigation water applied, the University of California Cooperative Extension (2000) suggests dividing the irrigation demand by the efficiency of the irrigation system. An efficiency factor of 80 percent was used for both



the lawn and agricultural irrigation systems in order to estimate the depth of irrigation water applied. Finally, the irrigation water applied was added to the water balance in the LSPC simulation. The daily amount applied was assumed distributed evenly over time. The LSPC model also uses demand-based irrigation values based on the PET time series.

Sediment Fractionation

SSURGO data were used to estimate the fraction of total sediment contributed from the land within each particle size class and hydrologic soil group (Table 12). Adjustments were made to account for deposition during runoff periods based on the assumption that 50 percent of the sand fraction and 30 percent of silt is deposited using watershed delivery ratios presented in Vanoni, 1975. The resulting particle size fractions used for modeling are shown in Table 13

Table 12. Sediment fractions by hydrologic soil group

Hydrologic Soils Group	Sand	Silt	Clay
B	65 %	23 %	12 %
C	68 %	19 %	14 %
D	54 %	21 %	24 %

Table 13. Sediment fractions adjusted for watershed delivery

Hydrologic Soils Group	Sand	Silt	Clay
B	33 %	16 %	51 %
C	34 %	13 %	53 %
D	27 %	15 %	58 %

Configuration of Key Model Components

The initial basis for model parameterization was derived from “Hydrology: San Diego Region TMDL Model” (CARWQCB and USEPA, 2005). Final model hydrologic parameters are provided in Appendix A. Model calibration and validation focused on accurate characterization of precipitation in the watershed. Precipitation data from Alert gages 22 and 24 provided long term rainfall records for the lower watershed. Two catchments in the upper watershed (1408 and 1409) had increased rainfall due to higher elevation which was greater than observed at the Alert gage. Proportionally scaling the rainfall data using median rainfall from the CIMIS 74 gage and Alert 24 provided a better representation of rainfall in those catchments. Little adjustment of model parameters from the regional calibration was required once good rainfall records were established.

Sediment calibration focused on maintaining sediment balance in the streams. Sediment land use model parameters were developed following BASINS Technical Note 8 (USEPA, 2006) and Ackerman and Weisberg (2006). Sediment shear stress thresholds for deposition and scour were adjusted independently for each reach to maintain a dynamic steady state bed for silt and clay during a decadal simulation. Sand in the reaches was simulated using the average velocity power function in the reach, again, maintaining a dynamic balance throughout the decadal simulation. Several parameters were adjusted during calibration to achieve reasonable

loading rates by land use type and to improve model fit to observed data collected in the Los Peñasquitos watershed.

Lagoon Model Description

The Los Peñasquitos Lagoon was simulated using the EFDC model. EFDC is a public domain, general purpose modeling package for simulating one-dimensional (1-D), two-dimensional (2-D), and three-dimensional (3-D) flow, sediment transport, and biogeochemical processes in surface water systems including rivers, lakes, estuaries, reservoirs, wetlands, and coastal regions. The EFDC model was originally developed at the Virginia Institute of Marine Science for estuarine and coastal applications. This model is now being supported by the USEPA and has been used extensively to support TMDL development throughout the United States. In addition to hydrodynamic, salinity, and temperature transport simulation capabilities, EFDC is capable of simulating cohesive and noncohesive sediment transport, near-field and far-field discharge dilution from multiple sources, eutrophication processes, the transport and fate of toxic contaminants in the water and sediment phases, and the transport and fate of various life stages of finfish and shellfish. The EFDC model has been extensively tested, documented, and applied to environmental studies worldwide by universities, governmental agencies, and other entities.

The EFDC model includes four primary modules: (1) a hydrodynamic model, (2) a water quality model, (3) a sediment transport model, and (4) a toxics model. The hydrodynamic model predicts water depth, velocities, and water temperature. The water quality portion of the model uses the results from the hydrodynamic model to compute the transport of the water quality variables. The water quality model then computes the fate of up to 22 water quality parameters including dissolved oxygen, phytoplankton (three groups), benthic algae, various components of carbon, nitrogen, phosphorus and silica cycles, and fecal coliform bacteria (Cercio and Cole 1994). The sediment transport and toxics modules use the hydrodynamic model results to calculate the settling of suspended sediment and toxics, resuspension of bottom sediments and toxics, and bed load movement of noncohesive sediments and associated toxics. For this project, the hydrodynamics and sediment transport models were used. The hydrodynamics model simulated the circulation, water temperature, and salinity in the lagoon driven by ocean tides and watershed inflows. The sediment transport model simulated the transport of sand, silt as non-cohesive sediments, and clay as cohesive sediment. Details of the EFDC model's hydrodynamic and eutrophication components are provided in Hamrick (1992) and Tetra Tech (2002, 2006a, 2006b, 2006c, 2006d).

The EFDC model was configured to simulate hydrodynamics and sediment transport in the Los Peñasquitos Lagoon. Specifically, water temperature and salinity were both modeled for hydrodynamics. Sediment fractions considered in the model include sand, silt, and clay. Sand and silt were modeled using the non-cohesive sediment module and clay was modeled using the cohesive sediment module in EFDC.

Lagoon Model Setup

Various data sources were used to develop the EFDC model for the Los Peñasquitos Lagoon. Model development requires defining the computation domain and boundary conditions. The general steps to set up the EFDC model for the Los Peñasquitos Lagoon included generating the modeling grid, defining meteorological conditions, estimating oceanic inputs, and linking the watershed (LSPC) model to EFDC. Key data sources were compiled to support development of the lagoon model. Model development steps and data used to identify initial conditions, boundary assignments, and calibration of key model parameters are further discussed below.



Grid Generation

The Los Peñasquitos Lagoon is composed of both deep and shallow channels and salt marsh areas. The lagoon connects with the ocean through a narrow inlet. Grid generation was primarily based on available bathymetry data, shoreline data, DEM data, and satellite imagery. The EFDC grid for the lagoon includes two portions—the lagoon itself and the ocean. During model development, hydrodynamic calibration was conducted first to ensure accurate exchange of salt and freshwater in the lagoon. A model grid was developed to include the ocean shoreline for hydrodynamic calibration. The grid including the ocean shoreline allowed for the use of tide elevation data for hydrodynamic calibration.

After the hydrodynamic calibration, a reduced grid was used to simulate sediment transport. The reduced grid set the ocean inlet, which is the location where the lagoon connects with the ocean, as the open boundary and does not include the ocean cells that were incorporated for hydrodynamic calibration. This was done because sediment, especially sand in the water column, are at relatively low levels in the ocean and sediment entering the lagoon are mainly due to beach erosion caused by various processes such as wave-breaking. Beach erosion processes cannot be modeled with the existing configuration which lacks wave, wave-breaking, and wave-current interaction components; therefore, sediment modeling used a reduced grid which sets the open ocean boundary immediately outside of the ocean inlet. The ocean part of the grid was not used for the sediment modeling. Note that for sediment modeling, the predicted tide elevations, water temperature, and salinity from the hydrodynamic calibration were assigned. In addition, bank erosion within lagoon channels was not simulated; therefore sediment erosion and resuspension are assumed to occur only with respect to the bottom sediment.

There are 374 computation cells in the full model grid, which includes the ocean cells, and 259 cells in the reduced grid that was used for modeling sediment transport. Lagoon channels near the ocean inlet are wider than upstream channels and have a finer resolution. Because of the complicated channel and salt marsh shapes, several grids were generated for each of the individual sections. The individual grids were then combined together to form one composite model grid for running EFDC. The full grid is shown in Figure 20. The grid includes the salt marsh area and two major channels. Two vertical layers were also included within the grid to better represent differences between upper and lower sections.

The channel that receives the flow and sediment loadings from Carmel Creek is called the Carmel Branch in this report. The channel that receives the flow and sediment from the merged Los Peñasquitos Creek and Carroll Canyon Creek is called the Los Peñasquitos Branch in this report. The small channels are coarsely represented together with the salt marsh area. In addition, the railroad track that bisects the lagoon was represented as a continuous berm that blocks flow and separates eastern and western portions of the lagoon, except for the railroad trestle (bridge) that crosses Carmel Branch. The model grid includes an opening at this location and allows flow through.

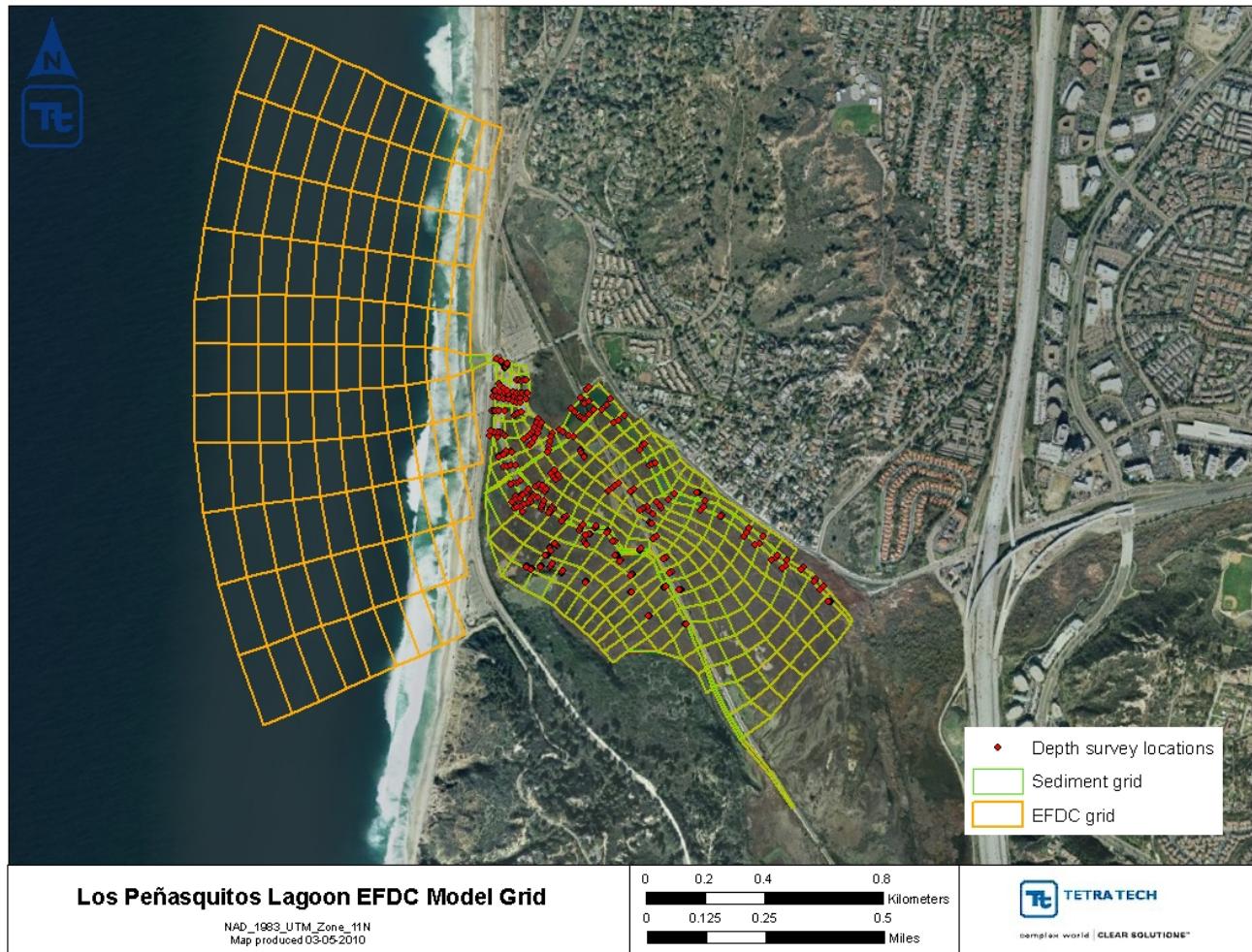


Figure 20. EFDC grid and bathymetry data for Los Peñasquitos Lagoon

As stated above, grid generation was based on available bathymetry data. A bathymetric survey of the Los Peñasquitos Lagoon was performed in March 2008 as part of the TMDL monitoring study (City of San Diego, 2009). The bathymetry for the two major channels were based on these data. These data include bottom elevations that were measured at several locations throughout the lagoon. Bottom elevation data were used to determine average grid bottom elevations. In addition, four lagoon mouth surveys were completed between October 2007 and April 2008 and were used to refine the ocean inlet. EFDC represents rectangular cross-sections; therefore, determination of grid bottom elevations cannot be assumed using average or lowest bottom elevations. Initial bottom elevations were estimated by reviewing these data and assigning the near deepest elevation values to each grid cell, where data are available. For grid cells where bottom elevations were not measured, initial bottom elevations were obtained through interpolation. Bottom elevations were refined during calibration for better hydrodynamic simulation.

For the salt marsh area, the more detailed USGS 1/9 arc second DEM data were downloaded. Average elevation within each EFDC cell was calculated using the DEM data. In addition to the DEM data, the 2006 Los Peñasquitos Lagoon Foundation monitoring report includes monitored elevation profiles in the lagoon (Hany et al, 2007). The elevations from the DEM were compared to the elevations in the report, and were adjusted slightly.

Boundary Conditions

As an open water system, conditions within the Los Peñasquitos Lagoon are continuously changing due to external forces. For example, flood tides allow for ocean water to flow into the lagoon, which increases salinity. Air temperature and solar radiation also have a strong influence on lagoon water temperature. These external forces are represented in the model using boundary conditions. In order to simulate water circulation and sediment transport using the EFDC model, boundary conditions must be specified. Boundary conditions include watershed freshwater inflows and associated sediment loading rates, the exchange of salt water and freshwater in the lagoon, and sediment carried by flood tide.

Watershed Inflow

Watershed inflows determine the amount of freshwater that is contributed to the lagoon and associated sediment loading rates. The lagoon primarily receives water from three main tributaries: Los Peñasquitos Creek, Carroll Canyon Creek, and Carmel Creek. Watershed hydrology and sediment loading were modeled using the LSPC model, as described earlier. Flow rates and sediment concentrations from catchments 1401, 1403, and 1404 were assigned as boundary conditions from the watershed to the EFDC model (Figure 21).

Modeled watershed flows were converted to EFDC format and assigned to the corresponding EFDC grid cells. Catchment 1401 is a small direct drainage to the lagoon and is input to grid cell (28,14). The reach in catchment 1403 is Carmel Creek and feeds into grid cell (26, 5), Los Peñasquitos Creek and Carroll Canyon Creek merge in catchment 1404 and feeds into grid cell (19, 3), and a small direct drainage area was specified at grid cell (19, 3). Water temperature for the watershed inflows were obtained from continuous temperature data provided by the City of San Diego (2009) and converted to EFDC format. Salinity from the direct drainage area was set to zero, and salinities from the three creeks were specified based on monitored salinity data. The LSPC model simulated three sediment particle sizes: sand, silt, and clay. LSPC modeled sand, silt, and clay concentrations were converted to EFDC format.

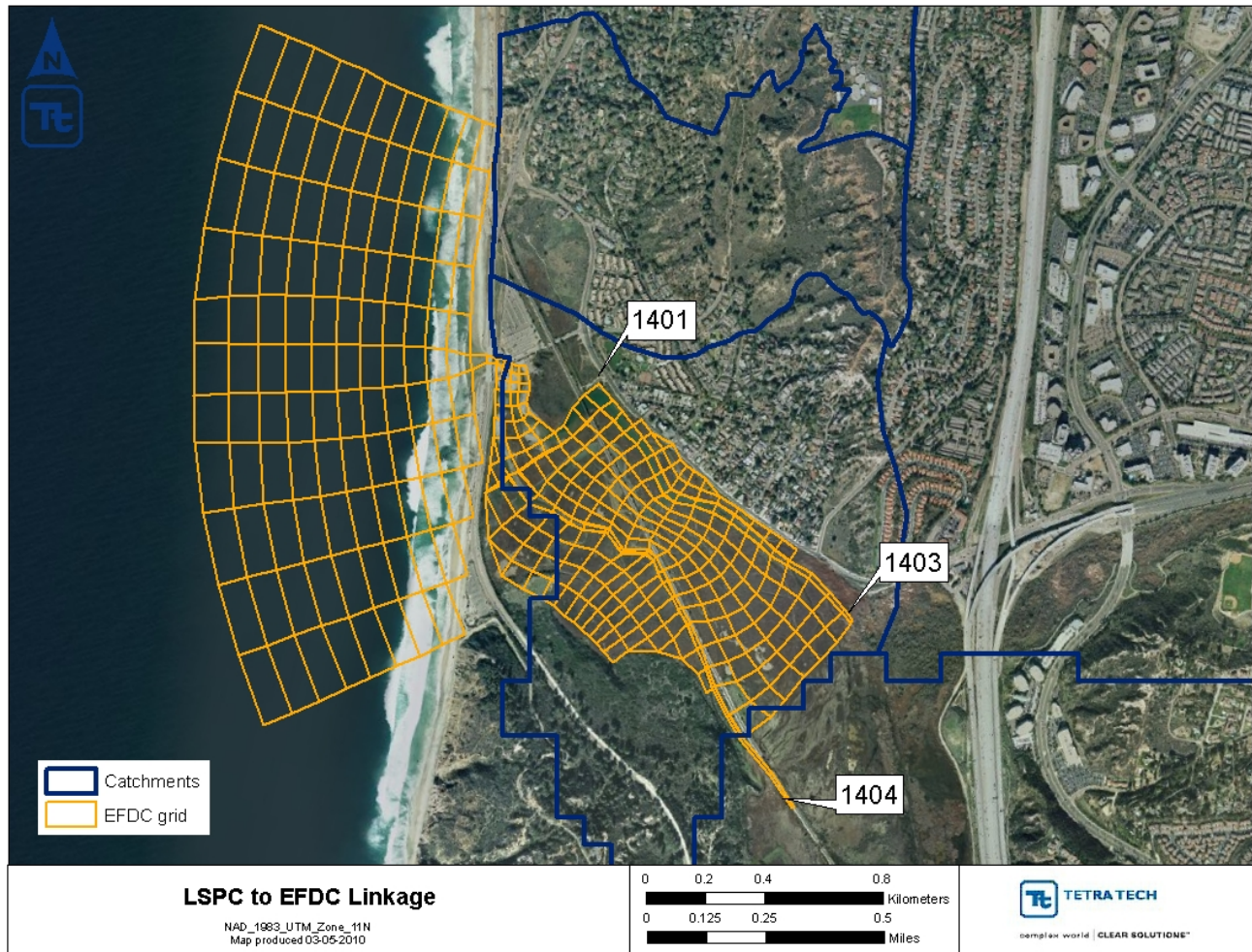


Figure 21. Assignment of watershed inputs to the EFDC grid

Representation of Ocean Boundary

In addition to the watershed, the ocean has both hydrodynamic and water quality influences on the lagoon. A narrow channel exists between the lagoon and the open ocean. The ocean is one of the major driving forces that influences lagoon circulation. Ocean water enters the lagoon during flood tides and leaves the lagoon during ebb tides. Changes in ocean water surface elevation determine the direction of flow and the transport of water quality constituents. Ocean water also increases or decreases the pollutant concentrations in the lagoon depending on water quality conditions along the ocean boundary. Required data for the ocean boundary include tidal elevation in the ocean, water temperature and salinity in the ocean water, and suspended sediment concentrations.

There are no monitoring stations located along the ocean boundary outside the lagoon mouth. Ocean inlet monitoring was conducted, however, this station is located at the lagoon/ocean interface. Conditions at this location are impacted by both the ocean and lagoon; therefore, data collected at the ocean inlet are not representative of ocean conditions. Tide data collected at the closest NOAA station in La Jolla were used to determine the open ocean water surface elevation boundaries for the lagoon model. The La Jolla station is located approximately 5 miles south of the Los Peñasquitos Lagoon. Tide data from La Jolla were used because it is similar to other available tide data in the vicinity and provides a more complete dataset in terms of the time period available. Mean sea level elevation data were downloaded from the NOAA site and were converted to EFDC



format (Figure 22). Water temperature data were also obtained from the La Jolla NOAA station, although salinity data were not available at this station. The salinity boundary condition was set to 35 psu at the ocean open boundary location.

For sediment simulations, the modeled water surface elevation, salinity, and water temperature immediately outside the lagoon (predicted from the full grid simulation) were specified as boundary conditions. Ocean sediment concentration data were not available. It is assumed that sediment entering the lagoon during flood tides primarily originates from beach erosion. The concentrations of sand, silt, and clay fractions were set to constant values initially and then adjusted during calibration.

Meteorological Data

Meteorological data are an important component of the EFDC model. Surface boundary conditions are determined by the meteorological conditions. Data required for model setup include atmospheric pressure, air temperature, relative humidity, precipitation, cloud cover, solar radiation, wind speed, and wind direction.

Meteorological data from station KCASAND153 located east of Interstate 5 in Torrey Woods Estates/Carmel Valley was downloaded from the website: www.weatherunderground.com. This website allows download of daily (5-minuted resolution) rainfall, wind speed and direction, air temperature, and percent humidity measurements (Figure 22). Solar radiation was estimated based on the latitude of the station and then adjusted based on the sky cover condition for each time-step. Sky condition data (i.e. cloud cover data) were not available and the estimated clear sky solar radiation data were adjusted/interpreted based on when precipitation occurred. Solar radiation data were further refined during calibration. Data for each day were provided by the City of San Diego (2009) from October 2007 through April 2008. These data were converted to the appropriate units and formatted for input into the EFDC model.

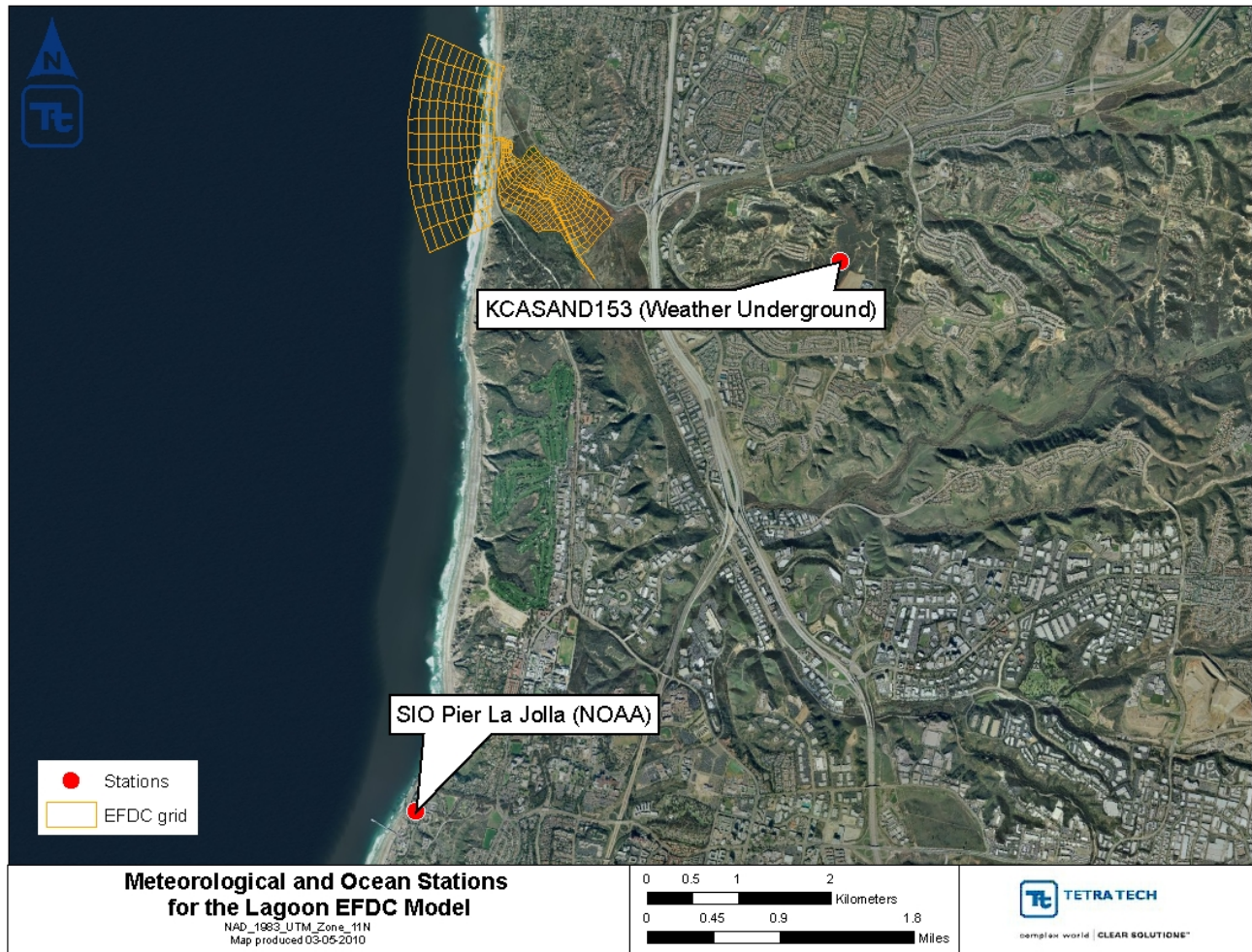


Figure 22. Meteorological and Ocean Boundary stations

Initial Conditions

For a dynamic model such as EFDC, initial conditions of water surface elevation, water temperature, salinity, water column sediments, and bottom sediments must be specified. Because the lagoon is an open system that is flushed by ocean water and watershed inflows frequently, the initial conditions of water surface elevation, water temperature, salinity, and water column sediments can be quickly replaced by boundary conditions. Model initial conditions were found to not be very sensitive to the model predictions. Initially assigned water surface elevation, water temperature, salinity, and water column sediment concentrations changed quickly as the model responds more readily to the driving boundary conditions from the ocean and watershed. Initial conditions were set to reasonable values based on modeling judgment. Water surface elevations were set to 0.92 meters above mean sea level (MSL) to ensure that all the grid cells were wet during the start of the simulation. Initial water temperatures were set to 10 degrees Celsius; salinities were set to 10 psu, and sand, silt, and clay fractions in the water column were set to 10 mg/L.

Sediment bottom conditions in the lagoon are the result of the long-term balance between deposition and erosion. Initial lagoon sediment depth at the beginning of the model simulation period determines the amount of sediment that can be eroded. Bottom sediment conditions were measured at the beginning of the modeling period on

10/1/2007. The only available data were collected (post storm) during 2/11/2008 and 2/15/2008 at 26 locations in the lagoon for sediment size distributions as part of the TMDL monitoring study. Sand, silt, and clay percentages from the sediment size distributions were set as the initial mass fractions for the sediment bed in the lagoon with the assumption that the sediment components have reached an equilibrium status and did not change dramatically from the beginning of the modeling period to the survey dates. In addition to mass fractions, other sediment properties including porosity and density must be specified in the model. These data were not collected; therefore default values for porosity (0.4) and density (1.99 gm/cm³) were used (Tetra Tech, 2007).

Model Calibration and Validation

Modeling parameters for the watershed and lagoon models were adjusted based on available monitoring data, as detailed below. For both models, it was essential that the physics of the system (hydrology and hydrodynamics) be accurately characterized in order to provide a sound foundation for simulating water quality conditions within the lagoon. Simulations of sediment fate and transport processes are dependent on an accurate representation of runoff, water movement and circulation, and other dynamic components. The time-step for the LSPC model is hourly and the time-step for the EFDC model is 0.5 seconds.

Watershed Model Calibration and Validation

Long term hydrology (1993-2008) was calibrated and validated using streamflow data from USGS gage 11023340 at the bottom of catchment 1406 (Figure 6). The period of record was divided into separate calibration and validation periods. Additional flow data were collected during TMDL monitoring by the City of San Diego (2009) at the bottom of catchments 1403 (Carmel Creek), 1405 (Los Peñasquitos Creek), and 1411 (Carroll Canyon Creek) were used for validation of the model hydrology (see Figure 19).

Hydrology

Measured and modeled average daily flows compared well throughout the model calibration and validation periods. Overall summary statistics comparing observed and simulated hydrology were within the recommended criteria based on HSPEXP (Lumb et al., 1994) for all metrics except summer volume error. Summer volume was primarily a function of the irrigation factor which was developed to balance observed summer low flows throughout the entirety of the simulation period.

Figure 23 through 30 compare modeled and measured flows during the calibration (1993-2000) and validation (2000-2008) periods. Table 4 presents the statistical comparison of modeled and measured flows at the USGS gage on Los Peñasquitos Creek (11023340).

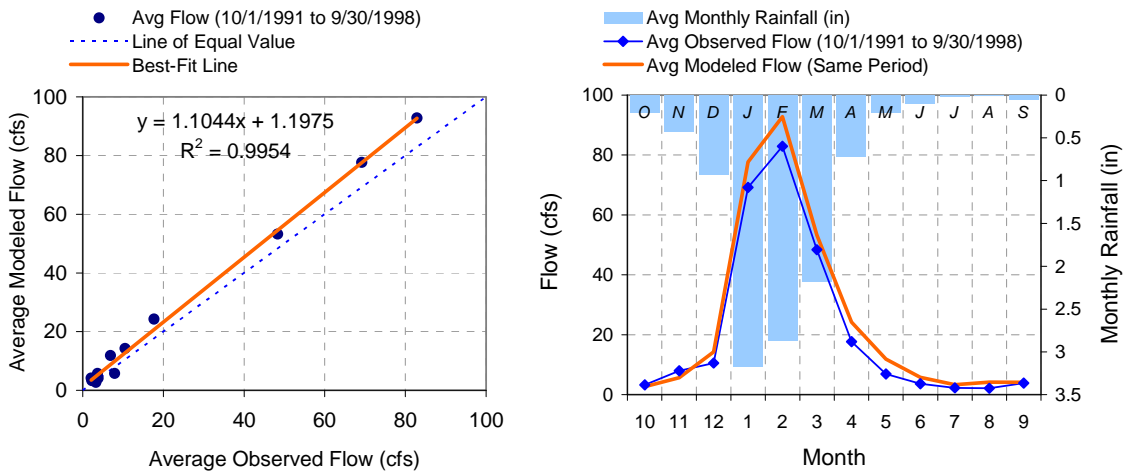


Figure 23. Mean monthly flow for calibration period (USGS 11023340)

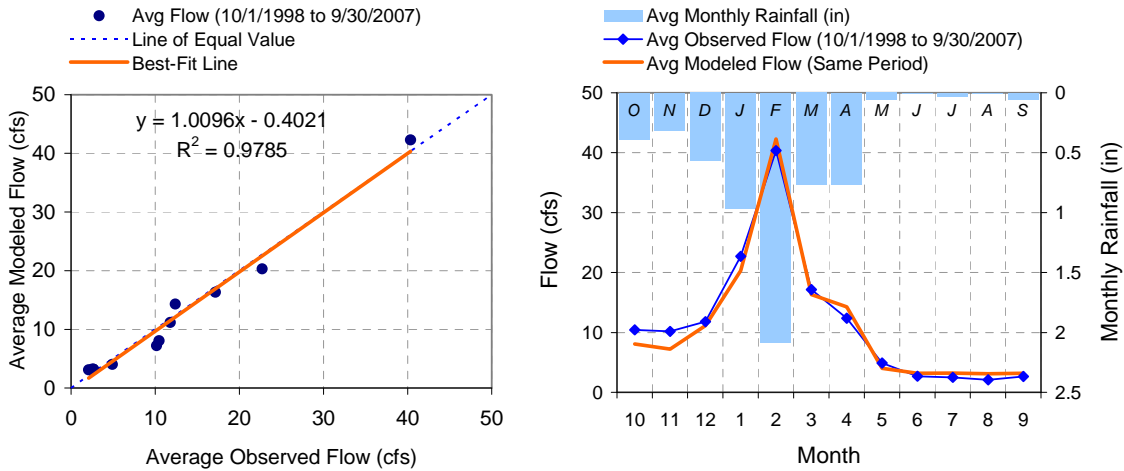


Figure 24. Mean monthly flow for validation period (USGS 11023340)

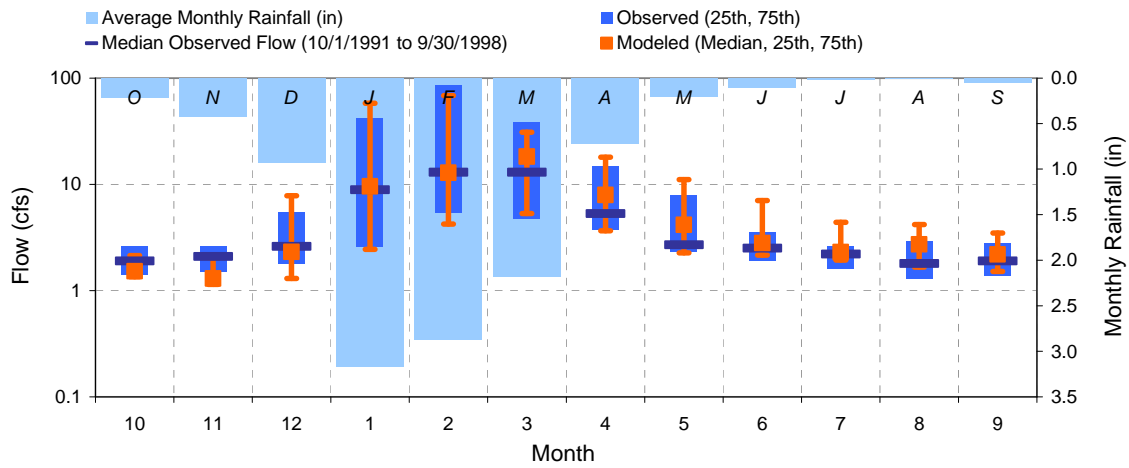


Figure 25. Monthly median and percentile flow comparison – calibration period

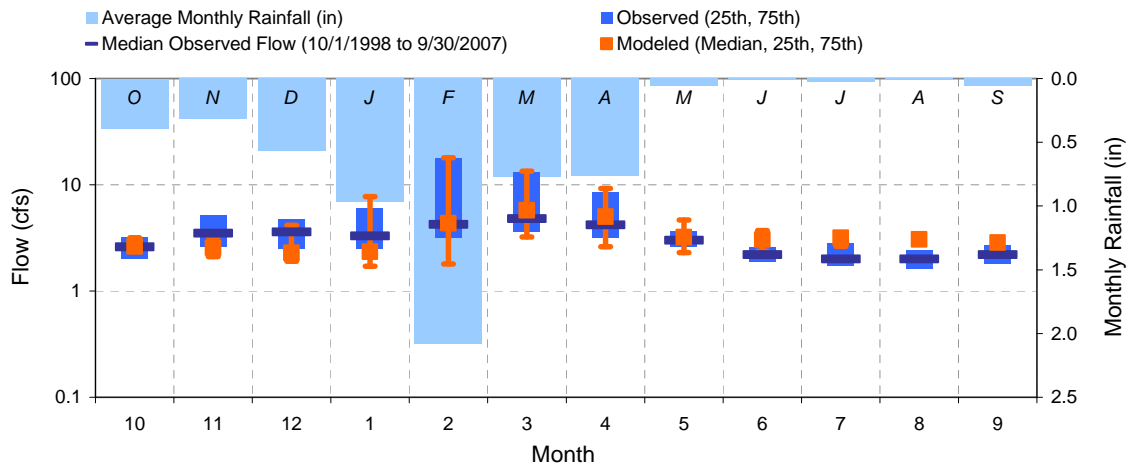


Figure 26. Monthly median and percentile flow comparison – validation period

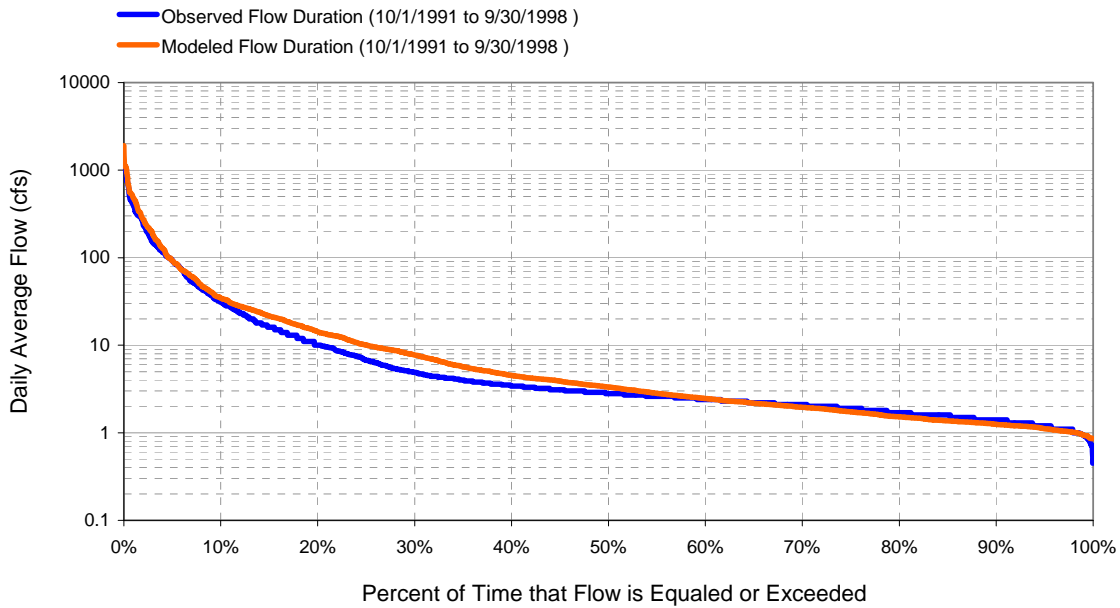


Figure 27. Flow exceedence output comparison – calibration period

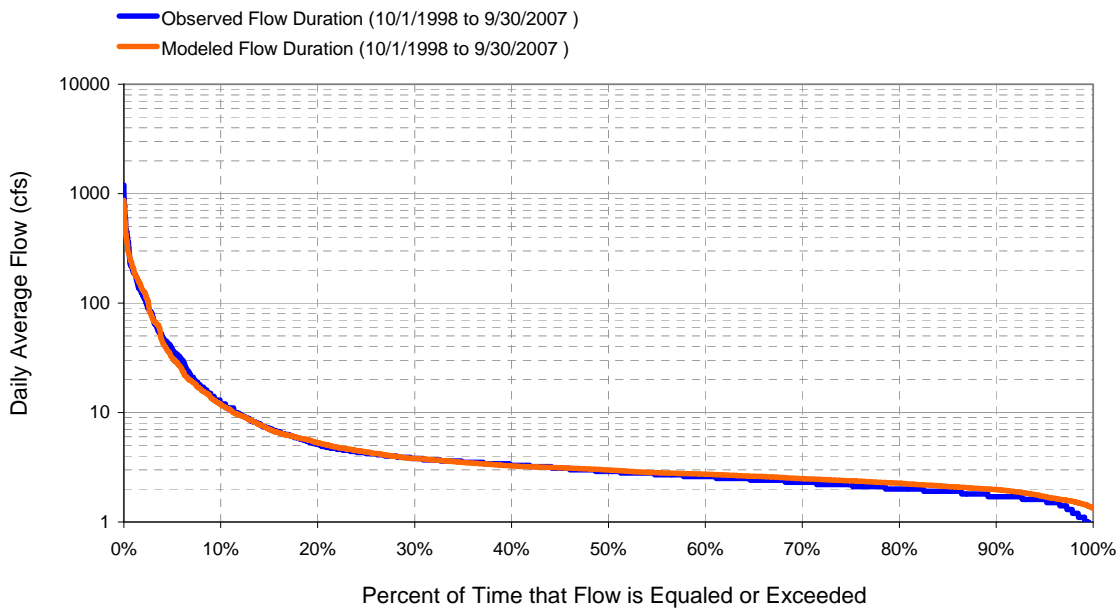


Figure 28. Flow exceedence output comparison – validation period

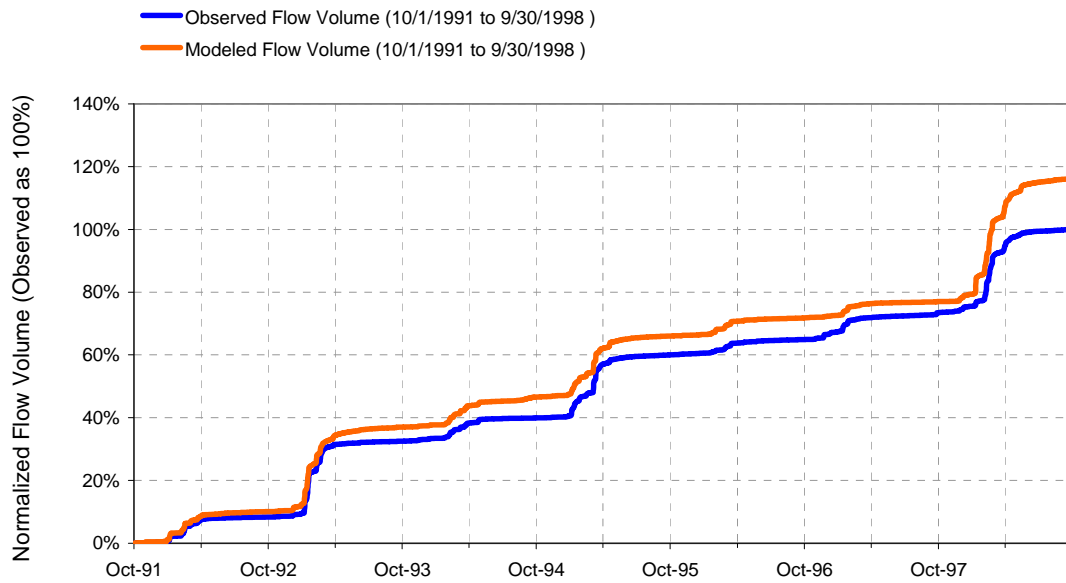


Figure 29. Cumulative volume comparison – calibration period

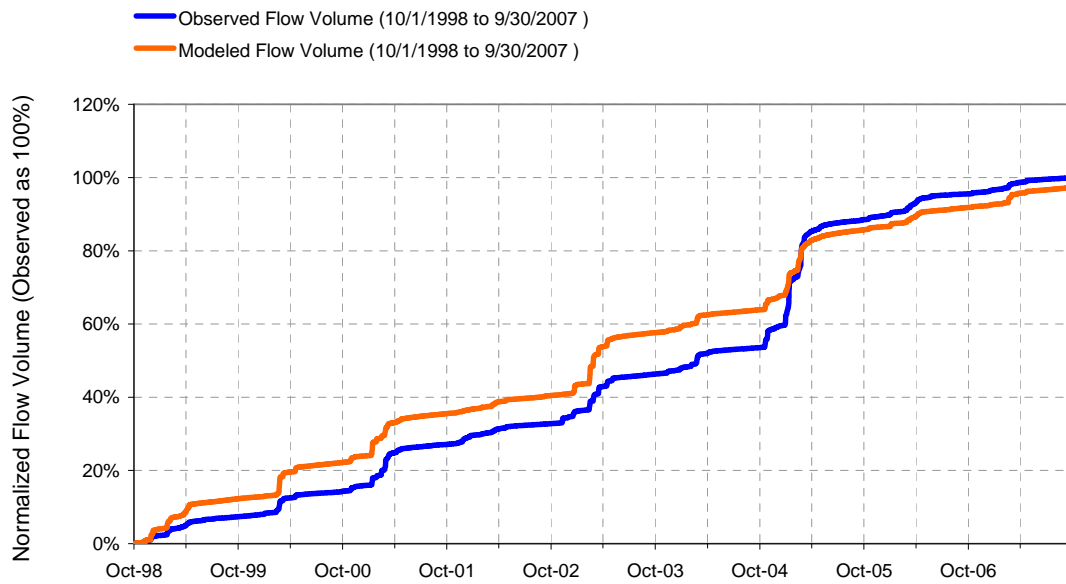


Figure 30. Cumulative volume comparison – validation period

Table 14. LSPC hydrologic model performance - entire simulation period

LSPC Simulated Flow		Observed Flow Gage		
OUTFLOW FROM CATCHMENT 1406		USGS 11023340 USGS Home		
15.16-Year Analysis Period: 1/1/1993 - 2/29/2008 Flow volumes are normalized, with total observed as 100				
Total Simulated In-stream Flow:	116.10	Total Observed In-stream Flow:		
Total of simulated highest 10% flows:	91.68	Total of Observed highest 10% flows:		
Total of Simulated lowest 50% flows:	4.36	Total of Observed Lowest 50% flows:		
Simulated Summer Flow Volume (months 7-9):	4.60	Observed Summer Flow Volume (7-9):		
Simulated Fall Flow Volume (months 10-12):	9.01	Observed Fall Flow Volume (10-12):		
Simulated Winter Flow Volume (months 1-3):	86.17	Observed Winter Flow Volume (1-3):		
Simulated Spring Flow Volume (months 4-6):	16.33	Observed Spring Flow Volume (4-6):		
Total Simulated Storm Volume:	54.53	Total Observed Storm Volume:		
Simulated Summer Storm Volume (7-9):	0.85	Observed Summer Storm Volume (7-9):		
Errors (Simulated-Observed)	Error Statistics	Recommended Criteria	1995-1999	2000-2004
Error in total volume:	16.10	10	-1.43	7.35
Error in 50% lowest flows:	-2.00	10	-1.60	-3.91
Error in 10% highest flows:	13.77	15	2.26	1.75
Seasonal volume error - Summer:	42.46	30	13.27	-2.52
Seasonal volume error - Fall:	5.02	30	4.49	12.42
Seasonal volume error - Winter:	11.62	30	-18.21	13.31
Seasonal volume error - Spring:	48.44	30	1.90	6.11
Error in storm volumes:	21.88	20	1.13	12.07
Error in summer storm volumes:	11.76	50	3.16	15.42
Nash-Sutcliffe Coefficient of Efficiency, E:	0.675	Model accuracy increases as E or E' approaches 1.0	0.688	0.814
Baseline adjusted coefficient (Garrick), E':	0.683		0.517	0.549

Additional validation flow data from the City of San Diego (2009) were available for comparison to model output. Los Peñasquitos Creek flows were monitored by the USGS (15 minute data at gage 11023340) and the City of San Diego (5 minute data at MLS) which represent drainages of 42 and 59 mi², respectively. Flows at the two monitoring stations reflected the amount of rainfall that was received within each drainage area. Peak stormflow (Figure 31) and storm volume (Figure 32) were greater at the upstream USGS gage (11023340) than measured at the MLS near the bottom of the watershed. Baseflow volume, defined as daily flows with more than 50% of flow from surface runoff using hydrograph separation techniques, was 9% greater at the downstream gage. For each of the three sampling events that were monitored, model output compared well to streamflow measurements at the USGS gaging station as opposed to the MLS (Figure 33 through 35). Timing differences may be due to several factors including possible data limitations, as described below.

Flows typically increase further downstream barring withdrawals and/or infiltration; however, storm volumes during the monitoring period at the downstream station were significantly lower than reported at the upstream USGS gaging station. This may indicate that the flow rating table for the downstream station may not characterize higher flows well, especially since the model calibrated well to the upstream USGS gaging station. As a result, significant adjustments were not made to the model in order to match the measured flows at the MLS.

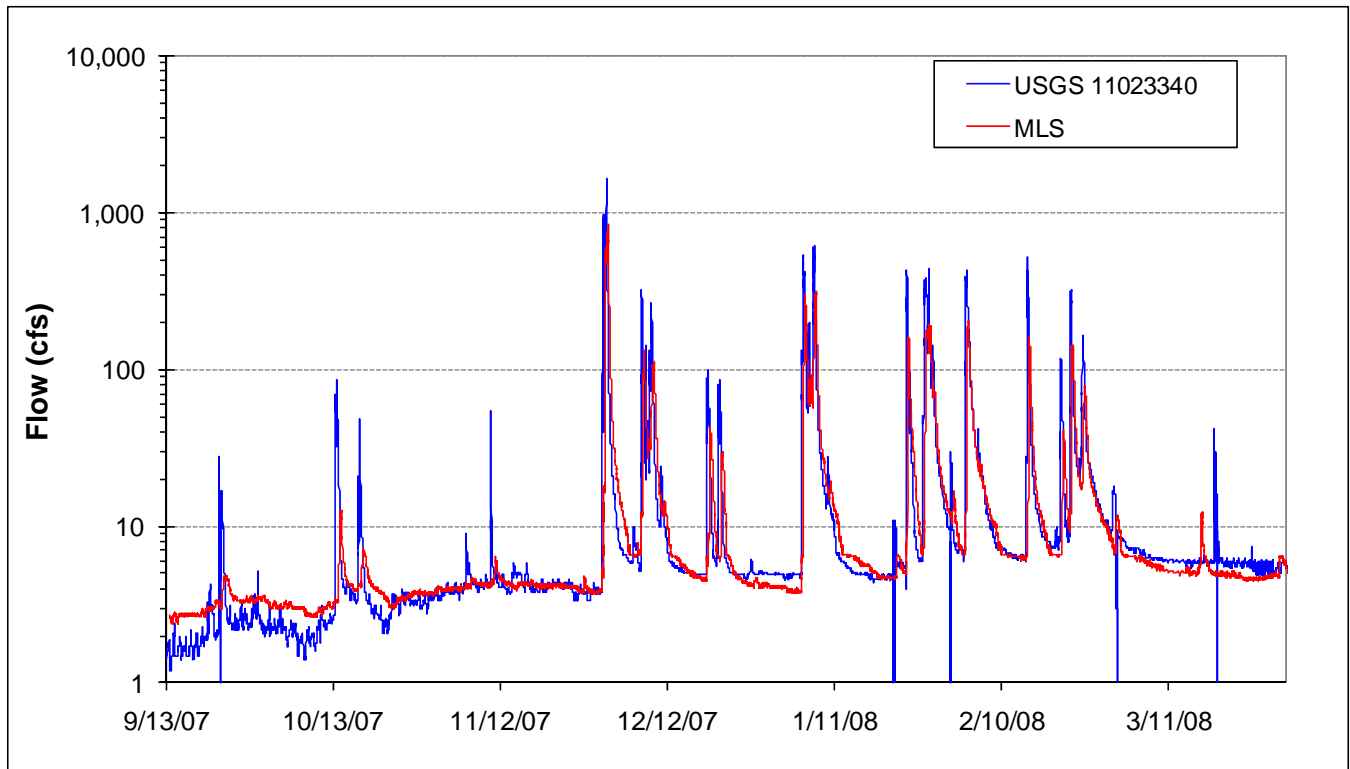


Figure 31. Time-series streamflow measured on Los Peñasquitos Creek

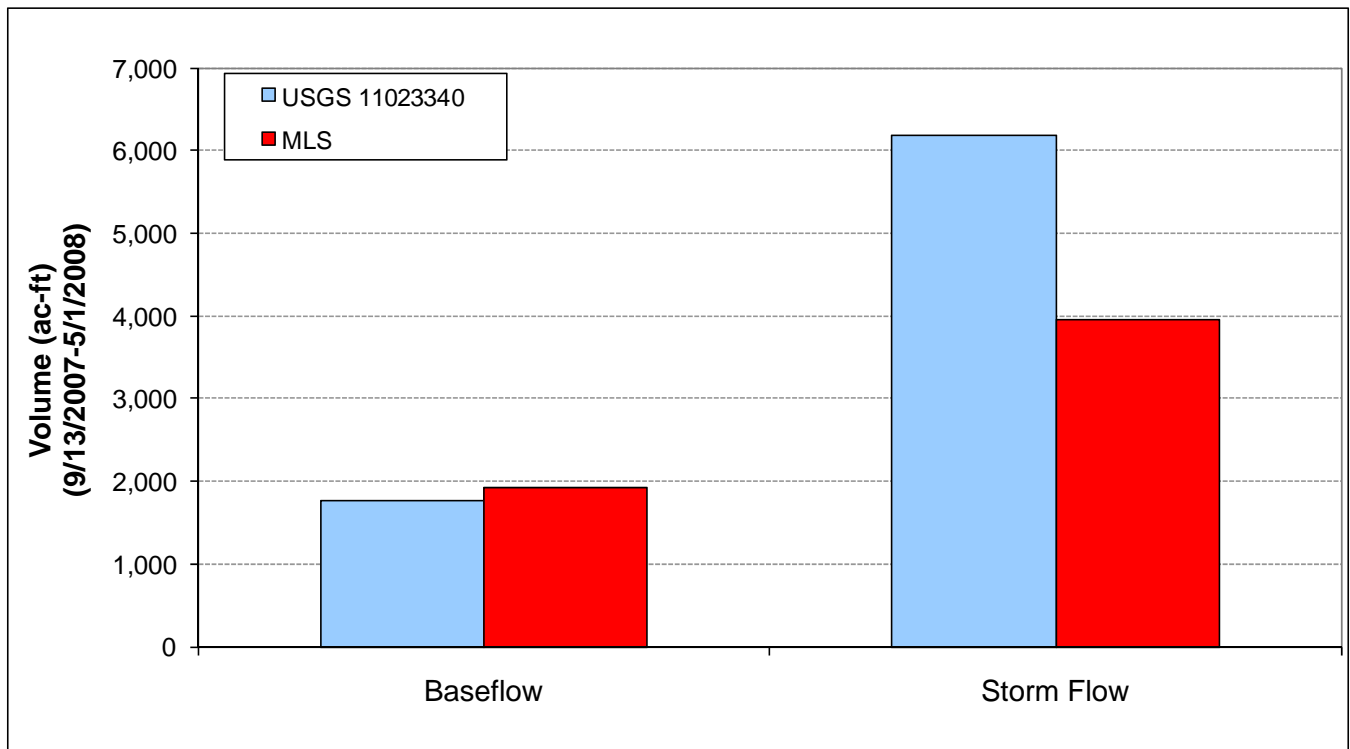


Figure 32. Baseflow and storm volumes measured on Los Peñasquitos Creek

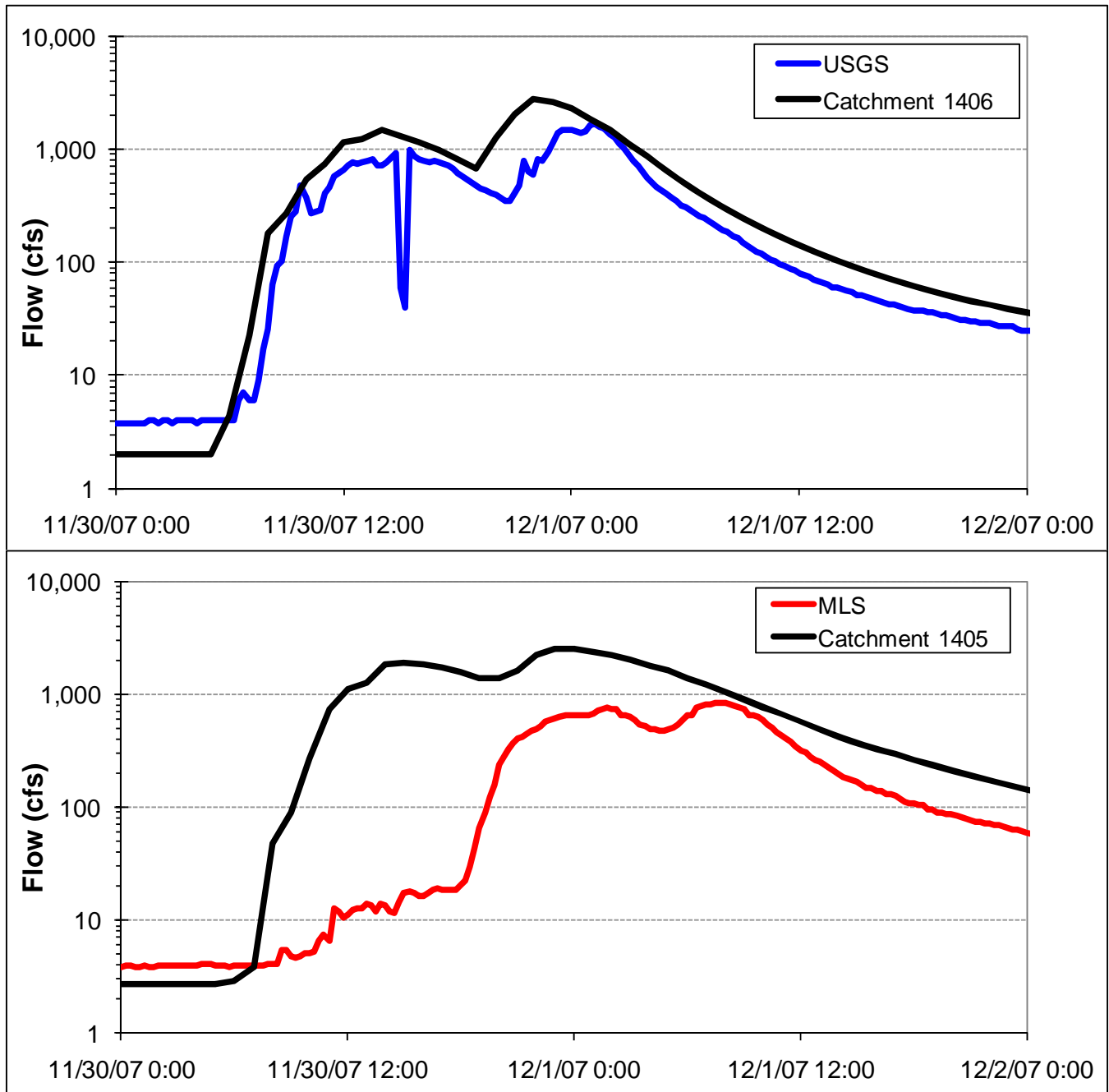


Figure 33. Comparison of modeled and observed flows at the USGS and MLS stations - 11/30/2007 storm

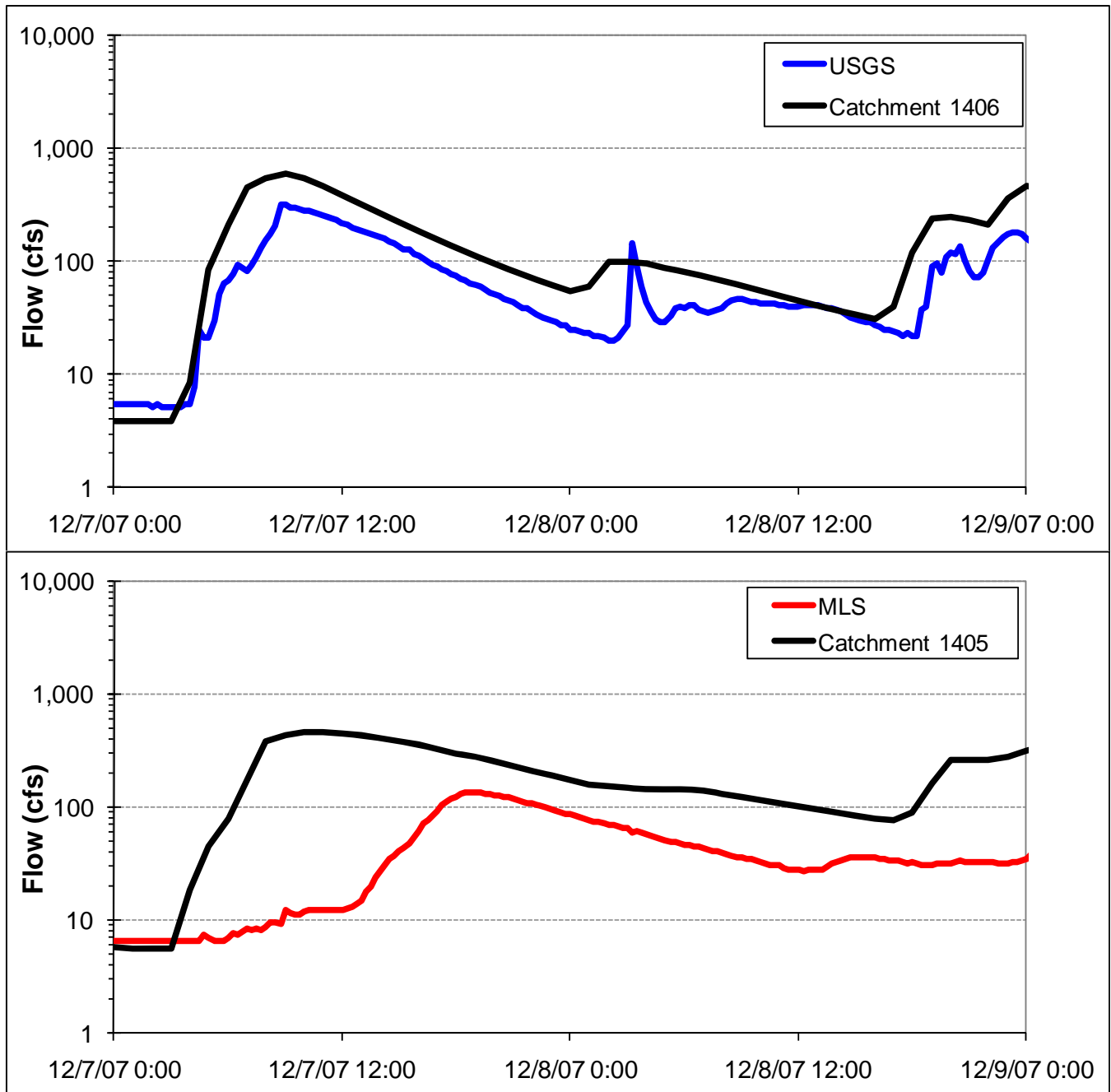


Figure 34. Comparison of modeled and observed flows at the USGS and MLS stations - 12/7/2007 storm

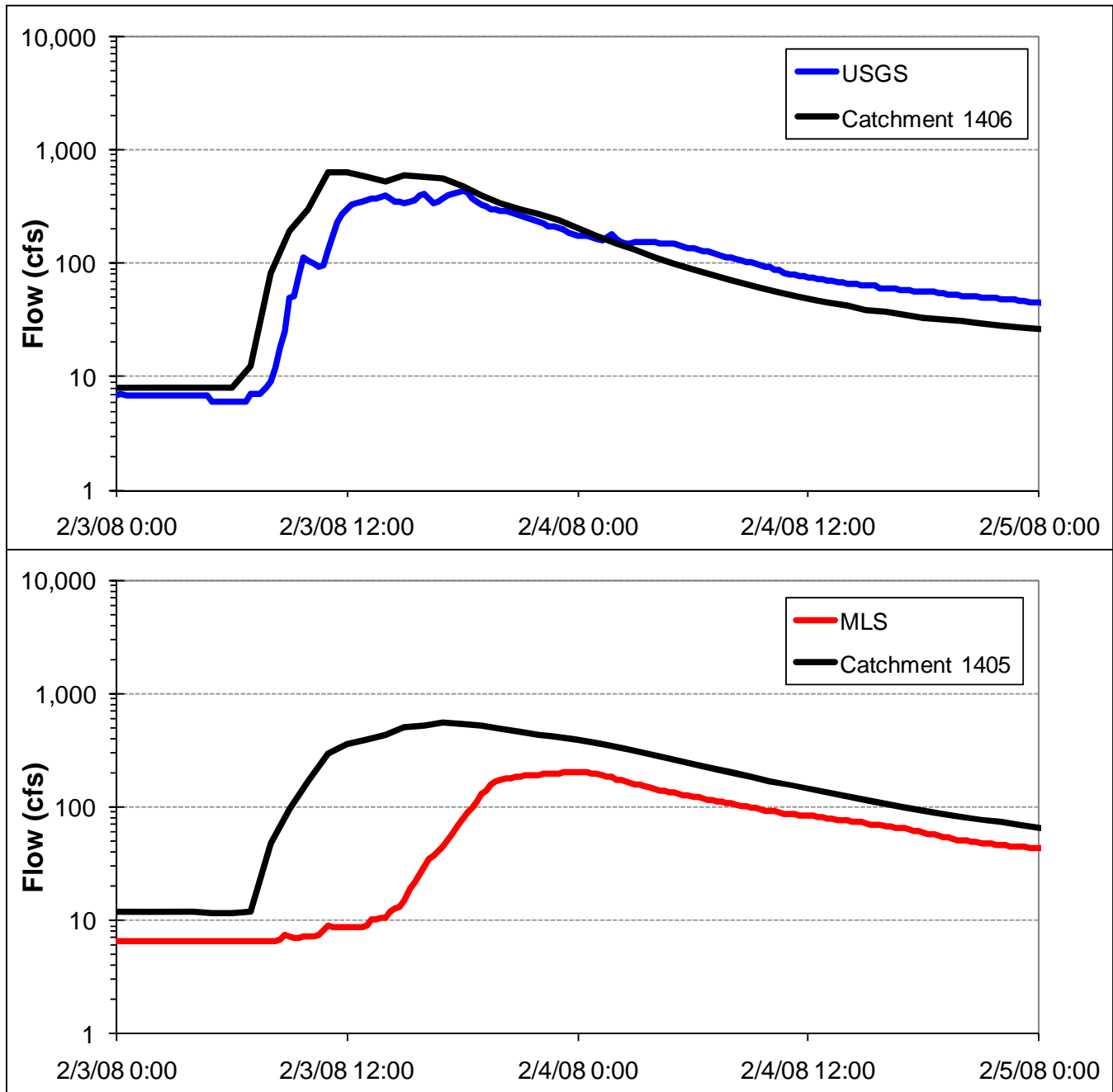


Figure 35. Comparison of modeled and observed flows at the USGS and MLS stations – 2/3/2008 storm

Suspended Sediment

Sediment deposition and scour can add or remove sediment from the modeled catchment reaches. Sand carrying capacity was assumed to be represented by a power function of velocity. The coefficient and exponent of the equation were modified to achieve a dynamic steady state where the sand in the bed remained relatively constant throughout a 16 year simulation period. The reach-specific shear stress required for deposition and resuspension of silt and clay were determined following the same methodology that was employed to define the sand dynamics.

At two of the monitoring locations, land use inputs were insufficient to replicate the observed suspended sediment concentrations. Both Carroll Canyon Creek and Carmel Creek required additional sediment inputs from the streambanks. The streambank erosion module in LSPC was used to account for the additional sediment load to the system (see Appendix B for those coefficients). The incorporation of streambank erosion provided a much improved calibration of the model at those two sites; however, care must be used in interpreting those results. The stream cross sections in the model were based on an algorithm relating stream cross section to upstream drainage basin. Sensitivity analyses were performed on the bank erosion processes where the linear term of the bank erosion equation was modified by ± 25 percent. Carmel Canyon Creek was relatively insensitive to the stream bank coefficients with a ± 7 percent change in total sediment load from the catchment. Carroll Canyon Creek was more sensitive with load changes of ± 21 percent when the stream bank coefficient was changed. To more accurately model the system, and the contribution from streambank erosion, accurate measurement of stream cross sections throughout the watershed would be required.

The primary dataset used in the calibration was pollutograph data for three storms that were sampled between November 2007 and February 2008 by the City of San Diego (2009) as part of the TMDL monitoring study. Both pollutograph samples and storm EMCs from the three events were used for comparison at the three monitoring sites (Figures 36 through 39). Note that flow calibration discrepancies shown in Figures 37 through 39 are likely due to possible problems with the flow rating tables and resulting streamflow estimates for these stations, as discussed in the previous section.

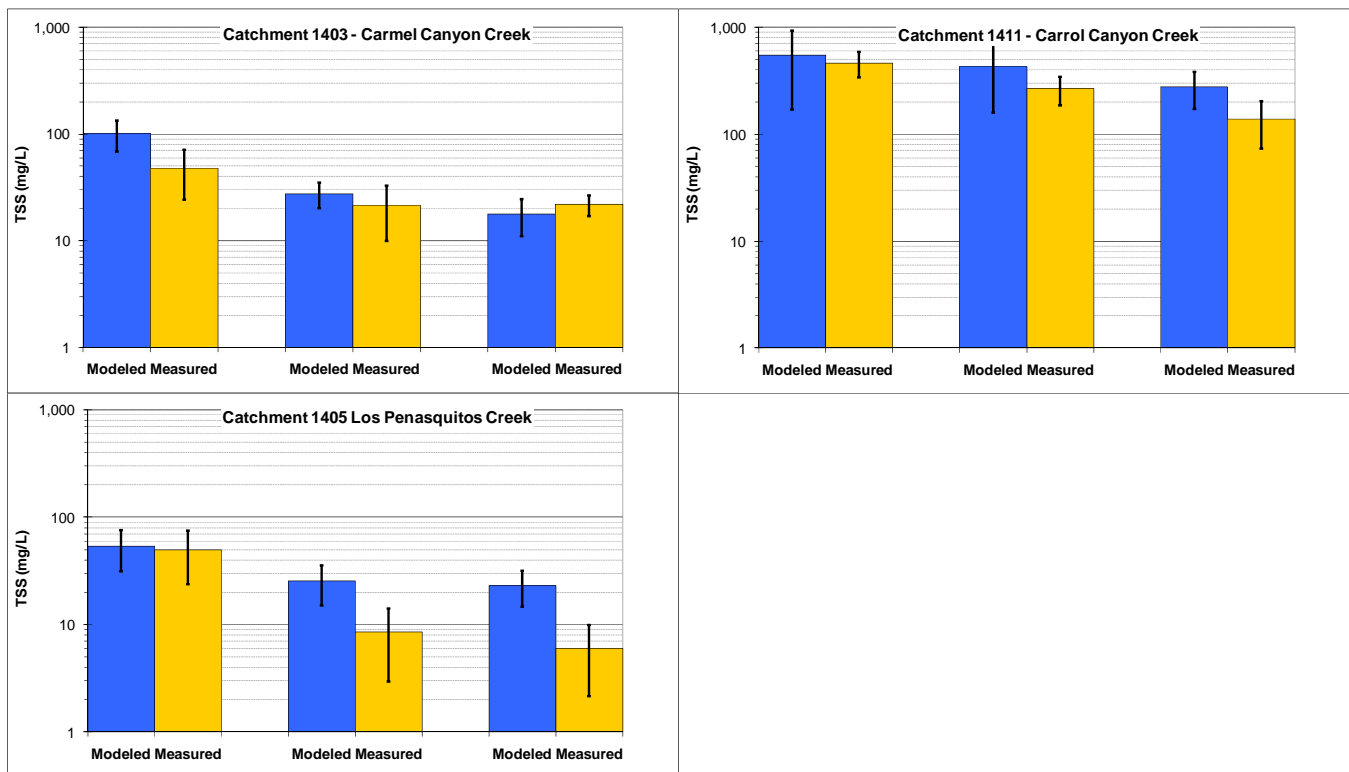


Figure 36. Comparison of EMC and 95th Percentile TSS data collected during each storm event

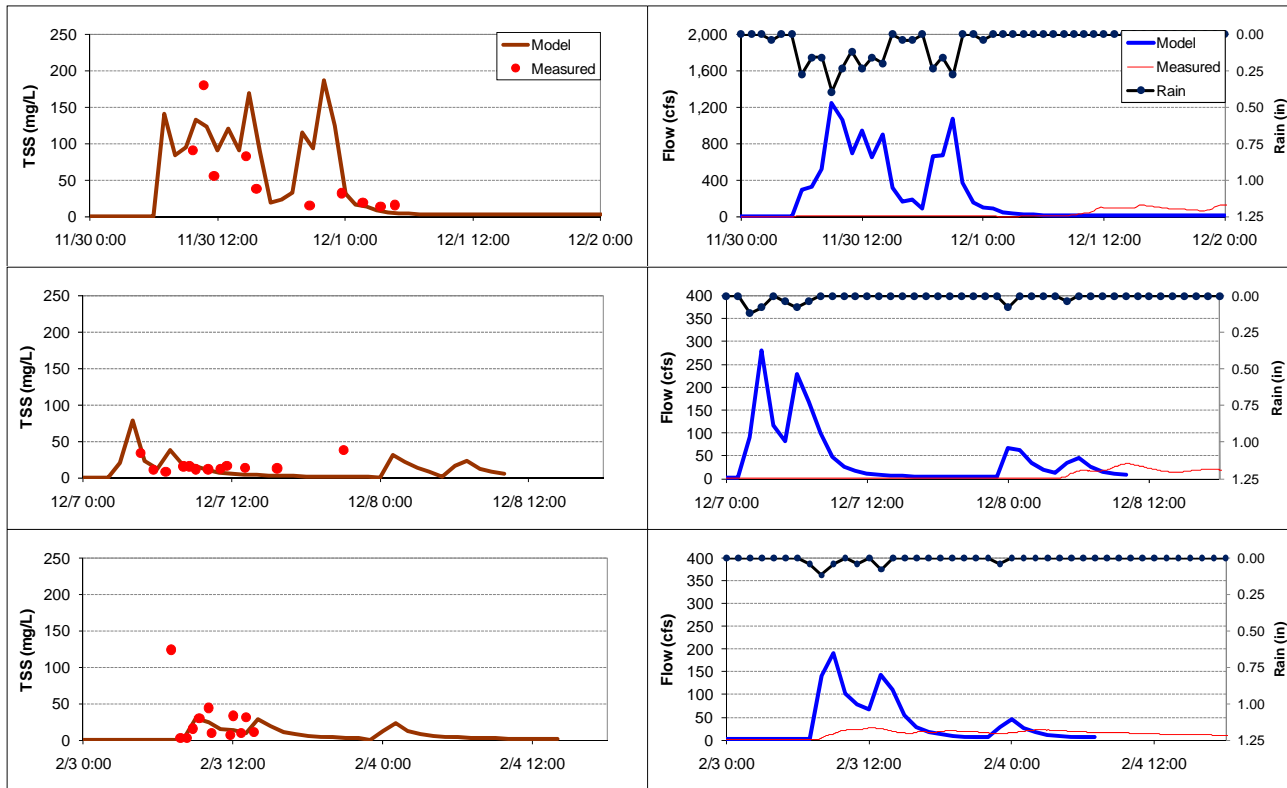


Figure 37. Pollutograph TSS calibration at Carmel Creek

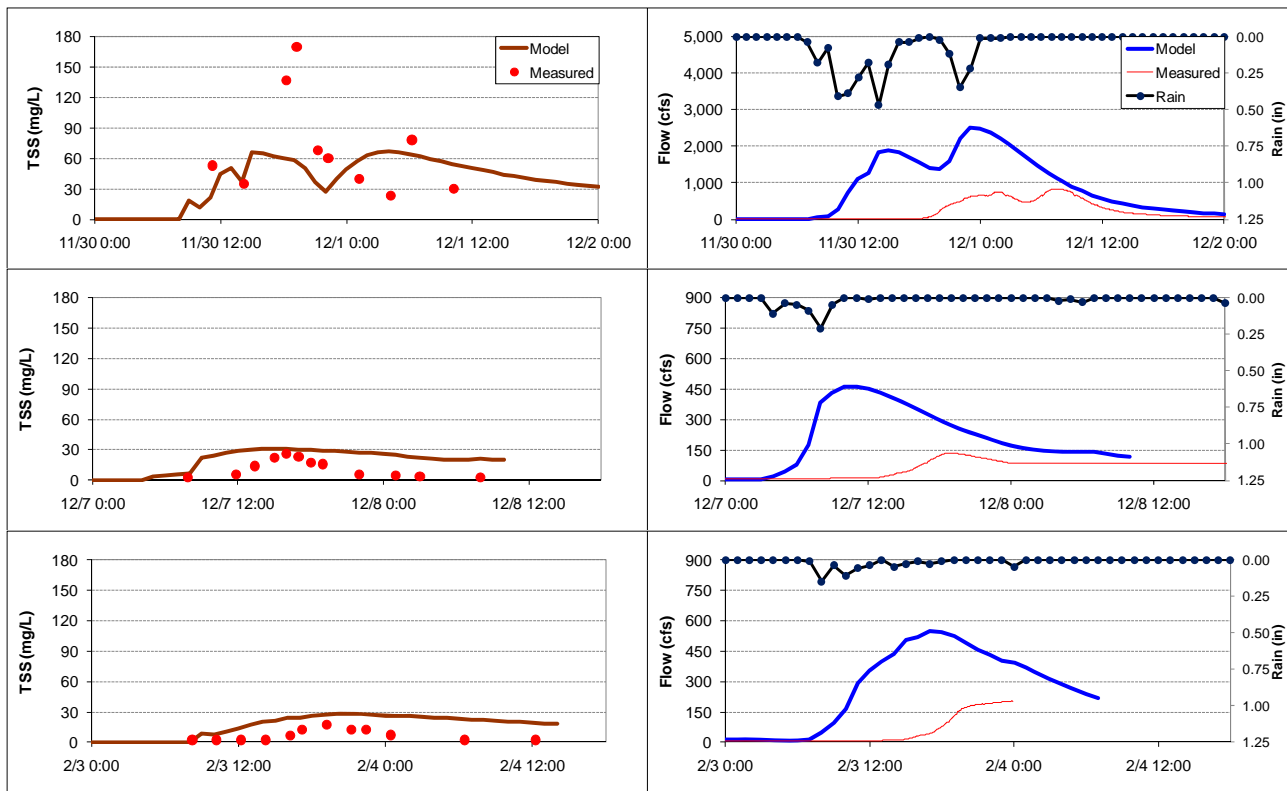


Figure 38. Pollutograph TSS calibration at Los Peñasquitos Creek

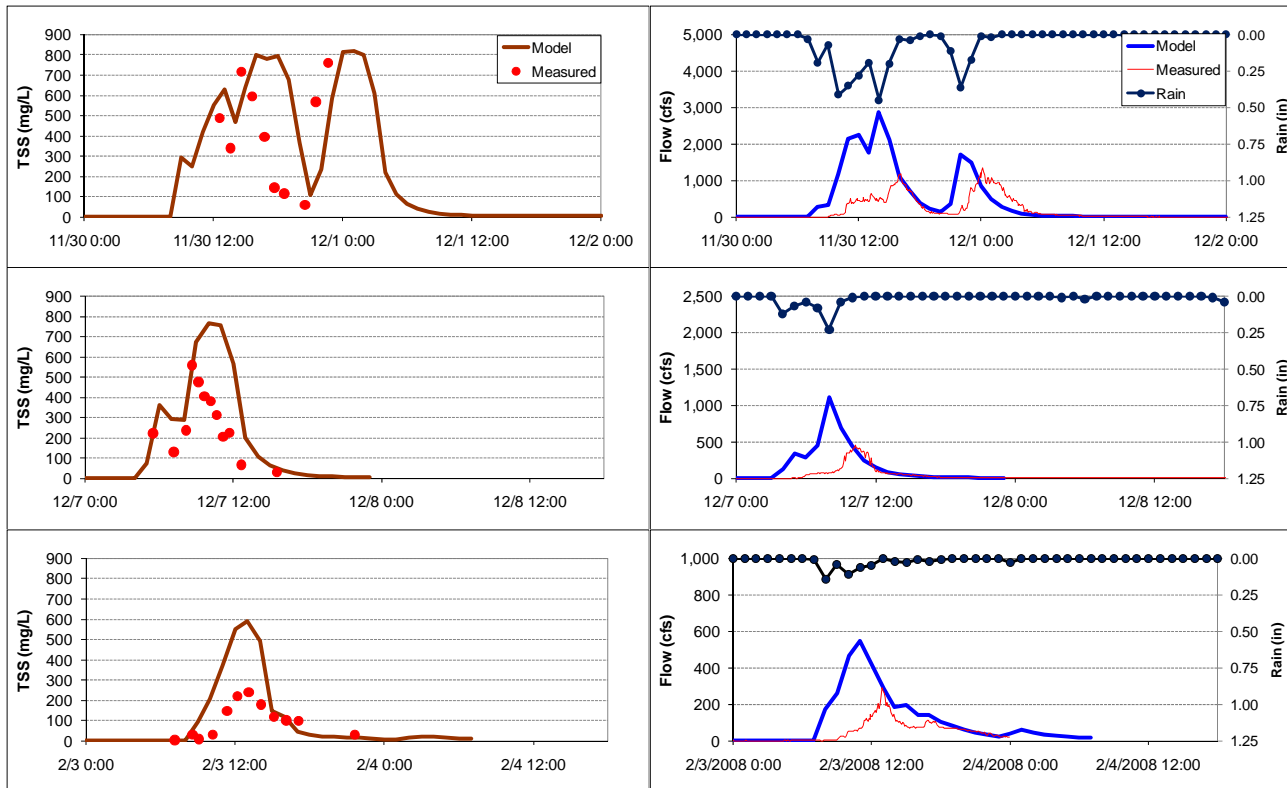


Figure 39. Pollutograph TSS calibration at Carroll Canyon Creek

Modeled particle size distributions were compared to the measured data presented in Figure 16 and 17. The measured particle size distributions were aggregated into sand (62.5-4000 μm), silt (3.1 – 53 μm) and clay (0.2 – 2 μm) fractions. Model output indicates a reasonable representation of the sand, silt and clay distributions observed in the 11/30/2007 and 12/7/2007 storms (Table 15).

Table 15. Comparison of modeled and measured sediment fractions for each storm event

	Sand		Silt		Clay	
	Measured	Modeled	Measured	Modeled	Measured	Modeled
11/30/2007						
Carmel Creek	41 %	32 %	48 %	36 %	11 %	32 %
Los Peñasquitos Creek	12 %	21 %	74 %	44 %	14 %	35 %
Carroll Canyon Creek	8 %	33 %	72 %	34 %	19 %	33 %
12/07/2007						
Carmel Creek	42 %	41 %	44 %	30 %	14 %	29 %
Los Peñasquitos Creek	42 %	28 %	49 %	38 %	9 %	34 %
Carroll Canyon Creek	26 %	32 %	40 %	34 %	34 %	34 %
02/03/2008						
Carmel Creek	n/a	36 %	n/a	32 %	n/a	32 %
Los Peñasquitos Creek	n/a	29 %	n/a	38 %	n/a	33 %
Carroll Canyon Creek	n/a	32 %	n/a	34 %	n/a	34 %

The model performed reasonably well with respect to the observed concentrations at the three monitoring locations. The average difference between modeled and measured EMCs for Carmel Creek, Los Peñasquitos Creek, and Carroll Canyon Creek was 83%, 51%, and 65%, respectively. However these predictions are highly influenced by mis-timing or simply a poor comparison of measured and modeled hydrographs. The difficulties of establishing a good relationship between flow and depth is discussed in the previous section. While the measured and modeled EMCs were dissimilar, the predicted concentrations agreed well with observed data (see Figure through 39).

Additional sampling efforts within the Los Peñasquitos watershed included stormwater TSS measurements. The USGS had two separate sampling efforts in the watershed in the 1980's (Table 5). NPDES monitoring on Los Peñasquitos Creek began in 2001 and is currently an ongoing effort. Two pollutograph sampling events (11/30/2007 and 12/7/2007) were also sampled during NPDES monitoring, providing both pollutograph and EMC data.

Output from a long term simulation (1/1/1998 – 2/28/2008) was used to validate the model. Storm TSS EMCs from the model output (Model) were compared against the USGS sampling results (USGS), NPDES monitoring (MLS), and paired NPDES (MLS-1 and -3)/pollutograph monitoring (Storms 1 and 3) (Figure 40). Model results were an order of magnitude lower than the USGS grab samples but were not significantly different at the 95th percentile level. Median model output was comparable to the long term NPDES EMC sampling. It is interesting to note that the EMCs from the two common storms for the pollutograph and NPDES sampling differed by more than double.

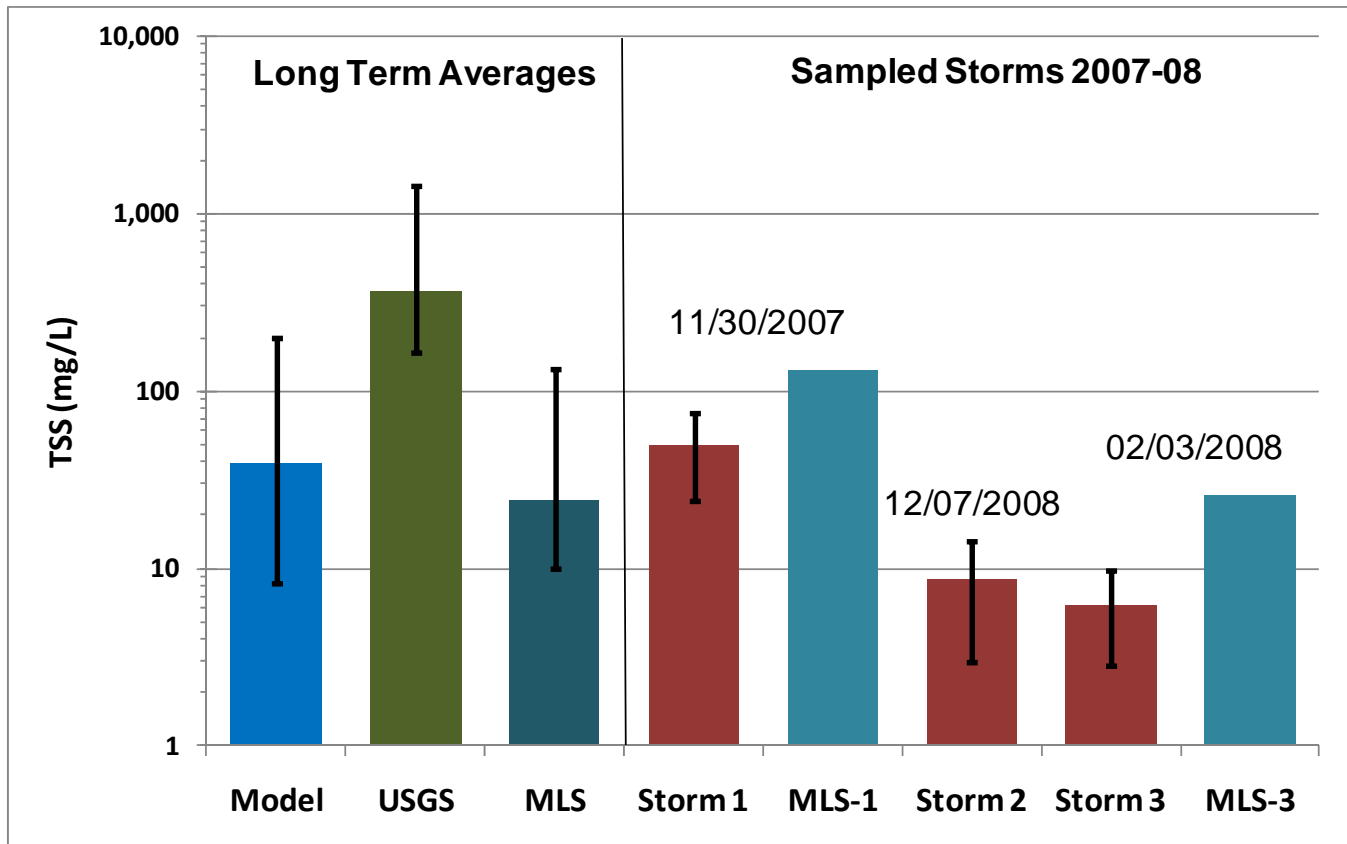


Figure 40. Comparison of modeled and measured TSS with 95th percentile confidence intervals

In 2005, the El Cuervo Norte wetlands were built upstream of the long-term MLS monitoring station. Flows from Los Peñasquitos Creek are diverted into the wetlands, creating the potential for solids to settle out and thus reduce the TSS measured at the MLS. Historic stormwater EMC monitoring data from the City of San Diego has not shown a significant reduction in TSS concentrations at the 95th percent confidence level (Figure 41).

Suspended sediment simulations reasonably predicted the observed stormwater TSS concentrations in the Los Peñasquitos watershed. Sediment transported via diffusive bed load processes also has the potential to be a significant source of sediment loadings; however, this source was neither characterized in the LSPC modeling or would be with traditional TSS sampling. Perennial flows into the lagoon were modeled with little to no sediment inputs throughout the majority of the simulation period. Because of the length of those periods without TSS at low levels, bed flow has the potential to be the dominate sediment transport pathway and could add significant sediment to the lagoon.

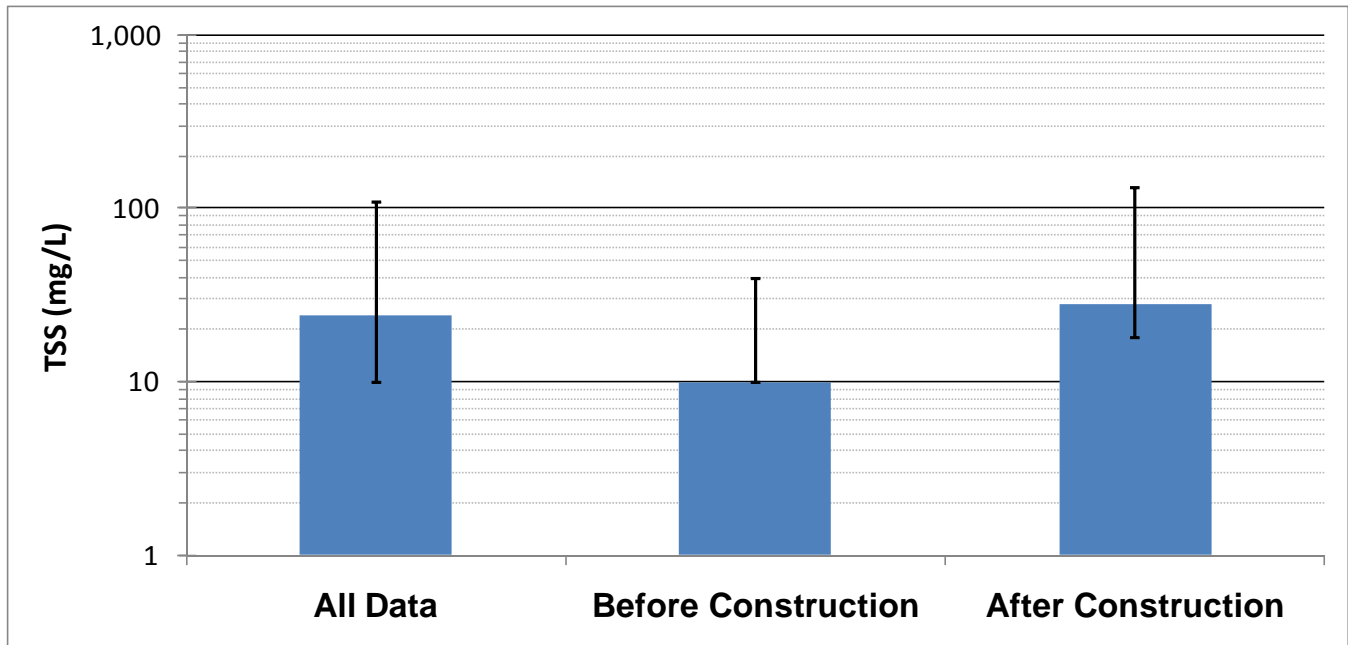


Figure 41. Measured TSS before/after construction of the El Cuervo Norte wetlands

Lagoon Model Calibration

Based on the TMDL monitoring study conducted by the City of San Diego (2009), two lagoon stations were available for model calibration. One station is located near the ocean inlet and one is located on the Carmel Branch lagoon segment. Figure 42 shows the locations where grab samples and continuous data were collected at these two locations within the lagoon. An inventory of all available monitoring data that were used during model calibration is provided in Table 16.

Table 16. Lagoon calibration data summary

Dates	Media	Sample type	Parameters	Location
11/30-12/1/07 12/07-12/8/07 2/02-2/04/08	Water	Pollutograph	TSS and Conductivity	Lagoon and ocean Inlet
11/30-12/1/07	Water	Storm composite	Percent composition of gravel, sand, silt, and clay	Lagoon segment and ocean inlet
10/07-4/08	Water	Continuous	Temperature, Conductivity, and Water Level (15 min data)	Lagoon segment and ocean inlet

In addition to these monitoring stations, the Los Peñasquitos Lagoon Foundation also routinely monitors salinity at station W2 (railroad trestle) (Figure 42). The EFDC model was calibrated based on monitoring data that were collected at these three locations. Note that monitoring data were not collected along the Los Peñasquitos/Canyon Creek lagoon segment (Los Peñasquitos Branch); therefore, comparisons could not be made to determine if the lagoon model results accurately predict conditions in this portion of the lagoon.

Model calibration involved adjusting parameters to achieve agreement between model results and observed data. The Los Peñasquitos lagoon model was calibrated in two steps. First, hydrodynamic parameters were calibrated, including examining the modeled water surface elevation, water temperature, and salinity at the two TMDL monitoring locations with the full grid. After hydrodynamics were calibrated, sediment processes were checked to ensure reasonable model representation of the lagoon using the reduced grid. The model was run from 10/1/2007 through 3/1/2008 in order to include the TMDL sampling events conducted by City of San Diego (2009).

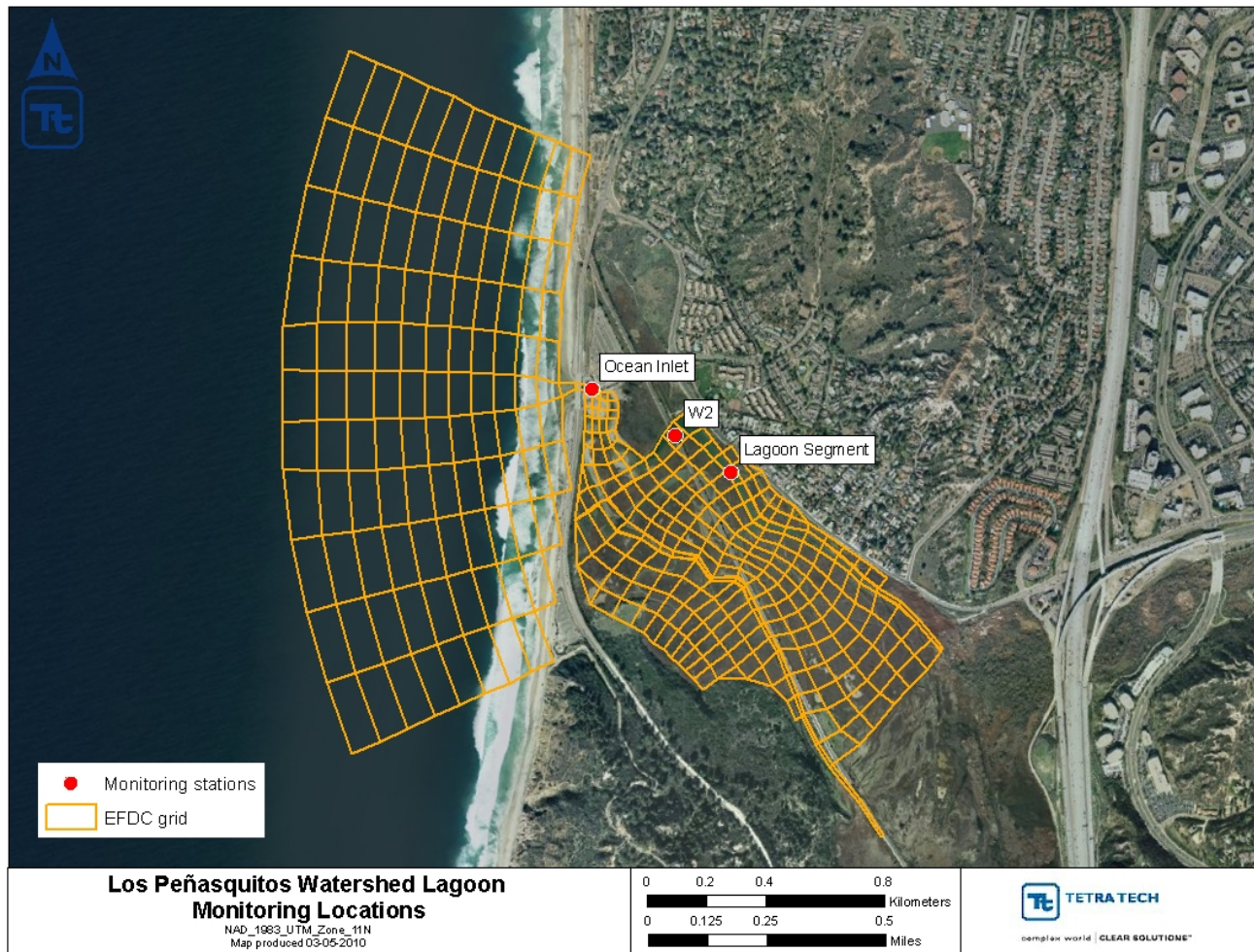


Figure 42. Calibration stations within Los Peñasquitos Lagoon

Hydrodynamics Calibration

During hydrodynamic calibration, roughness height and lagoon bottom elevations for the model grid cells were adjusted slightly. The cross-section of EFDC cells is rectangular; therefore, measured cross-section data cannot be used directly. Original bottom elevations were estimated using the relatively deep measurements across the cross-section data. Final bottom elevations were determined during calibration.

Modeled water surface elevations, water temperature, and salinities were compared against observed data. Available observed data do not include water surface elevations and salinity measurements. Instead, TMDL monitoring data collected by City of San Diego (2009) included depth and specific conductance. Because model results are average depths and observed depths were determined at the sampling points, they cannot be compared

directly. As a result, observed depths were converted to water surface elevations. The datum used for depth measurements was not recorded; therefore, conversion from depths to water surface elevations were estimated by assuming that average depths were near 0.5 meters above MSL.

Specific conductance data were measured continuously at the two sampling locations. EFDC can directly simulate the specific conductance as tracer. However, the impact of specific conductance on density cannot be considered as a tracer, therefore, salinity was modeled for the lagoon. Salinities were converted from specific conductance using the UNESCO algorithm (UNESCO, 1983). An Excel VBA function was developed to convert the specific conductance to salinity using the UNESCO algorithm.

Model calibration results for water surface elevation are shown in Figure 43. In general, modeled water surface elevations agree well with the elevations converted from observed depths at both of the locations. The model was able to capture the magnitude and timing of the fluctuations of water surface elevations driven by the tide and watershed inflows. The modeled elevations show some spikes with much higher elevations. These spikes are caused by modeled peak flows from the watershed, which can be different from the actual flows due to the uncertainties caused by rainfall and other parameters. In addition to uncertainty associated with the watershed inflows, the ocean inlet can change due to the sediment deposition and erosion by strong wave and/or flood tides during the simulation period. Changes in ocean inlet bathymetry can also affect the exchange of ocean water and the resulting water surface elevation. Note that for the entire calibration period (10/1/2007 – 2/28/2008), the ocean inlet was open with closures starting to occur sometime in March of 2008 as indicated in the Los Peñasquitos Lagoon TMDL monitoring report (City of San Diego, 2009)

Lagoon water temperature is mainly governed by the temperature associated with watershed inflows, ocean water temperature, and meteorological conditions. Modeled water temperature agrees well with observed water temperature at both of the monitoring locations. The model slightly over-predicted water temperature in the beginning of the simulation. This was mainly due to the open boundary water temperature data used in the model. Water temperature data were from the La Jolla station, which is approximately 5 miles south of the lagoon. 4 shows the temperature calibration at the two locations.

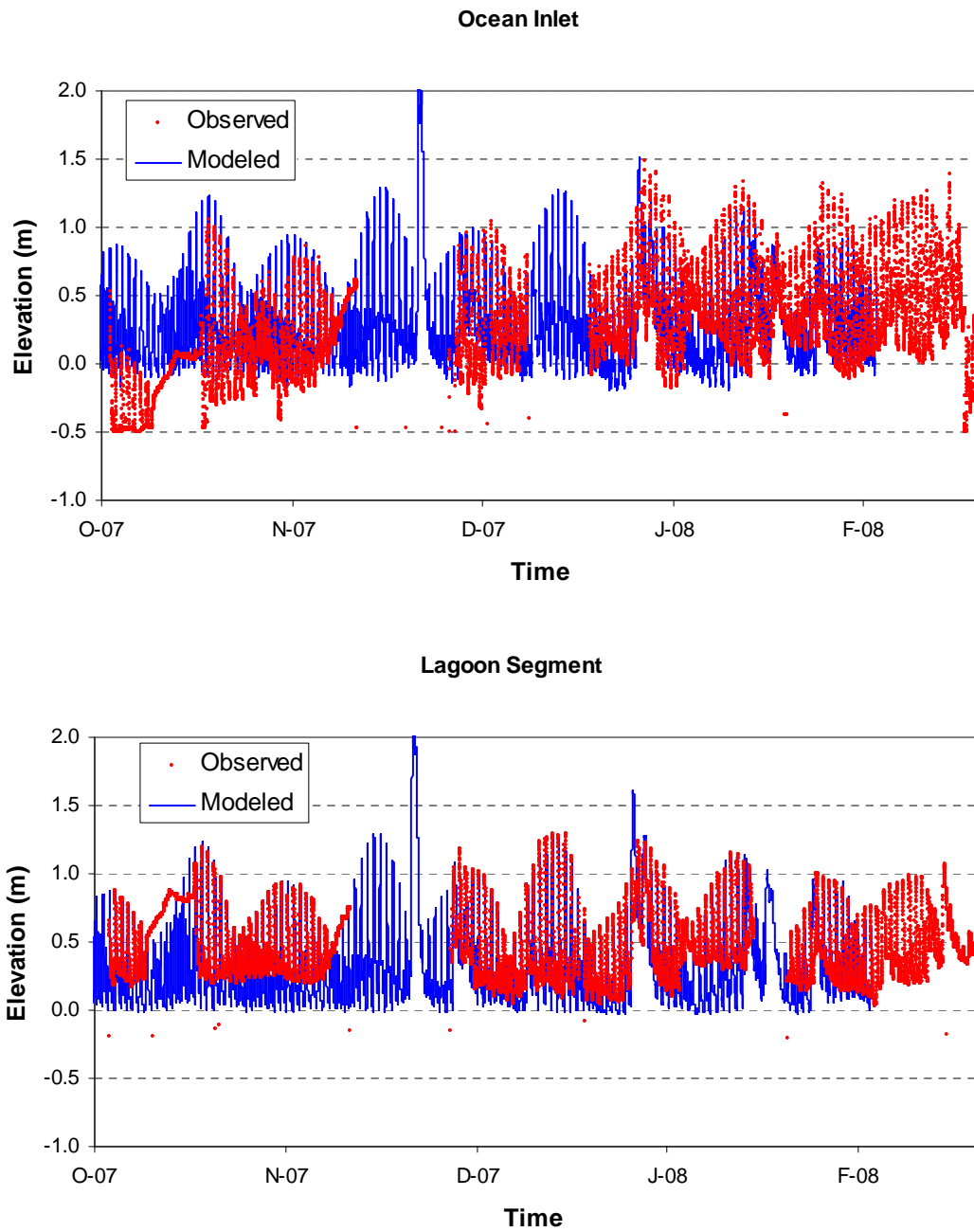


Figure 43. Water surface elevation calibration results

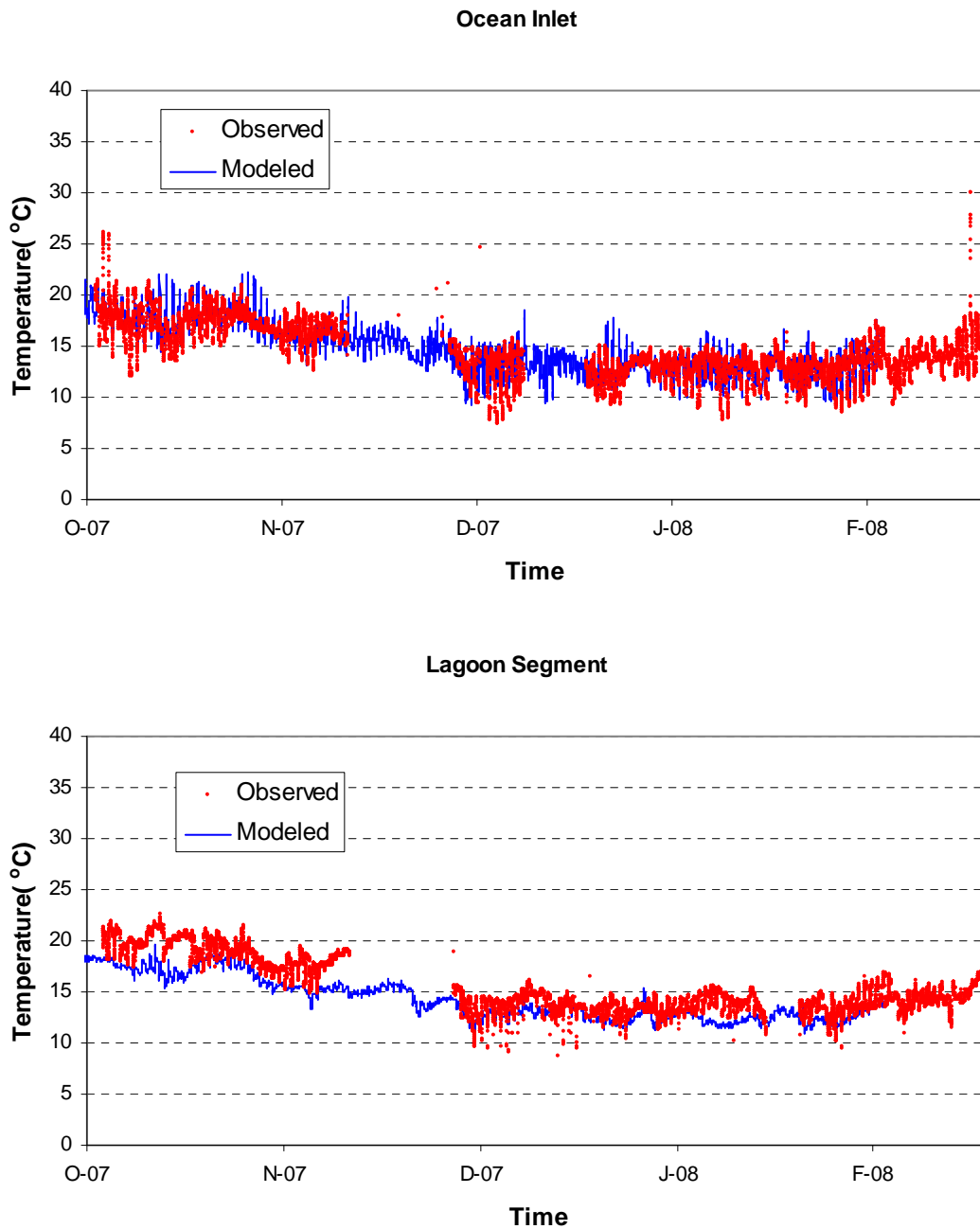


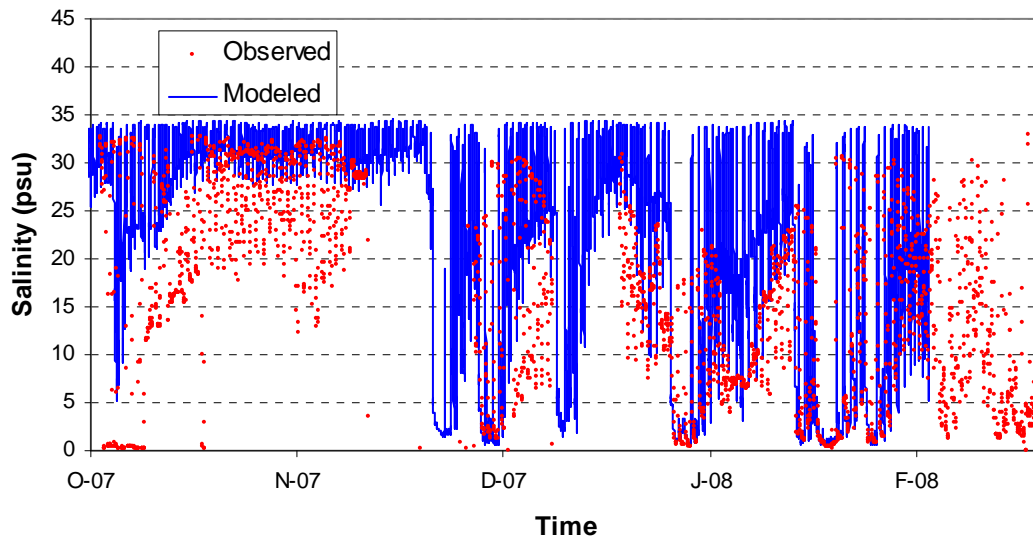
Figure 44. Temperature calibration results

Figure 45 presents the modeled and measured salinity results at the three lagoon monitoring stations. Overall, the model captured the fluctuation of salinity caused by the exchange of the ocean water and freshwater from watershed. Whenever there are storm events, the lagoon salinity decreases significantly. Salinity also changes along with the flood and ebb tides. Modeled salinity at the Ocean Inlet location agrees well with salinity data which were converted from specific conductance in terms of magnitude and fluctuation. The model under-predicted the fluctuation frequency of salinity at the Lagoon Segment location. Because the lagoon is very small compared to the watershed area, freshwater inflow has significant impact on salinity in the lagoon. The uncertainties associated with the estimation of the watershed inflows can be transported to the lagoon. In addition,

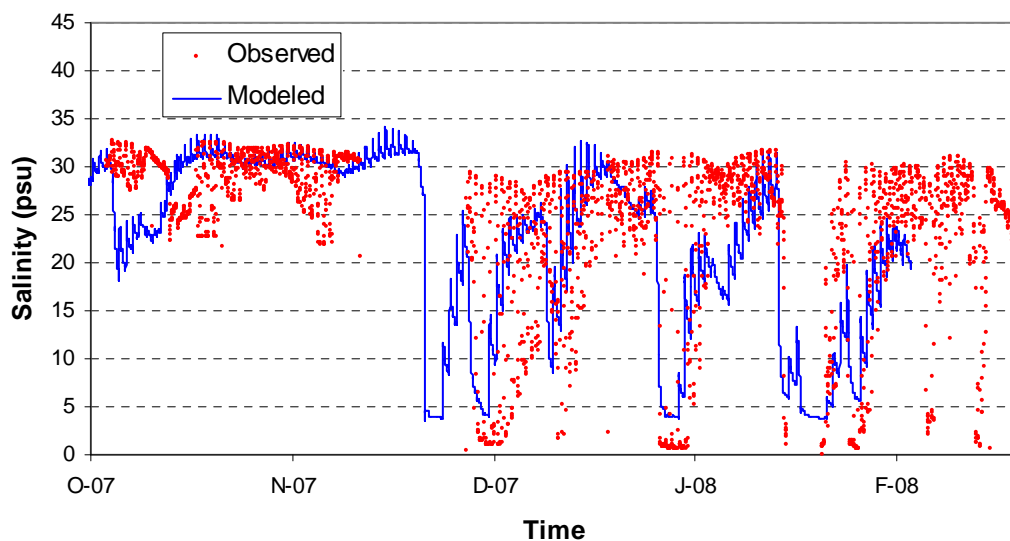


the lagoon mouth is constantly changing, but the model can only represent a fixed configuration. This approximation also brings in uncertainties in the model to calculate the salt water entering the lagoon. There are also questions related to the accuracy of the monitoring data. For example, salinity levels at the Lagoon Segment location are frequently higher than salinity levels at the Ocean Inlet location. Salinity levels at the Lagoon Segment and Ocean Inlet show a strong fluctuation in a relatively short time period, while salinities observed by the Los Peñasquitos Lagoon Foundation at station W2 show consistent high salinity during dry weather conditions. Therefore, these data can only serve for qualitative evaluation of the model performance.

Ocean Inlet



Lagoon Segment



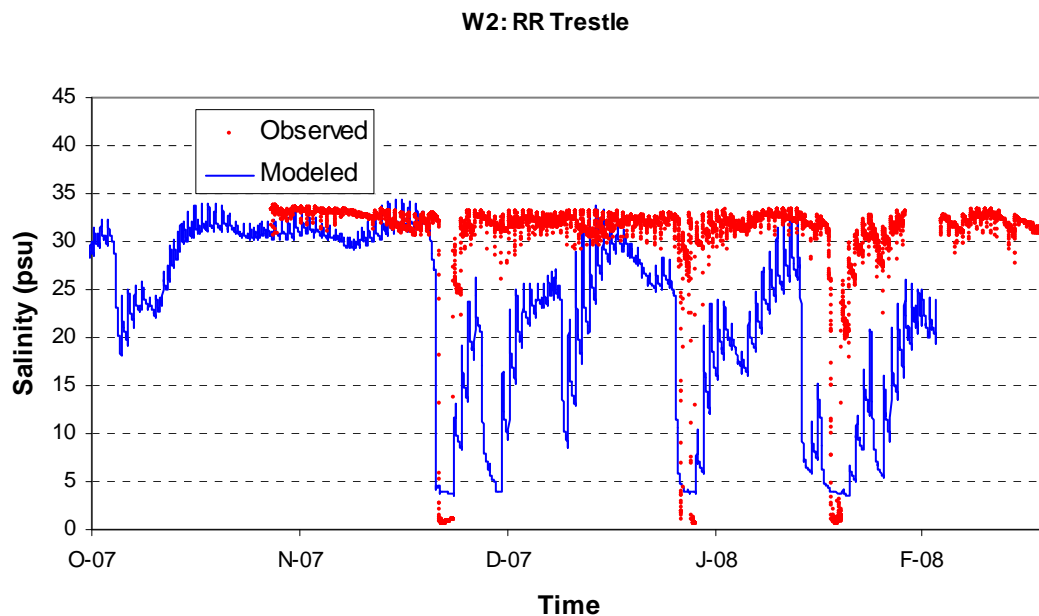


Figure 45. Salinity Calibration results for all stations (including Station W2)

Sediment Calibration

Sediment modeling in the lagoon mainly focused on the deposition and re-suspension of sand, silt, and clay fractions. The bed load transport of sand and silt was not modeled due to the lack of data needed for model representation. Sediment calibration mainly included adjustment of settling velocities for sediment deposition and critical shear stresses for sediment re-suspension. In addition, sand carried into the lagoon from the beach by flood tide represents a major source of sand based on the sediment bottom monitoring results. Monitoring was not conducted to measure the sand carried by the flood tide entering the lagoon; therefore, the concentrations of sediment at the open ocean boundary of the reduced grid were estimated during calibration. Modeled sediment components were compared against observed data during calibration.

TSS calibration plots for the Ocean Inlet and Lagoon Segment monitoring locations are shown in Figures 46 through 71. The entire calibration period is shown (Figures 46 and 59), as well as individual plots for each of the three storm events that occurred during the calibration period (Figures 47 through 49; Figures 60 through 62). In general, the model is able to capture the main pattern of sediment transport in the lagoon, which is related to storm events. The lagoon sediment in the water column increases during storm events due to the high watershed loading of sediment associated with storm events. Because the lagoon is sensitive to the watershed loadings, uncertainties associated with watershed modeling are transported to the lagoon modeling. The timing of modeled peak flow can be shifted several hours (earlier or later) and the peak concentrations of sediment may be different as compared to the observed data. For example, there appears to be a time lag in the TSS calibration results at the Lagoon Segment station (refer to Figure 60). Flow data collected at the MLS station on Los Peñasquitos Creek also indicate possible timing differences with the watershed model results, however, other information including the flow calibration results at the USGS gage upstream, TSS calibration results at each pollutograph station, and TSS calibration results at the Ocean Inlet station all indicate a good correlation with respect to time. Note that TSS grab samples were not collected at the Lagoon Segment station on 11/30/07 due to sampling problems; therefore, TSS samples were first collected on 12/1/07. Other data limitations are discussed below.



The calibration results for the Lagoon Segment station for the two later storm events (12/7/2007 and 2/3/2008) do not match because watershed flow into the lagoon during these storm events is relatively low in comparison to the first storm event (11/30/2007) (refer to Figures 59 through 62). Watershed contributions have a much greater influence on water quality conditions at this station, versus the Ocean Inlet station which showed better agreement in the calibration results. TSS calibration results for the watershed model showed good agreement for Carmel Creek; therefore, it is expected that TSS contributions from the watershed were correct. The lagoon model response for TSS was proportionate to the flow and sediment contributions from the watershed for all three storm events. It is also interesting to note that the TSS measurements from the Lagoon Segment station were similar in magnitude between the first and third storms, although watershed flows into the lagoon were much higher during the first storm. There may also be significant localized processes that affected TSS concentrations. For example, localized scour of bed or bank sediment may occur during storm events with high water velocity. The model represents the averaged condition of the channel and uses average width and depth for each grid cell. The modeled velocity for each grid cell represents average velocity and is, therefore, lower than the actual maximum velocity that can occur. Higher velocities can cause scouring and increase the sediment concentration locally, while the model will not mimic such local phenomenon. Other factors may also cause a discrepancy in the calibration results, including possible data quality issues, sample collection methods, and spatial differences in TSS concentration within lagoon channels (depth, distance from bank, etc.).

A detailed comparison of the three sediment size classes for both stations is also shown (Figures 50 through 58; Figures 63 through 71). Observed sand, silt, and clay fractions were estimated based on the TSS measurements and particle size distribution data that were derived from water column samples collected during the 11/30/07 monitoring event at these two locations. Among the three sediment classes modeled, sand is under-predicted. Sand from the ocean and watershed can settle out quickly due to its high settling velocity. Sand also moves throughout the lagoon primarily through bed load transport processes; therefore, sand concentrations near the bottom can be much higher than concentrations near the water surface. Modeled silt and clay fractions show better agreement with observed data at both stations. Note that the watershed model was calibrated using TSS rather than the individual sediment fractions. Also, particle size distributions for the observed data were based on sample results from one monitored storm event (11/30/2007). TSS data for all three storm events were separated into the three sediment classes based on the results from this single event. In addition, the particle size distribution for suspended sediment is highly time variable because of the different settling velocities for sand, silt, and clay fractions; therefore the size distribution from one storm sample cannot fully represent the size distribution of sediment throughout each storm event. Given the uncertainty of the sediment particle size distributions, model calibration focused on TSS and individual sediment class data only serve as supplemental evaluation of model performance.

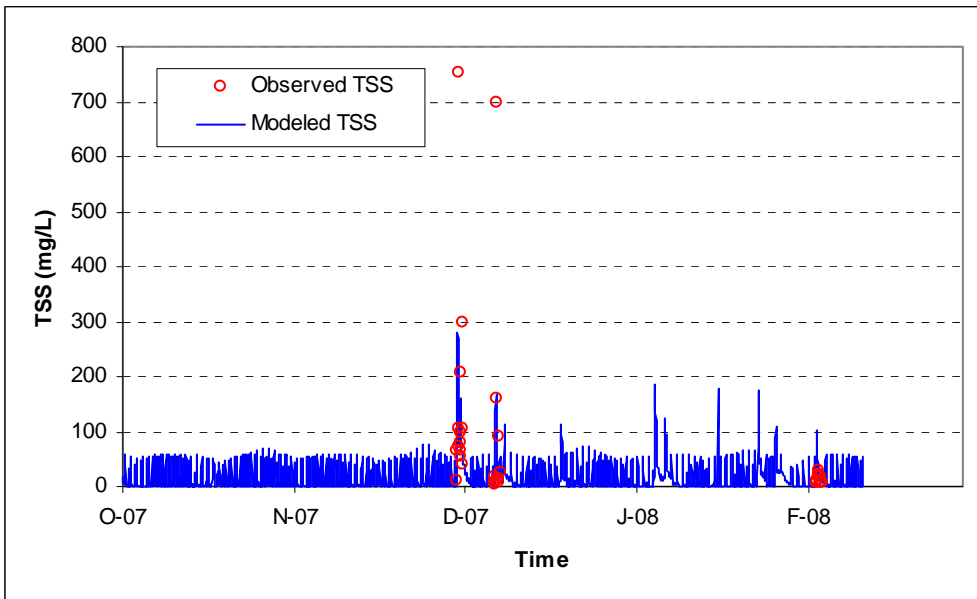


Figure 46. TSS calibration at Ocean Inlet – entire calibration period

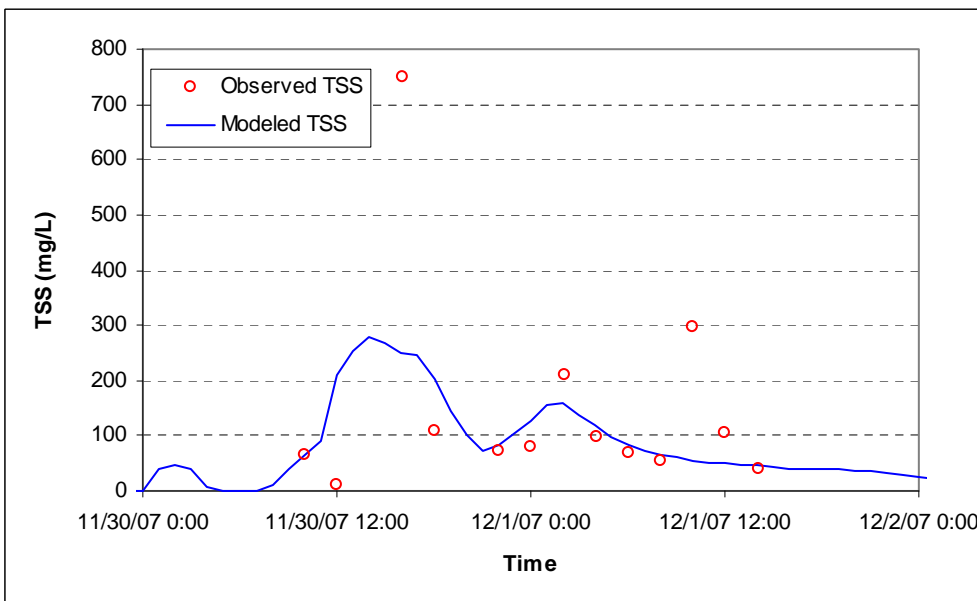


Figure 47. TSS calibration at Ocean Inlet – 11/30/2007 storm

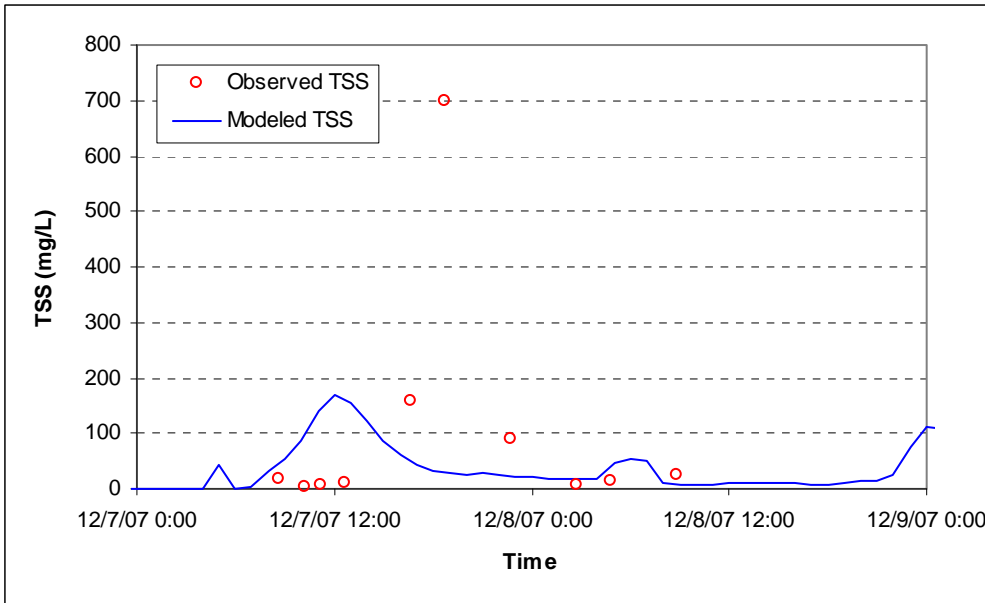


Figure 48. TSS calibration at Ocean Inlet – 12/7/2007 storm

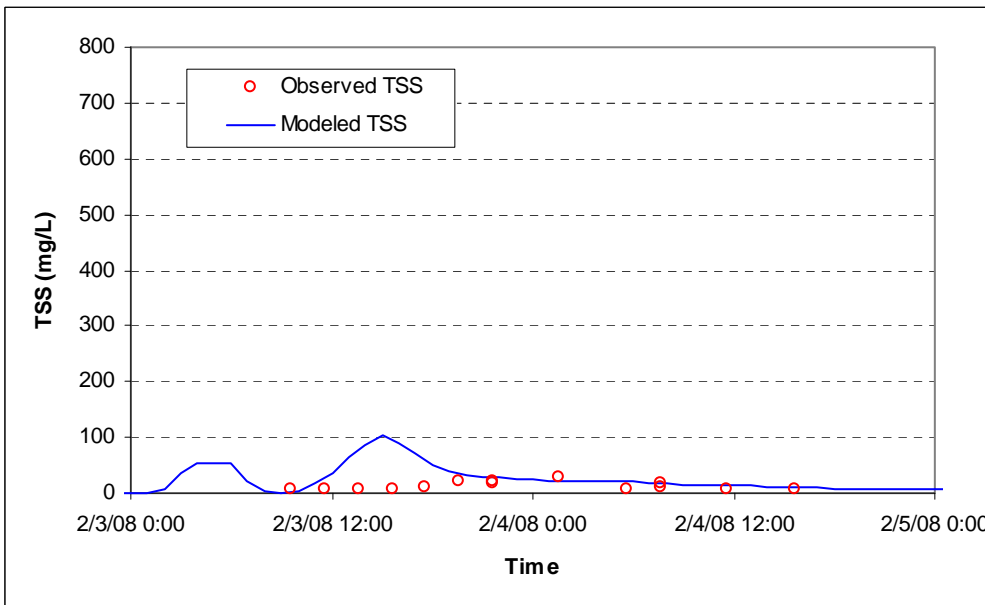


Figure 49. TSS calibration at Ocean Inlet – 2/3/2008 storm

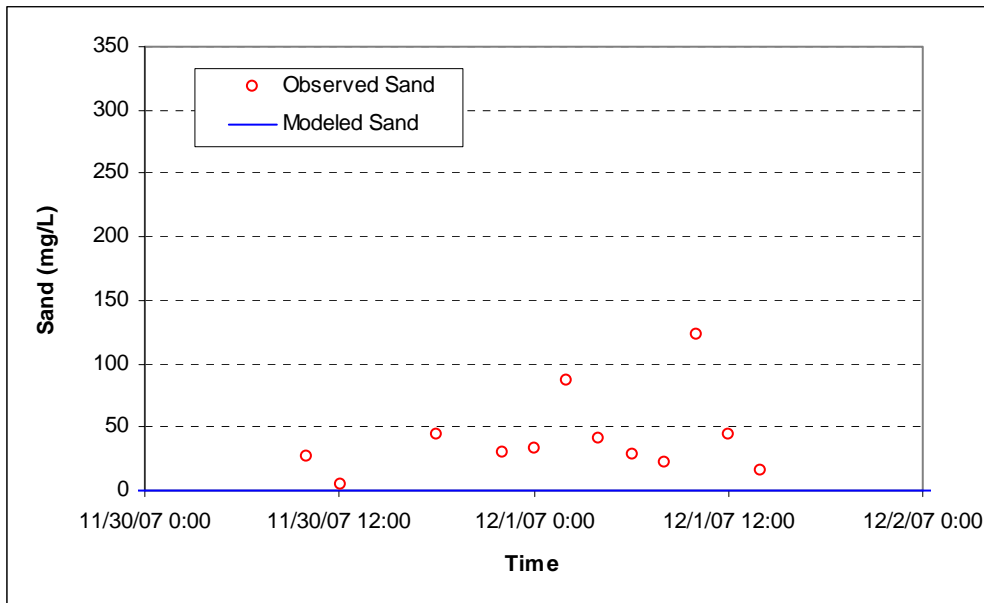


Figure 50. Modeled vs. observed sand fraction at Ocean Inlet - 11/30/2007 storm

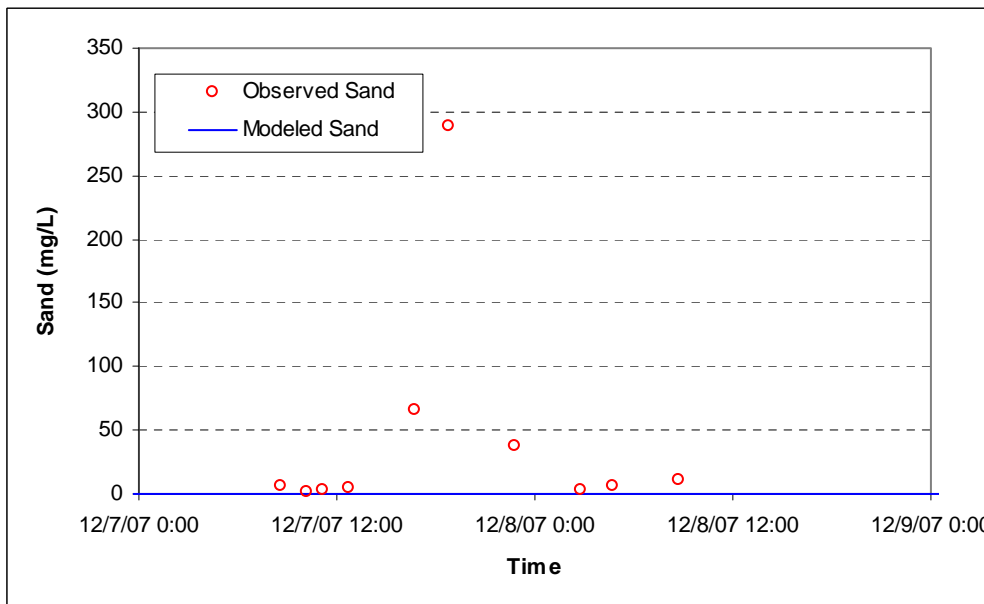


Figure 51. Modeled vs. observed sand fraction at Ocean Inlet - 12/7/2007 storm

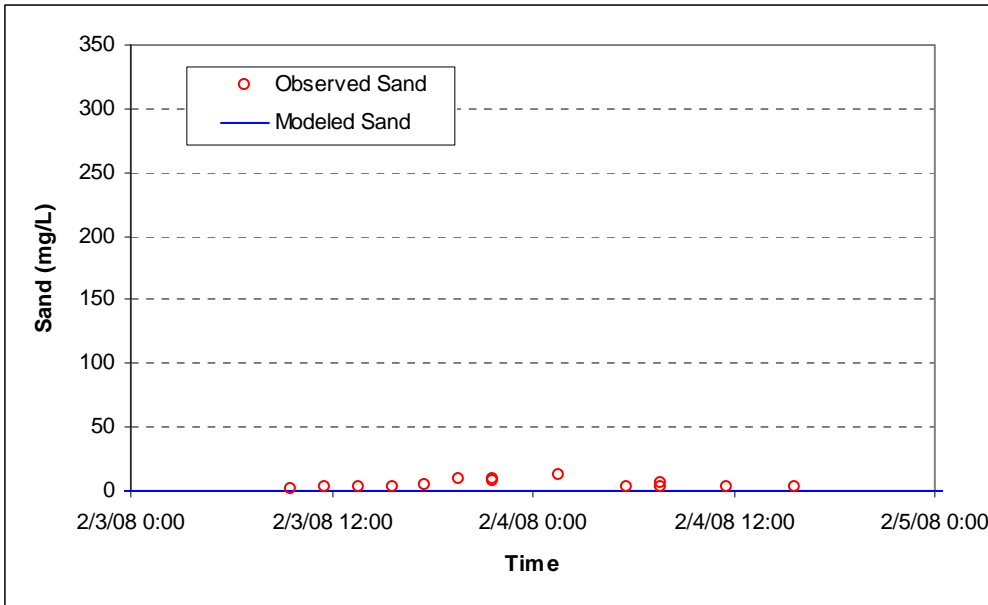


Figure 52. Modeled vs. observed sand fraction at Ocean Inlet – 2/3/2008 storm

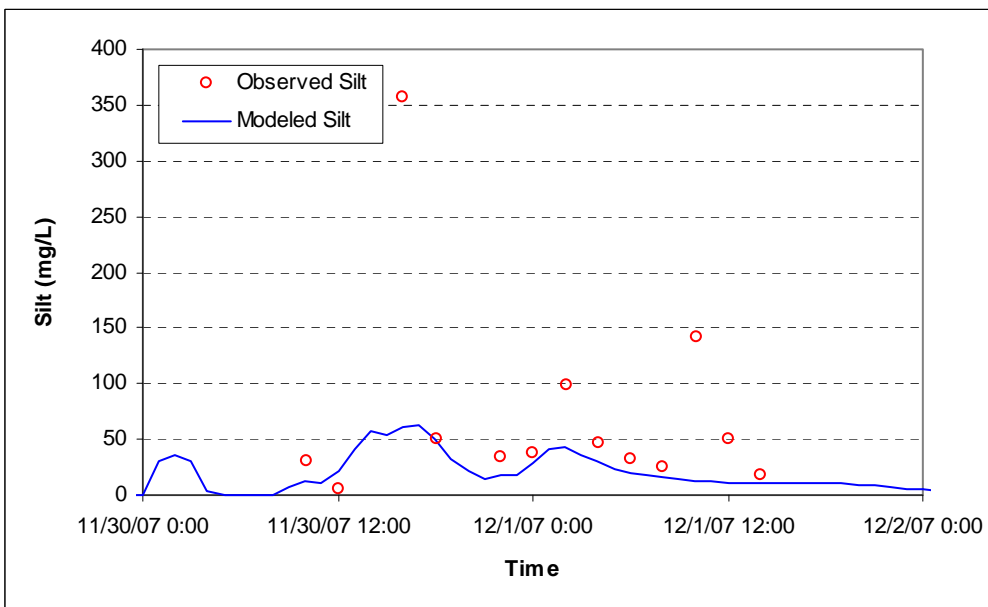


Figure 53. Modeled vs. observed silt fraction at Ocean Inlet – 11/30/2007 storm

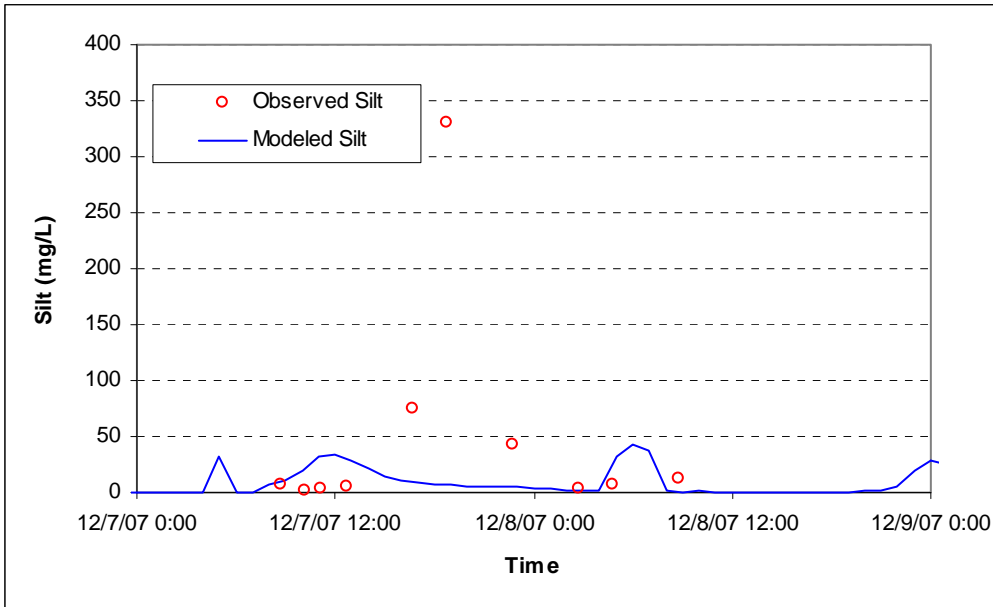


Figure 54. Modeled vs. observed silt fraction at Ocean Inlet – 12/7/2007 storm

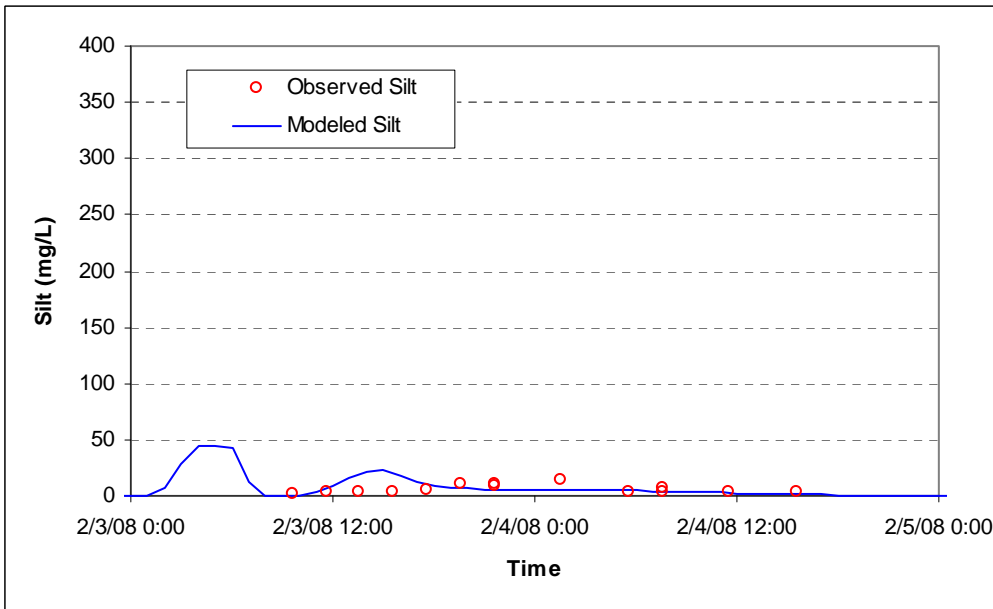


Figure 55. Modeled vs. observed silt fraction at Ocean Inlet – 2/3/2008 storm

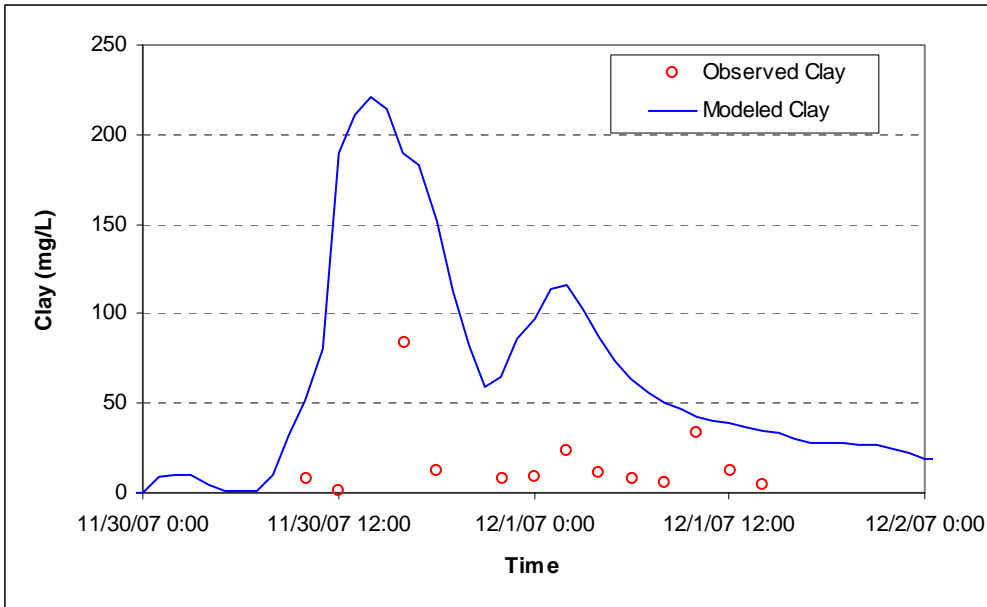


Figure 56. Modeled vs. observed clay fraction at Ocean Inlet – 11/30/2007 storm

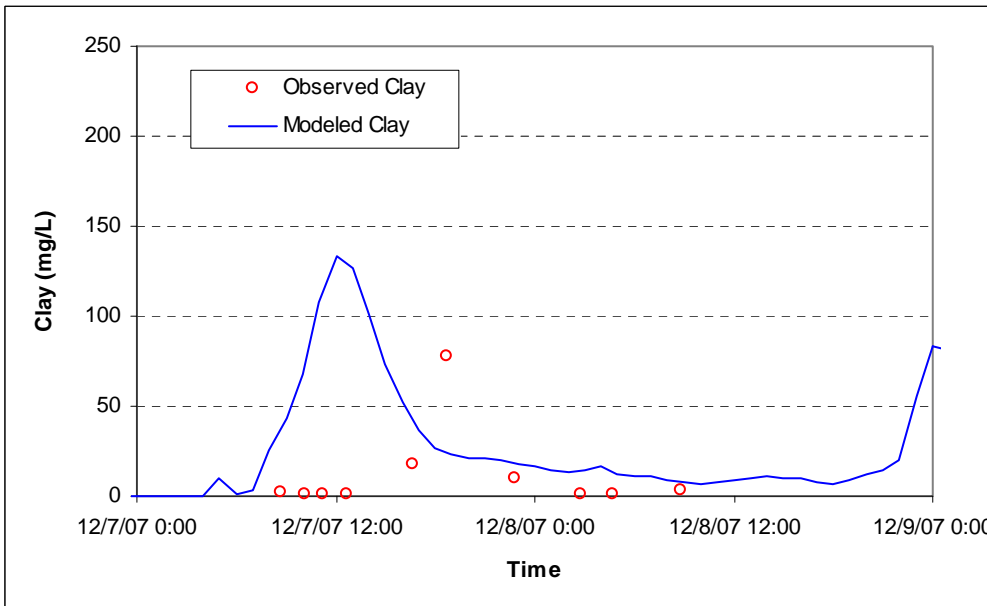


Figure 57. Modeled vs. observed clay fraction at Ocean Inlet – 12/7/2007 storm

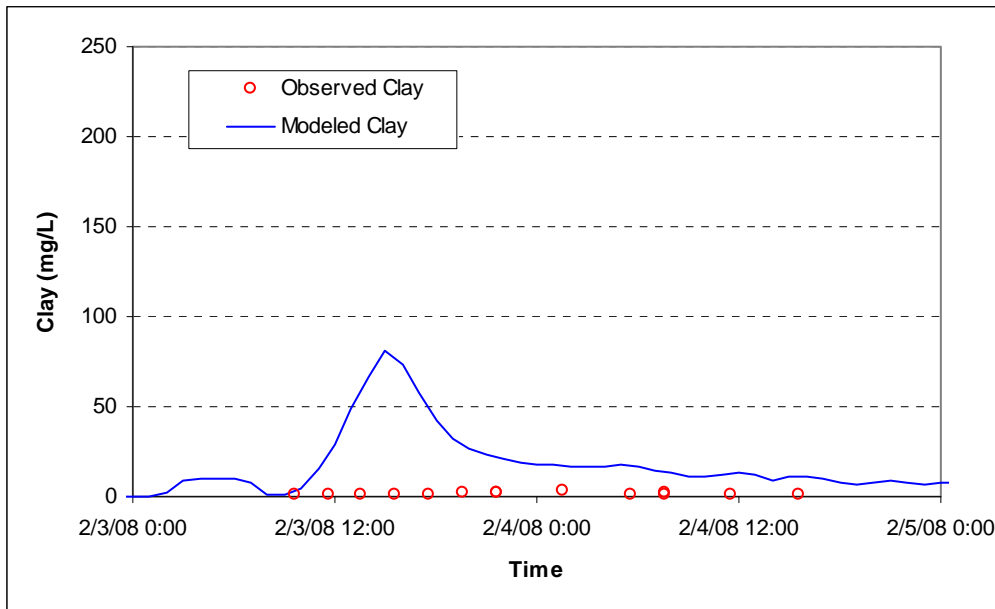


Figure 58. Modeled vs. observed clay fraction at Ocean Inlet – 2/3/2008 storm

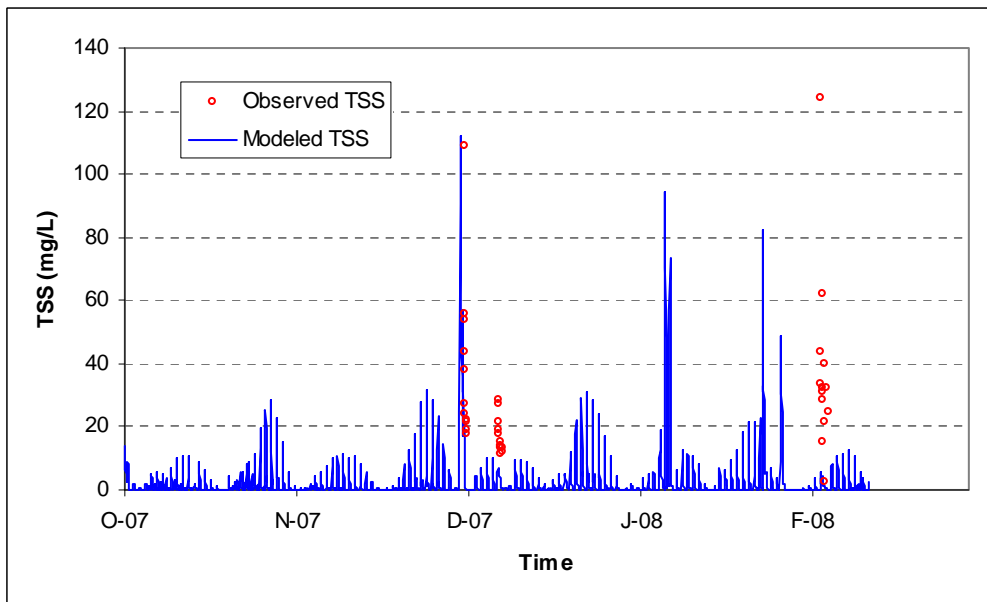


Figure 59. TSS calibration at Lagoon Segment – entire calibration period

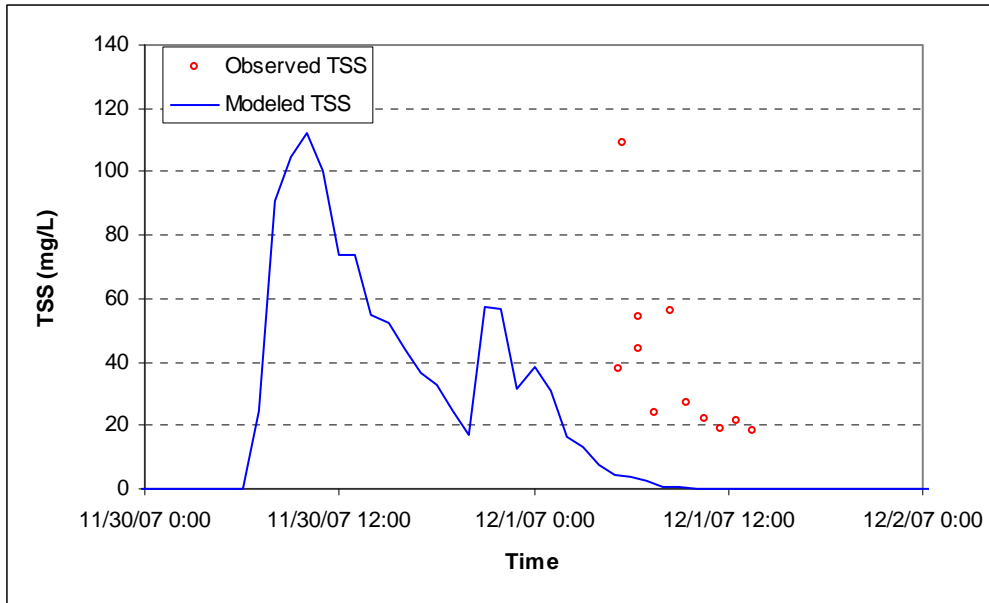


Figure 60. TSS calibration at Lagoon Segment – 11/30/2007 storm

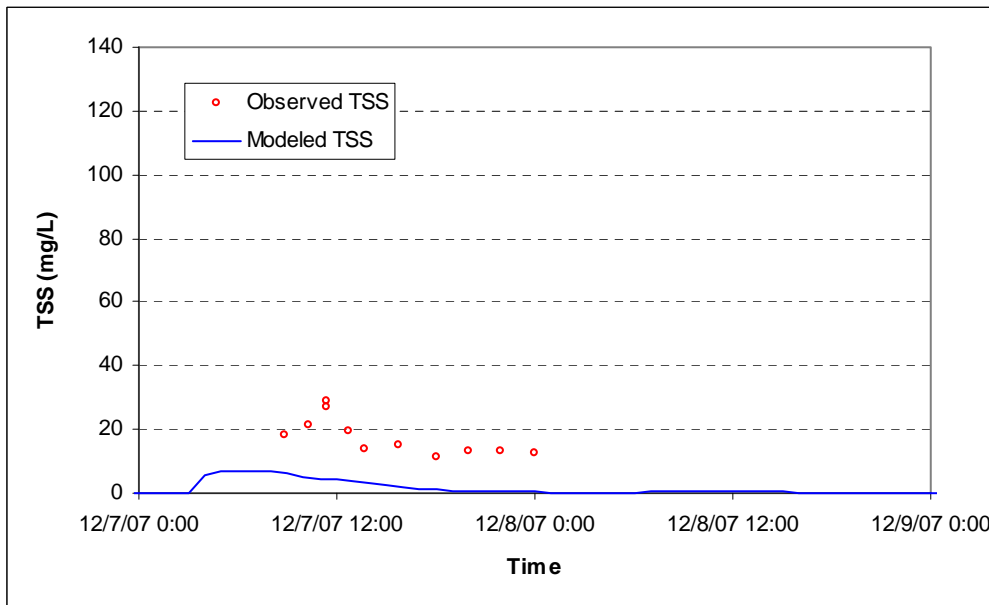


Figure 61. TSS calibration at Lagoon Segment – 12/7/2007 storm

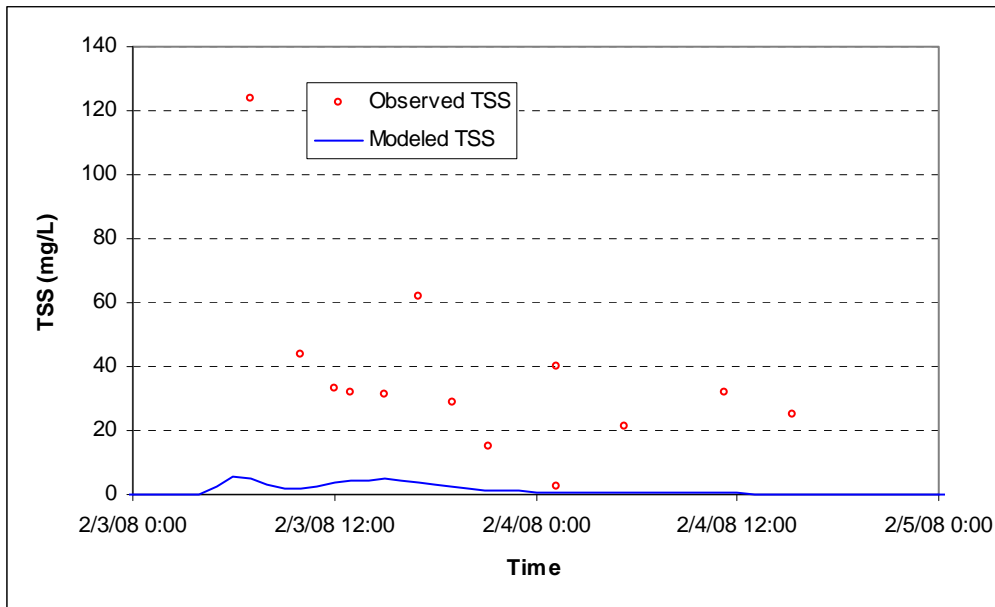


Figure 62. TSS calibration at Lagoon Segment – 2/3/2008 storm

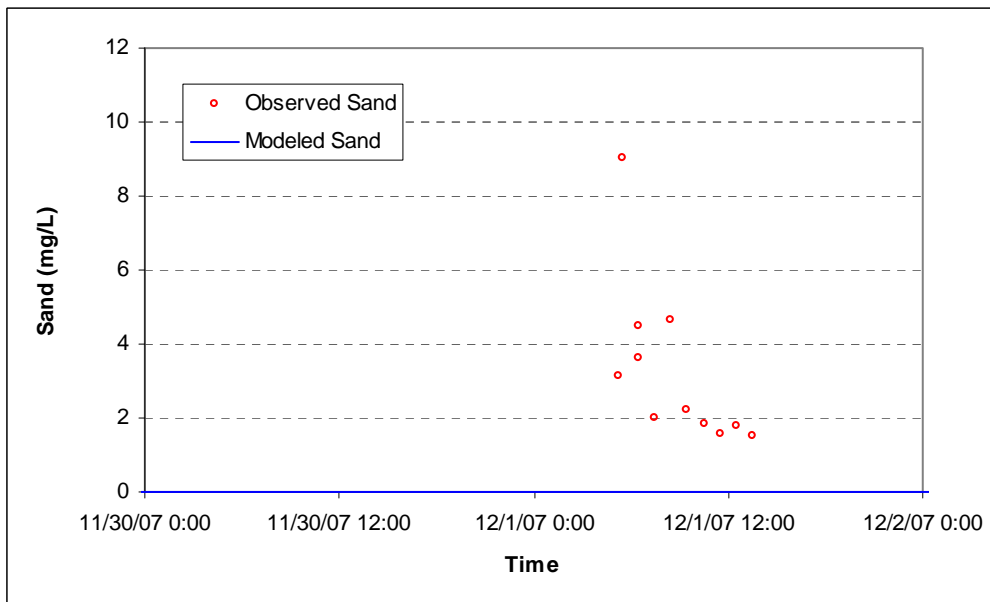


Figure 63. Modeled vs. observed sand fraction at Lagoon Segment – 11/30/2007 storm

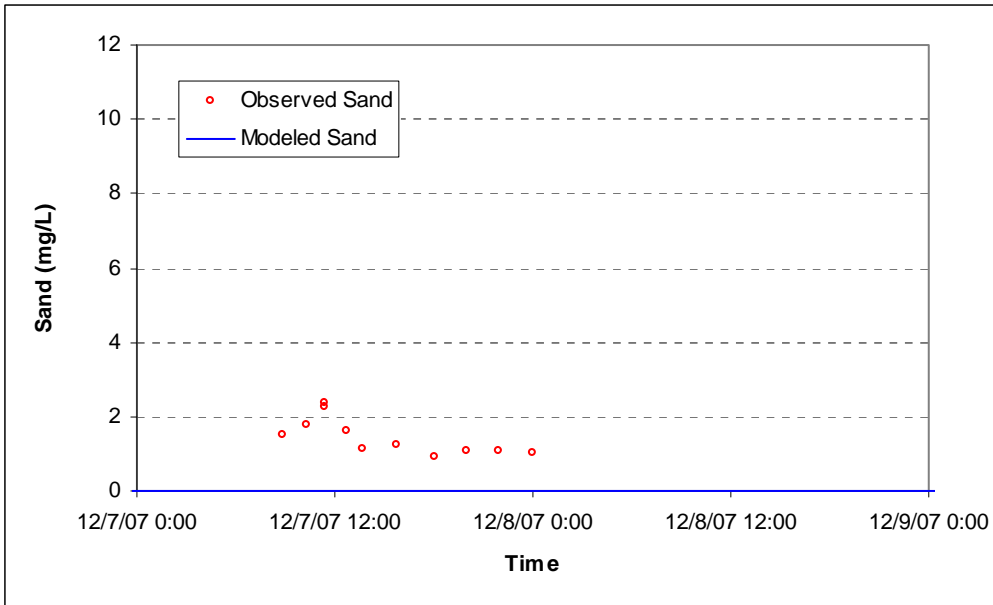


Figure 64. Modeled vs. observed sand fraction at Lagoon Segment – 12/7/2007 storm

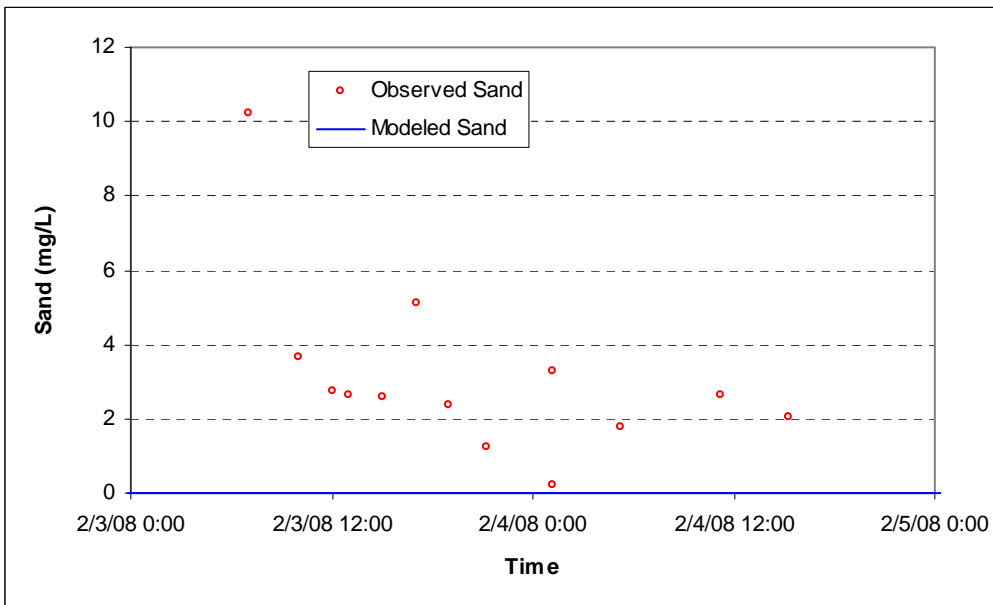


Figure 65. Modeled vs. observed sand fraction at Lagoon Segment – 2/3/2008 storm

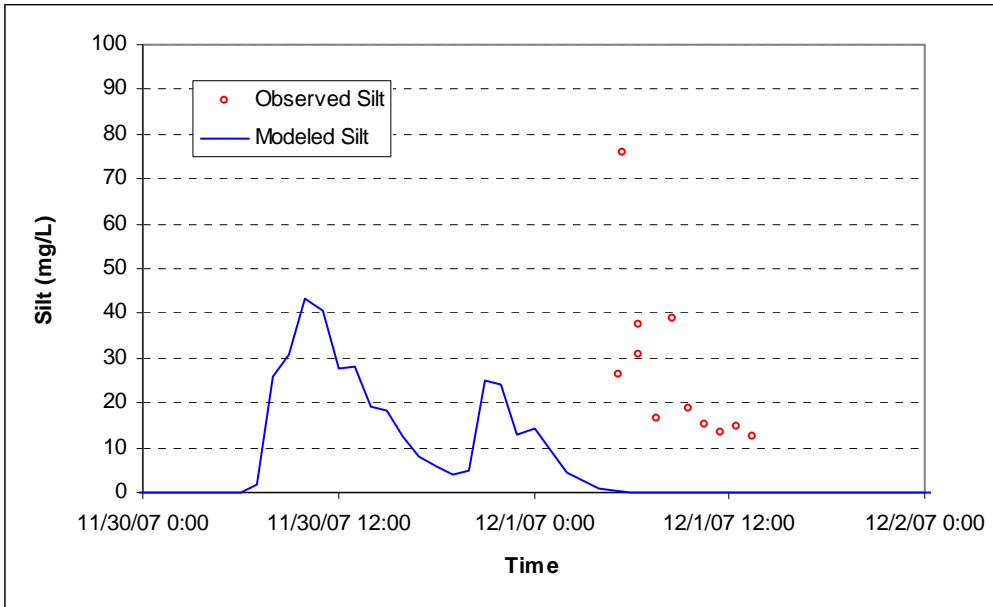


Figure 66. Modeled vs. observed silt fraction at Lagoon Segment - 11/30/2007 storm

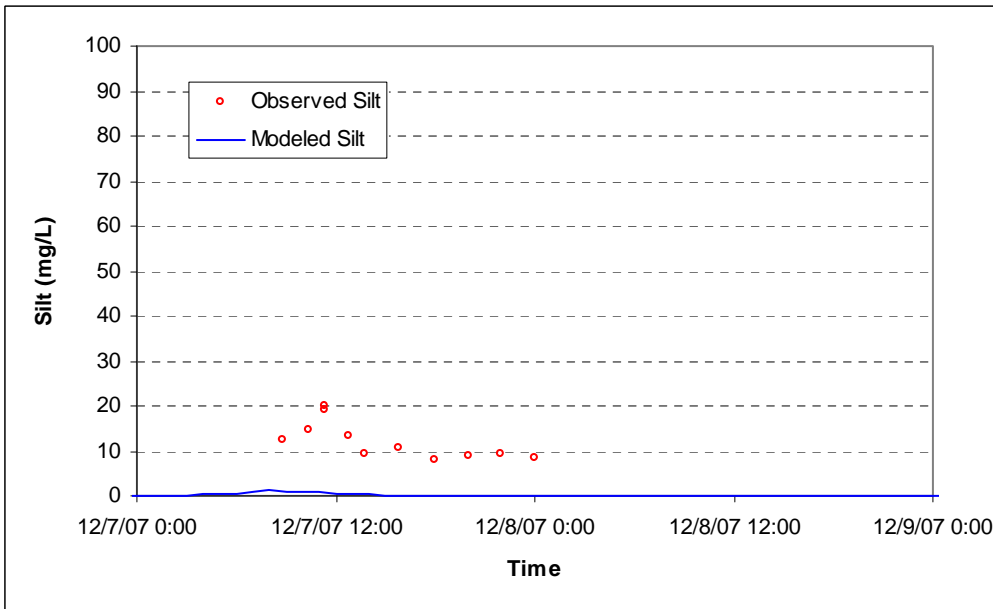


Figure 67. Modeled vs. observed silt fraction at Lagoon Segment - 12/7/2007 storm

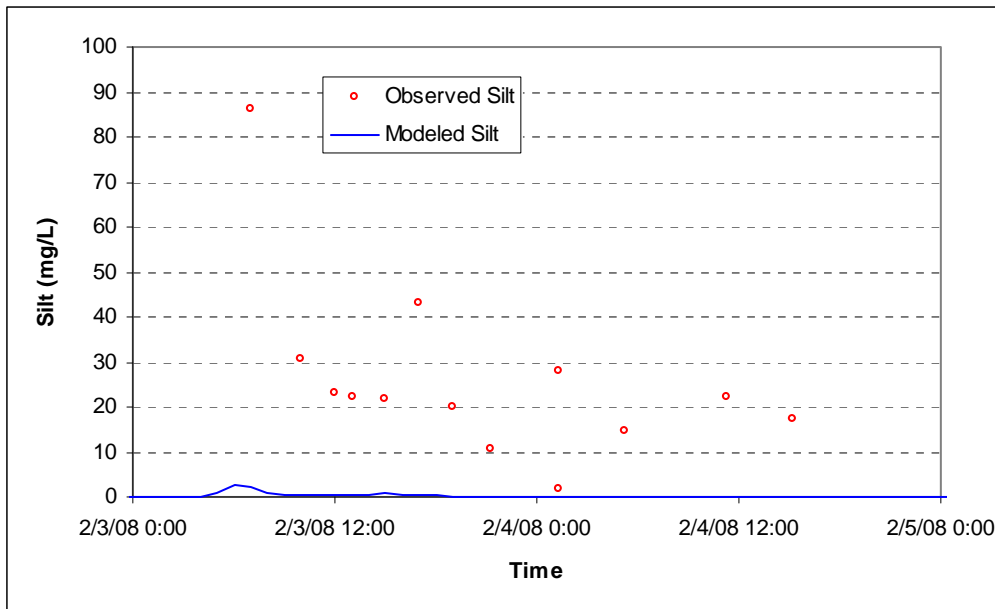
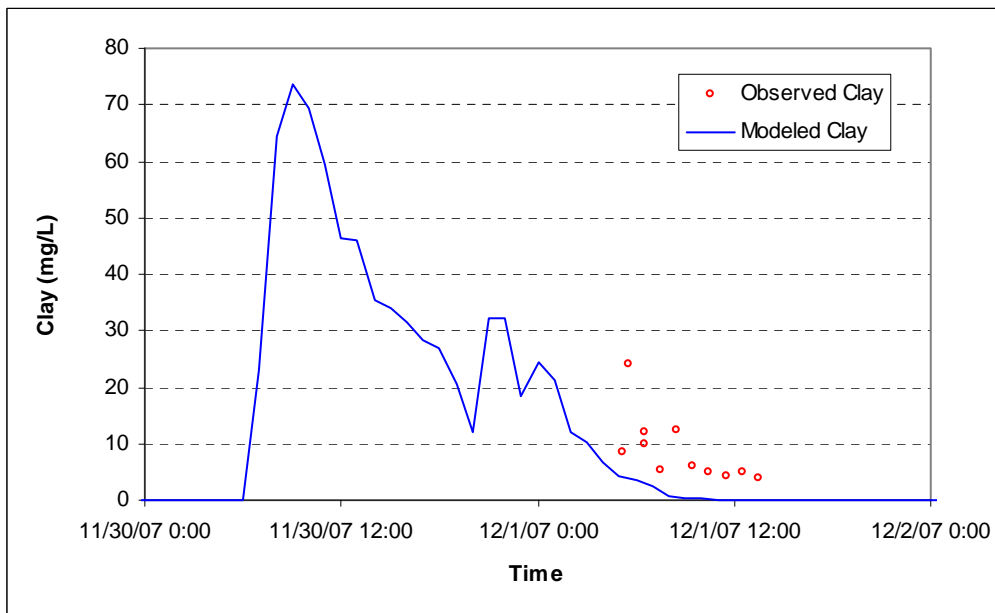


Figure 68. Modeled vs. observed silt fraction at Lagoon Segment – 2/3/2008 storm



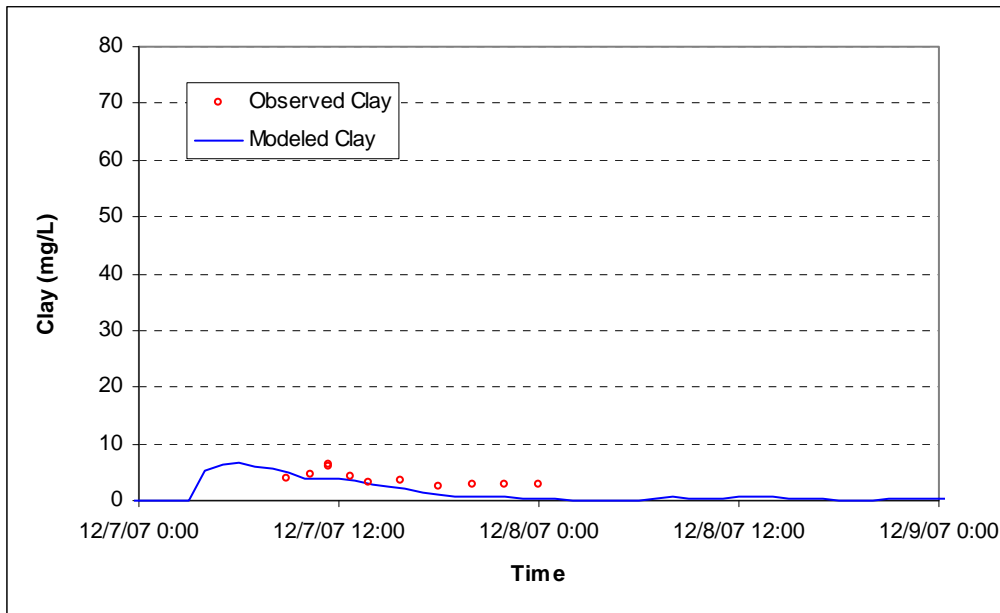


Figure 70. Modeled vs. observed clay fraction at Lagoon Segment – 12/7/2007 storm

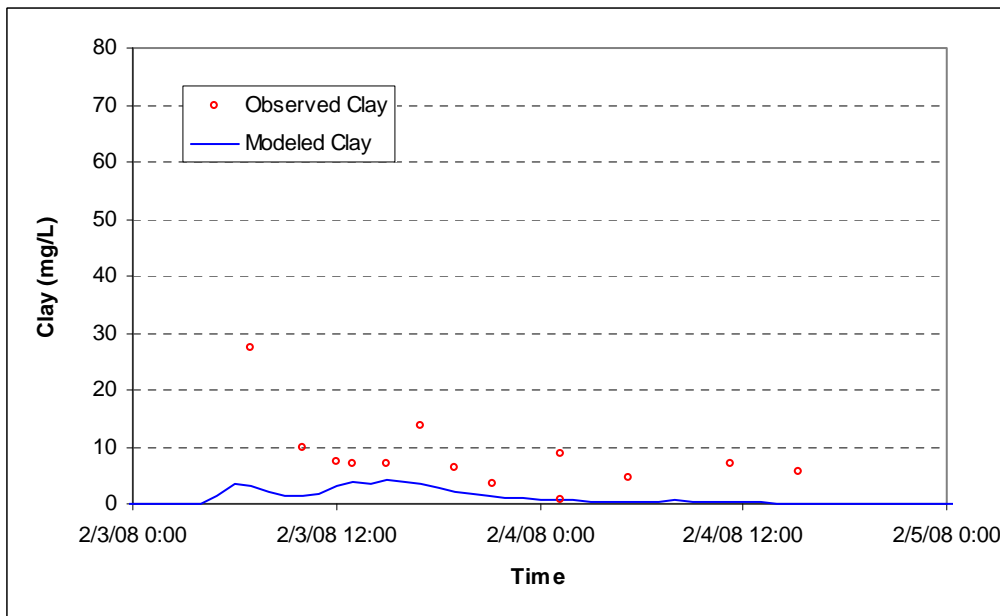


Figure 71. Modeled vs. observed clay fraction at Lagoon Segment – 2/3/2008 storm



Summary and Conclusions

A dynamic model was developed for the Los Peñasquitos Lagoon for simulating the transport of sediment through the lagoon using the EFDC framework. The model considered the ocean and watershed contributions of sediment. Model development involved two steps. In the first step, the model grid was extended into the ocean to use the tide elevation, salinity, and water temperature in the open ocean to drive the simulation of hydrodynamic conditions. After hydrodynamic calibration, the model was run using a reduced grid that incorporated the modeled water surface elevation, salinity, and water temperature at the immediate outside of the ocean inlet as the driving boundary conditions because the open ocean sediment conditions are significantly different from those at the ocean inlet. The sediment model was then calibrated using the reduced grid.

The Los Peñasquitos modeling framework can be used to simulate various management scenarios and for TMDL development purposes. In order to examine management scenarios related to controlling ocean and/or watershed inputs of sediment, model boundary conditions, the watershed model configuration, and the lagoon model grid can all be modified accordingly. For example, if the ocean inlet is widened, the model grid size can be increased at the ocean inlet. The application of BMPs within the watershed to control sediment input to the lagoon can also be examined through modifications to the sediment time series from the watershed, based on estimated BMP efficiencies, which can then be used to examine future changes in lagoon conditions. For management scenarios that involve dredging and other lagoon modifications, initial sediment bed conditions, such as the particle size distributions, can be updated accordingly.

References

- Ackerman, D. and SW Weisberg, 2006. Evaluating HSPF runoff and water quality predictions at multiple time and spatial scales. Southern California Coastal Water Research Project 2005-06 Annual Report. pp.293-303.
- Bicknell, B.R., J.C. Imhoff, J.L. Kittle, Jr., A.S. Donigian, Jr., and R.C. Johanson, 1997. Hydrological Simulation Program–FORTRAN, Users Manual for Version 11. EPA/600/R-97/080, U.S. Environmental Protection Agency, National Exposure Research Laboratory. Athens, Georgia, 755 pp.
- California Regional Water Quality Control Board, San Diego Region (CARWQCB) and US Environmental Protection Agency (USEPA). 2005. Bacteria-Impaired Waters TMDL Project II for Lagoons and Adjacent Beaches in the San Diego Region. Technical Draft.
- Cerco, C. F. and T. Cole. 1994. Three-Dimensional Eutrophication Model of Chesapeake Bay, Volume I: Main Report U.S. Army Corps of Engineers Waterway Experiment Station, Vicksburg, MS., EL-94.4.
- City of San Diego. 2009. TMDL Monitoring For Sedimentation/Siltation in Los Peñasquitos Lagoon. Report prepared for the City of Poway, City of Del Mar, City of San Diego, County of San Diego, and California Department of Transportation by Weston Solutions, Carlsbad, California.
- Hamrick, J.M. 1992. A Three-Dimensional Environmental Fluid Dynamics Computer Code: Theoretical and Computational Aspects, Special Report 317. The College of William and Mary, Virginia Institute of Marine Science, Gloucester Point, VA.
- Hany, E., White, M., and Goodell, K. 2007. 2006 Annual Monitoring of Sedimentation in Los Peñasquitos Lagoon. Submitted to: Los Peñasquitos Lagoon Foundation
- Li, Yingxia, Lau, Kayhanian, and Stenstrom. 2005. Particle Size Distribution in Highway Runoff. Journal of Environmental Engineering. Volume 131(9): 1267-1276.
- Lumb, A.M., McCammon, R.B., and Kittle, J.L., Jr. 1994. Users manual for an expert system (HSPexp) for calibration of the Hydrologic Simulation Program–Fortran: U.S. Geological Survey Water-Resources Investigations Report 94-4168, 102 p.
- Shen, J., A. Parker, and J. Riverson. 2004. A New Approach for a Windows-based Watershed Modeling System Based on a Database-supporting Architecture. Environmental Modeling and Software, July 2004.
- Solomon, K.H. 1988. Irrigation Notes: Irrigation System Selection, Irrigation Systems and Water Application Efficiencies. Center for Irrigation Technology, California State University, Fresno, CA.
<http://cati.csufresno.edu/cit/rese>.
- Tetra Tech and USEPA (U.S. Environmental Protection Agency). 2002. The Loading Simulation Program in C++ (LSPC) Watershed Modeling System – User’s Manual.
- Tetra Tech. 2002. User’s Manual for Environmental Fluid Dynamics Code: Hydrodynamics. Prepared for the U.S. Environmental Protection Agency, Region 4, by Tetra Tech, Inc., Fairfax, VA.
- Tetra Tech. 2006a. User’s Manual for Environmental Fluid Dynamics Code: Water Quality. Prepared for the U.S. Environmental Protection Agency, Region 4, Tetra Tech, Inc., Fairfax, VA.
- Tetra Tech. 2006b. The Environmental Fluid Dynamics Code, Theory and Computation: Volume 1: Hydrodynamics. Tetra Tech, Inc., Fairfax, VA.
- Tetra Tech. 2006c. The Environmental Fluid Dynamics Code, Theory and Computation: Volume 2: Sediment and Contaminant Transport and Fate. Tetra Tech, Inc., Fairfax, VA.



Tetra Tech. 2006d. The Environmental Fluid Dynamics Code, Theory and Computation: Volume 3: Water Quality and Eutrophication. Tetra Tech, Inc., Fairfax, VA.

Tetra Tech, Inc. 2007. Green River, MA Sediment Stability Analysis. Memorandum May 25, 2007. Prepared by John Hamrick.

USEPA (U.S. Environmental Protection Agency). 2006. BASINS Technical Note 8: Sediment Parameter and Calibration Guidance for HSPF. U. S. Environmental Protection Agency, Office of Water, Washington, D.C.

USEPA (U.S. Environmental Protection Agency). 2003. Fact Sheet: Loading Simulation Program in C++. USEPA, Watershed and Water Quality Modeling Technical Support Center, Athens, GA. Available at: <http://www.epa.gov/athens/wwqtsc/LSPC.pdf>.

UNESCO. 1983. Algorithms for computation of fundamental properties of seawater. UNESCO technical papers in marine science 44:1-55

University of California Cooperative Extensive. 2000. A Guide to Estimating Irrigation Water Needs of Landscape Plantings in California. California Department of Water Resources, Sacramento, CA. Available at: <http://www.owue.water.ca.gov/docs/wucols00.pdf>.

USGS. 2009. <http://waterdata.usgs.gov/nwis/qw>. Accessed 09/01/2009.

Vanoni, V. A. ed., 1975. Sedimentation engineering. New York, American Society of Civil Engineers, 745 p.

Williams, G.D. 1997. The physical, chemical, and biological monitoring of Los Peñasquitos Lagoon, 1996-97. Annual report prepared for the Los Peñasquitos Lagoon Foundation. Prepared by Pacific Estuarine Research Laboratory. November 1997.

Wischmeier, W.H. and D.D. Smith. 1978. Predicting Rainfall Erosion Losses – A Guide to Conservation Planning. Agricultural Handbook 537. U.S. Department of Agriculture, Washington, DC.



Appendix A: Model Hydrology Parameters

Table A-1. 110 pwat-parm2

defid	deluid	lzsnn	infiltr	kvary	agwrc
2	1	3.4	0.01	0.2	0.99
2	2	3.4	0.01	0.2	0.99
2	3	3.4	0.01	0.2	0.99
2	4	3.4	0.01	0.2	0.99
2	5	8	0.33	0.2	0.99
2	6	4	0.01	0.2	0.99
2	7	4.5	0.3	0.2	0.99
2	8	6.2	0.35	0.2	0.99
2	9	6.2	0.35	0.2	0.99
2	10	6.2	0.35	0.2	0.99
2	11	6.3	0.4	0.2	0.99
2	13	4.5	0.4	0.2	0.99
2	14	4	0.01	0.2	0.99
2	15	4	0.01	0.2	0.99
2	16	4	0.01	0.2	0.99
2	17	4	0.01	0.2	0.99
2	18	4	0.01	0.2	0.99
2	19	4	0.01	0.2	0.99
2	1	3.5	0.01	0.2	0.99
2	2	3.5	0.01	0.2	0.99
2	3	3.5	0.01	0.2	0.99
2	4	3.5	0.01	0.2	0.99
2	5	6.4	0.31	0.2	0.99
2	6	5	0.01	0.2	0.99
2	7	5.3	0.25	0.2	0.99
2	8	6.4	0.3	0.2	0.99
2	9	6.4	0.3	0.2	0.99
2	10	6.4	0.3	0.2	0.99
2	11	5	0.2	0.2	0.99
2	13	4.7	0.05	0.2	0.99
2	14	3.7	0.01	0.2	0.99
2	15	3.7	0.01	0.2	0.99
2	16	3.7	0.01	0.2	0.99
2	17	3.7	0.01	0.2	0.99
2	18	3.7	0.01	0.2	0.99
2	19	3.7	0.01	0.2	0.99
2	1	3.6	0.01	0.2	0.99
2	2	3.6	0.01	0.2	0.99
2	3	3.6	0.01	0.2	0.99
2	4	3.6	0.01	0.2	0.99
2	5	8	0.3	0.2	0.99
2	6	5.3	0.01	0.2	0.99
2	7	5.5	0.23	0.2	0.99

defid	deluid	lzsnn	infiltr	kvary	agwrc
2	8	6.5	0.23	0.2	0.99
2	9	6.5	0.23	0.2	0.99
2	10	6.5	0.23	0.2	0.99
2	11	5	0.1	0.2	0.99
2	13	4.7	0.05	0.2	0.99
2	14	3.8	0.01	0.2	0.99
2	15	3.8	0.01	0.2	0.99
2	16	3.8	0.01	0.2	0.99
2	17	3.8	0.01	0.2	0.99
2	18	3.8	0.01	0.2	0.99
2	19	3.8	0.01	0.2	0.99
2	1	3.4	0.01	0.2	0.99
2	2	3.4	0.01	0.2	0.99
2	3	3.4	0.01	0.2	0.99
2	4	3.4	0.01	0.2	0.99
2	5	8	0.33	0.2	0.99
2	6	4	0.01	0.2	0.99
2	7	4.5	0.3	0.2	0.99
2	8	6.2	0.35	0.2	0.99
2	9	6.2	0.35	0.2	0.99
2	10	6.2	0.35	0.2	0.99
2	11	6.3	0.4	0.2	0.99
2	13	4.5	0.4	0.2	0.99
2	14	4	0.01	0.2	0.99
2	15	4	0.01	0.2	0.99
2	16	4	0.01	0.2	0.99
2	17	4	0.01	0.2	0.99
2	18	4	0.01	0.2	0.99
2	19	4	0.01	0.2	0.99

defid parameter group id

deluid land use id

lzsnn lower zone nominal soil moisture storage (inches)

infiltr index to the infiltration capacity of the soil (in/hr)

kvary variable groundwater recession (1/inches)

agwrc base groundwater recession (none)



Table A-2. 120 pwat-parm3

defid	deluid	petmax	petmin	infexp	infilid	deepfr	basetp	agwetp
2	1	40	35	2	2	0.1	0	0.01
2	2	40	35	2	2	0.1	0	0.01
2	3	40	35	2	2	0.1	0	0.01
2	4	40	35	2	2	0.1	0	0.01
2	5	40	35	2	2	0.1	0.03	0.05
2	6	40	35	2	2	0.1	0	0.01
2	7	40	35	2	2	0.1	0	0.01
2	8	40	35	2	2	0.1	0	0.01
2	9	40	35	2	2	0.1	0	0.05
2	10	40	35	2	2	0.1	0	0.05
2	11	40	35	2	2	0.1	0.03	0.03
2	13	40	35	2	2	0.1	0	0.03
2	14	40	35	2	2	0.1	0	0
2	15	40	35	2	2	0.1	0	0
2	16	40	35	2	2	0.1	0	0
2	17	40	35	2	2	0.1	0	0
2	18	40	35	2	2	0.1	0	0
2	19	40	35	2	2	0.1	0	0
3	1	40	35	2	2	0.1	0	0.01
3	2	40	35	2	2	0.1	0	0.01
3	3	35	30	2	2	0.1	0	0.01
3	4	35	30	2	2	0.1	0	0.01
3	5	40	35	2	2	0.1	0.03	0.05
3	6	40	35	2	2	0.1	0	0.01
3	7	40	35	2	2	0.1	0	0.01
3	8	40	35	2	2	0.1	0	0.01
3	9	40	35	2	2	0.1	0	0.05
3	10	40	35	2	2	0.1	0	0.05
3	11	40	35	2	2	0.1	0.02	0.03
3	13	40	35	2	2	0.1	0	0.03
3	14	35	30	2	2	0.1	0	0
3	15	40	35	2	2	0.1	0	0
3	16	40	35	2	2	0.1	0	0
3	17	35	30	2	2	0.1	0	0
3	18	40	35	2	2	0.1	0	0
3	19	40	35	2	2	0.1	0	0
4	1	40	35	2	2	0.1	0	0.01
4	2	40	35	2	2	0.1	0	0.01
4	3	40	35	2	2	0.1	0	0.01
4	4	40	35	2	2	0.1	0	0.01
4	5	40	35	2	2	0.1	0.03	0.05
4	6	40	35	2	2	0.1	0	0.01
4	7	40	35	2	2	0.1	0	0.01
4	8	40	35	2	2	0.1	0	0.01
4	9	40	35	2	2	0.1	0	0.05



defid	deluid	petmax	petmin	infexp	infil	deepfr	basetp	agwetp
4	10	40	35	2	2	0.1	0	0.05
4	11	40	35	2	2	0.1	0.02	0.03
4	13	40	35	2	2	0.1	0	0.03
4	14	40	35	2	2	0.1	0	0
4	15	40	35	2	2	0.1	0	0
4	16	40	35	2	2	0.1	0	0
4	17	40	35	2	2	0.1	0	0
4	18	40	35	2	2	0.1	0	0
4	19	40	35	2	2	0.1	0	0

defid parameter group id

deluid land use id

petmax air temperature below which e-t will is reduced (deg F)

petmin air temperature below which e-t is set to zero (deg F)

infexp exponent in the infiltration equation (none)

infil ratio between the maximum and mean infiltration capacities over the PLS (none)

deepfr fraction of groundwater inflow that will enter deep groundwater (none)

basetp fraction of remaining potential e-t that can be satisfied from baseflow (none)

agwetp fraction of remaining potential e-t that can be satisfied from active groundwater (none)



Table A-3. 130 pwat-parm4

defid	deluid	cepssc	uzsn	nsur	intfw	irc	lzetp
2	1	0.08	0.204	0.2	1	0.5	0.3
2	2	0.08	0.204	0.2	1	0.5	0.3
2	3	0.08	0.204	0.2	1	0.5	0.3
2	4	0.08	0.204	0.2	1	0.5	0.2
2	5	0.27	0.48	0.3	1	0.5	0.5
2	6	0.15	0.24	0.2	1	0.5	0.3
2	7	0.15	0.27	0.3	1	0.5	0.4
2	8	0.15	0.372	0.3	1	0.5	0.7
2	9	0.3	0.372	0.3	1	0.5	0.6
2	10	0.3	0.372	0.3	1	0.5	0.6
2	11	0.15	0.378	0.3	1	0.5	0.55
2	13	0.15	0.27	0.3	1	0.5	0.4
2	14	0.05	0.24	0.08	1	0.5	0.3
2	15	0.05	0.24	0.08	1	0.5	0.3
2	16	0.05	0.24	0.08	1	0.5	0.3
2	17	0.05	0.24	0.08	1	0.5	0.3
2	18	0.05	0.24	0.08	1	0.5	0.3
2	19	0.1	0.24	0.08	1	0.5	0.3
3	1	0.08	0.21	0.2	1	0.5	0.2
3	2	0.08	0.21	0.2	1	0.5	0.15
3	3	0.08	0.21	0.2	1	0.5	0.15
3	4	0.08	0.21	0.2	1	0.5	0.15
3	5	0.27	0.384	0.3	1	0.5	0.5
3	6	0.15	0.3	0.2	1	0.5	0.3
3	7	0.15	0.318	0.3	1	0.5	0.4
3	8	0.15	0.384	0.3	1	0.5	0.7
3	9	0.3	0.384	0.3	1	0.5	0.6
3	10	0.3	0.384	0.3	1	0.5	0.6
3	11	0.15	0.3	0.3	1	0.5	0.5
3	13	0.15	0.282	0.1	1	0.5	0.2
3	14	0.05	0.222	0.08	1	0.5	0.3
3	15	0.05	0.222	0.08	1	0.5	0.3
3	16	0.05	0.222	0.08	1	0.5	0.2
3	17	0.05	0.222	0.08	1	0.5	0.2
3	18	0.05	0.222	0.08	1	0.5	0.3
3	19	0.1	0.222	0.08	1	0.5	0.3
4	1	0.08	0.216	0.2	1	0.5	0.2
4	2	0.08	0.216	0.2	1	0.5	0.15
4	3	0.08	0.216	0.2	1	0.5	0.15
4	4	0.08	0.216	0.2	1	0.5	0.15
4	5	0.27	0.48	0.3	1	0.5	0.65
4	6	0.15	0.318	0.2	1	0.5	0.3
4	7	0.15	0.33	0.3	1	0.5	0.4
4	8	0.15	0.39	0.3	1	0.5	0.7
4	9	0.3	0.39	0.3	1	0.5	0.6
4	10	0.3	0.39	0.3	1	0.5	0.6



defid	deluid	cepssc	uzsn	nsur	intfw	irc	lzetp
4	11	0.15	0.3	0.3	1	0.5	0.5
4	13	0.15	0.282	0.1	1	0.5	0.2
4	14	0.05	0.228	0.08	1	0.5	0.3
4	15	0.05	0.228	0.08	1	0.5	0.3
4	16	0.05	0.228	0.08	1	0.5	0.2
4	17	0.05	0.228	0.08	1	0.5	0.2
4	18	0.05	0.228	0.08	1	0.5	0.3
4	19	0.1	0.228	0.08	1	0.5	0.3

defid parameter group id

deluid land use id

cepssc interception storage capacity (inches)

uzsn upper zone nominal storage (inches)

nsur Manning's n for the assumed overland flow plane (none)

intfw interflow inflow parameter (none)

irc interflow recession parameter (none)

lzetp lower zone evapotranspiration parameter (none)

Appendix B: Model Sediment Parameters

Based on the SCWRRP regional sediment approach, the following parameters for the sediment module were used as initial values. Some adjustment was necessary based on local conditions and observed data.

Pervious Lands (PERLNDs)

SMPF 1.0

KRER The presented model varies this parameter by soil group and land use (area-weighted average) as follows:

SSUGRO soil data for San Diego County was utilized to calculate weighted KRER values for each land use and soil hydrologic group (HSG) within the Los Peñasquitos watershed. A weighted average of soil slope (S) and soil erodibility factors (K) were calculated for each soil map unit in ArcGIS using Soil Data Viewer. The land use classification layer (which contained HSG values for each parcel) was subsequently intersected with both the aggregated slope and K factor layers. In a spreadsheet program, slope and K factor values were subtotaled and area weighted for each land use classification and soil hydrologic group across the watershed. In order to calculate $KRER$ values, length-slope (LS) factors were first calculated according to the Wischmeier and Smith (1978) equation:

$$LS = (0.045 L)^b \cdot (65.41 \sin^2 \theta_k + 4.56 \sin \theta_k + 0.065)$$

where $\theta_k = \tan^{-1}(S/100)$, S in the slope in percent, L is the slope length, and b equals the following values: 0.5 for $S \geq 5$, 0.4 for $3.5 \leq S \leq 5$, 0.3 for $1 \leq S \leq 3$, and 0.2 for $S < 1$. An L value of 15 meters was used for all LS calculations, and LS values were not allowed to exceed 5. Finally, $KRER$ values were calculated using the following equations:

$$KRER = G \cdot K \cdot LS$$

where G accounts for unit conversion and was assigned a value of 4.102.

JRER Set all to 1.81 (SCWRRP used 2.0)

AFFIX All set at 0.005

COVER All set at 0.10 by SCWRRP

NVSI Set to 0

KSER Set to 1.8

JSER Set to 2.0

KGER Set to 0

JGER Set to 2.0 (inactive)

DETS 0.5 tons/ac

Impervious Lands (IMPLNDs)

KEIM and JEIM varies by land use. The following values for impervious surfaces for general land use categories were used.



Table B-1. Impervious surface coefficients (KEIM and JEIM) by landuse

	Industrial	LDR	HDR	Commercial	Open/Park
KEIM	soils B = 0.10 soils C/D = 0.07	0.03	0.015	0.10	0.20
JEIM	2.5	2.5	2.5	2.5	2.5

ACCSDP 0.1 tons/ac/d
REMDSP Set at 0.20

Upland Sediment Fractions

SSURGO data was used to set the fraction of total sediment from land that is sediment class (Table). Adjustments to account for deposition en route were made based on the assumption that 50 percent of the sand and 30 percent of silt is deposited using watershed delivery ratios in Vanoni, 1975. Table provides the resulting land fractions for the model.

Table B-2. Sediment fractions by hydrologic soil group

HSG	Sand	Silt	Clay
B	65	23	12
C	68	19	14
D	54	21	24

Table B-3. Sediment fractions adjusted for watershed delivery

HSG	Sand	Silt	Clay
B	33	16	51
C	34	13	53
D	27	15	58

Reaches (RCHRES)

The primary calibration parameters for maintaining dynamic steady state in each reach was defining the stresses for deposition and scour. The stream cross sections were defined by internal LSPC algorithms based on upstream watershed area. Properties for fall velocity in still water (w) and density (Rho) were set uniformly for all reaches (Table).

Table B-4. Model reach parameters

	Sand	Silt	Clay
Fall velocity (in/s)	1.0	0.05	0.0002
Rho (g/cm ³)	2.5	2.2	2.0



Sand transport in the reaches was simulated using the power function of velocity subroutine. The KSAND parameter was set to 1.0 and EXPSND to 2.0 within each reach. Critical shear stress deposition and scour stress and erodibility coefficient were unique by reach and calibrated to maintain a dynamic steady state during the long term calibration simulations.

Table B-5. Model reach sand and silt stress and erodibility coefficients

Reach	Sediment Class	Critical shear stress		Erodibility coefficient (m) (lb/ft ² ·d)
		Deposition (lb/ft ²)	Scour (lb/ft ²)	
1	Silt	0.7	1.3	0.001
1	Clay	0.6	1.1	0.001
2	Silt	0.4	0.9	0.001
2	Clay	0.35	0.7	0.001
3	Silt	0.08	0.8	0.001
3	Clay	0.07	0.7	0.001
4	Silt	0.35	1	0.001
4	Clay	0.3	0.95	0.001
5	Silt	0.35	0.75	0.001
5	Clay	0.3	0.6	0.001
6	Silt	0.35	0.8	0.001
6	Clay	0.3	0.6	0.001
7	Silt	0.5	1	0.001
7	Clay	0.4	0.9	0.001
8	Silt	1.5	2.2	0.001
8	Clay	1.2	1.8	0.001
9	Silt	1.2	2	0.001
9	Clay	1	1.5	0.001
10	Silt	0.48	1.2	0.001
10	Clay	0.4	1	0.001
11	Silt	0.35	0.75	0.001



Reach	Sediment Class	Critical shear stress		Erodibility coefficient (m) (lb/ft ² · d)
11	Clay	0.3	0.6	0.001
12	Silt	0.6	1.2	0.001
12	Clay	0.5	1	0.001

kber coefficient for scour of the bank matrix soil (calibration)

jber exponent for scour of the bank matrix soil (calibration)

qber bank erosion flow threshold causing channel bank soil erosion (cfs)

RCHID	KBER	JBER	QBER	Sand	Silt	Clay
1	0	0.001	8.972199	0.34	0.33	0.33
2	0	0.001	94.98709	0.34	0.33	0.33
3	1.0	0.001	238.4284	0.34	0.33	0.33
4	0	0.001	92.76765	0.34	0.33	0.33
5	0	0.001	81.77471	0.34	0.33	0.33
6	0	0.001	68.26335	0.34	0.33	0.33
7	0	0.001	62.12131	0.34	0.33	0.33
8	0	0.001	78.1442	0.34	0.33	0.33
9	0	0.001	101.9106	0.34	0.33	0.33
10	0	0.001	43.68436	0.34	0.33	0.33
11	0.5	0.1	154.2955	0.34	0.33	0.33
12	0.5	0.1	223.6453	0.34	0.33	0.33